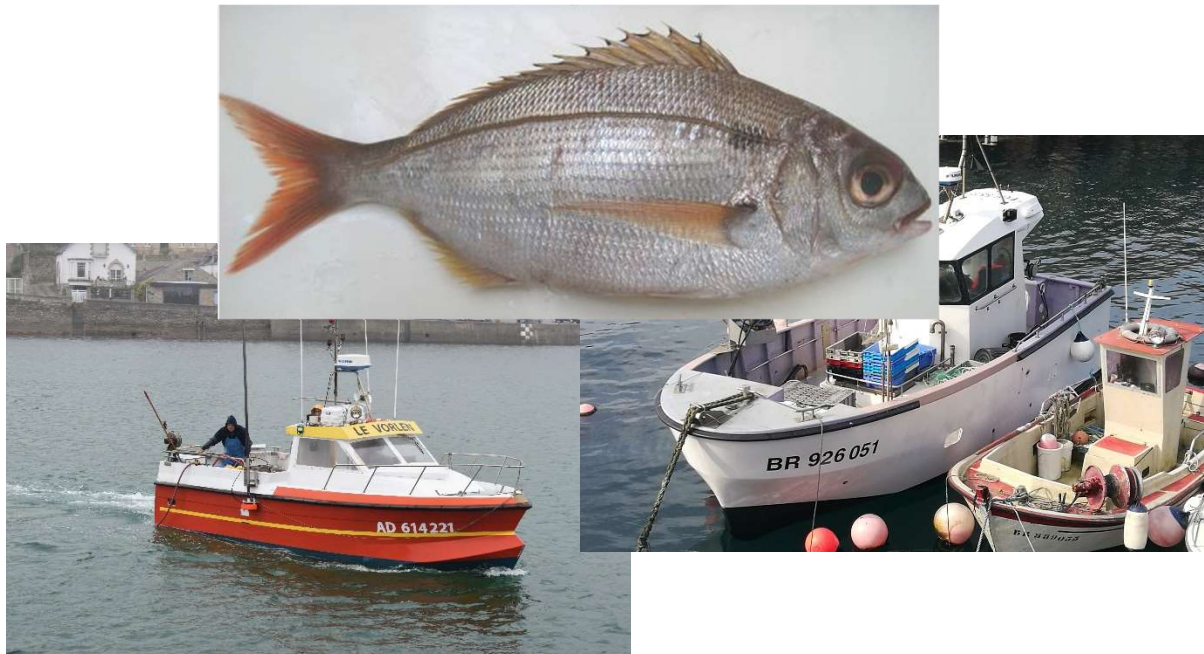


# Projet France-Filière Pêche DynRose

## Rapport Final



## 1. Introduction

La dorade rose (*Pagellus bogaraveo*) était la quatrième espèce de poissons démersaux dans les débarquements en poids du golfe de Gascogne et probablement la deuxième en valeur au cours des années 60 et 70. Le stock du golfe de Gascogne s'est effondré du fait de la surpêche au cours des années 1980 et les captures internationales sont restées à un niveau bas depuis, d'environ 100 tonnes ces dernières années. La dorade rose est une espèce sensible à l'exploitation qui ne peut soutenir qu'une mortalité par pêche modérée du fait de son cycle de vie où l'espèce est hermaphrodite protandre, mâle puis femelle, ce qui a pour conséquence que la biomasse de femelles fécondes décroît fortement même pour sous une pression de pêche modérée. De plus la croissance individuelle est lente ce qui conduit à une productivité biologique des stocks faible. Enfin, le comportement agrégatif de cette espèce a pour conséquence que des captures élevées peuvent avoir lieu même lorsque l'abondance totale est basse tandis que sa grande qualité organoleptique lui confère une haute valeur marchande et donc un fort intérêt pour les pêcheries.

Malgré l'effondrement du stock de dorade rose dans les années 1980, aucune gestion n'a contraint les captures jusqu'en 2003 où des quotas européens ont été introduits pour ce stock considéré couvrir les sous-région 6, 7 et 8 du CIEM. Ces quotas ont été graduellement réduits à 105 tonnes depuis 2020. Il n'y a ni données pour évaluer quantitativement la biomasse du stock ni indicateur pour évaluer sa tendance de sorte que l'application par le CIEM du cadre pour les stocks à données limitées conduit à une recommandation de captures nulles. Le très faible quota français de 4 tonnes depuis 2020 semble bien inférieur à la fraction réellement inévitable des captures accessoires réelles. Les organisations de producteurs (OPs) ont pris des mesures pour s'adapter à ce faible quota, notamment l'interdiction des débarquements par les engins actifs et un système de licences. Néanmoins, l'interdiction des débarquements est problématique dans le cadre de l'obligation à débarquer.

Au cours de son cycle de vie la dorade rose passe de nourriceries situées dans la zone littorale au plateau côtier avec un hivernage dans les zones plus profondes de la pente continentale habitées par les adultes (Olivier, 1928; Mytilineou et al., 2013). Pour le stock du golfe de Gascogne, des marquages ont montré des migrations saisonnières de l'ordre de 1000 km entre des zones d'hivernage profonde et Méridionales, en Mer Cantabrique et des zones de reproduction et d'alimentation estivale au nord du golfe de Gascogne (Guéguen, 1974). L'analyse génétique a montré une distinction génétique entre les populations de dorade rose des Açores et celles de la côte Portugaise et de Madère (Stockley et al., 2005). En revanche, aucune différentiation génétique n'a été trouvée autour de la Péninsule Ibérique (Piñera et al., 2007). Une nouvelle étude, publiée pendant le projet DynRose par une équipe portugaise et utilisant des échantillons collectés à la pointe Bretagne en 2019 (Robalo et al., 2021) a montré la même structure et en particulier a confirmé l'absence de différence significative entre les dorades roses de la mer Cantabrique et celles de la Pointe Bretagne. Cela confirme la pertinence d'une seule unité de gestion pour la dorade rose du golfe de Gascogne (y compris mer Cantabrique) et de la mer Celtique.

Dans le cadre du projet européen H2020 Pandora, ifremer a réalisé une campagne acoustique d'estimation de la biomasse de dorade rose en 2019 et l'espèce a aussi été choisie comme cas d'étude dans un projet sur fonds propres, sur le développement des approches par ADN environnemental (eDNA). Dans ce contexte, le projet Dynrose avait pour objectif général de contribuer à la collecte et l'analyse des données nouvelles sur cette espèce par des études portant sur : (i) la distribution géographique actuelle de la dorade rose sur la côte Atlantique ; (ii) l'évolution des pêcheries et (iii) l'évaluation de stock et la stratégie de gestion. Il est apparu au cours du projet que des résultats

tangibles sur ce dernier objectif étaient hors de portée et le travail a été reporté sur une approche du budget énergétique de stock de dorade rose.

## 2. Principaux résultats

Les principaux résultats du projet DynRose portent sur trois aspects : la distribution spatiale et les habitats de l'espèce à l'échelle de l'Atlantique Nord-Est et de la Méditerranée, le budget énergétique de l'espèce et les relations entre les quantités débarquées et les prix au cours des 50 dernières années.

Une analyse de la distribution spatiale de la dorade rose a été réalisée avec une approche de modélisation de distribution d'espèce conjointe (ensemble Species Distribution Modelling, eSDM), qui met en œuvre plusieurs catégories de modèle d'habitat et une procédure statistique pour estimer des cartes d'habitat (habitat suitability maps) puis des cartes de présence-absence binaire. Les facteurs d'habitats de la dorade rose sélectionnés pour tracer des cartes d'habitat sont au nombre de neuf. Cette analyse a été réalisée sur l'ensemble de l'Atlantique Nord-Est et du bassin occidental de la Méditerranée sur des cellules spatiales de 0.05 degrés. Les neuf prédicteurs en termes d'habitat pour la dorade rose, à l'échelle de ces cellules sont (1) région, (2) type de fond, (3) moyenne et (4) écart-type de la profondeur, (5) maximum de la température de surface, (6) moyenne et (7) minimum de la vitesse du courant, (8) écart-type de la salinité, (9) écart-type de la température au fond. Les facteurs 5 à 9 concernent les minimum, maximum, moyenne et écart-type au cours de l'année. Les cartes de présence-absence binaire sont des projections qui reposent sur des sous-ensembles optimisés de six prédicteurs. L'habitat potentiel de la dorade rose inclut les côtes et pentes insulaires des Açores, le plateau continental et la pente continentale supérieure du Nord-Est Atlantique, principalement au sud de 48° nord (golfe de Gascogne) et, pour une extension moindre, dans le sud des mers Celtiques ainsi que les plateaux et pentes nord de la Méditerranée occidentale, avec des zones plus étendues au Détrict de Gibraltar, dans le golfe du Lion et le long des côtes italiennes. L'importance du prédicteur région, qui revient à estimer des paramètres différents pour les zones des Açores, de l'Atlantique et de la Méditerranée, est interprétée comme liée à l'état des stocks de dorade rose dans les trois régions, avec les stocks des côtes Atlantique européennes dans un état d'abondance plus réduite que ceux de Méditerranée ou des Açores. Par suite, dans le golfe de Gascogne l'habitat potentiel couvre l'essentiel du plateau continental tandis que l'habitat actuellement occupé (realised habitat dans la modélisation) représenté par les cartes de présence-absence binaire est beaucoup plus réduit. Enfin, l'estimation de l'habitat potentiel couvrant l'ensemble du golfe de Gascogne, suggère que cette zone reste adéquate pour l'espèce, qui devrait donc être capable de la recoloniser, et ce malgré les changements environnementaux survenus depuis les années 1980. Les détails de cette étude peuvent être trouvés en annexe 1 de ce rapport.

La dynamique du budget énergétique (modèle Dynamic Energy Budget, DEB) est une approche basée sur les principes de la thermodynamique. L'étude menée sur la dorade rose a permis de compiler un grand nombre de données physio-écologiques de l'espèce. Comme classiquement dans ce type d'étude, certaines données ne sont pas disponibles pour l'espèce et ont été remplacées par des pseudo-données correspondant à un organisme généralisé qui permettent d'assurer la cohérence de du paramétrage du modèle pour l'espèce. Le rapport technique fournit en annexe 2 détaille l'état d'avancement du modèle développé. La poursuite de ce travail permettra d'étudier plusieurs aspects non compris de la biologie et la dynamique de la dorade rose dont les facteurs du changement de sexe et du cycle migratoire.

Les relations entre les quantités débarquées et les prix au cours des 50 dernières années ont été traitées dans une approche comparative ou les variations observées pour la dorade rose ont été comparées à celles d'autres espèces exploitées dans le golfe de Gascogne. Trois catégories d'espèces exploitées dans le golfe de Gascogne et pertinentes pour des comparaisons avec la dorade rose ont été sélectionnées : les principales espèces benthico-démersales (merlu, baudroies, sole), les espèces à prix élevés (bar, saint-pierre, dorade royale, pagre, maigre, turbot, barbue, lieu jaune, rouget barbet et thon rouge) et des espèces de la même famille (Sparidae) que la dorade rose (pageot acarné, pageot commun, dorade grise, sar commun). A l'exception du thon rouge, l'étude est limitée à des espèces benthico-démersales plus pertinentes pour comparaison avec la dorade rose en terme de prix et marchés auxquels elles sont destinées. Les données de prix disponibles ont été corrigées de l'inflation en utilisant les indices de l'INSEE. L'effondrement du stock de dorade rose dans les années 1980 a été associé à une augmentation de son prix tandis que pour d'autres espèces dont les débarquements ont diminué, mais sans connaître un effondrement similaire, la baisse des débarquements de l'époque a été accompagnée d'une baisse des prix (corrigés de l'inflation).

Dans la période 2000-2020, les débarquements de dorade rose ont d'abord augmenté puis ont diminué sous l'effet des quotas limitant et son prix corrigé de l'inflation a augmenté de 0.42 €/an. Aucune autre espèce étudiée n'a connu une telle augmentation au cours de la même période et la plupart des prix au débarquement des espèces étudiées ont, au contraire, faiblement baissé. Depuis 2010, la dorade rose est devenue l'espèce de poisson démersale la plus chère débarquée par les bateaux actifs dans le golfe de Gascogne. Sur le long terme, la diminution des débarquements de dorade rose pourrait avoir conduit au report éventuel des consommateurs vers d'autres espèces de qualité similaire et prix élevés, mais les variations observées des prix et débarquement ne permettent pas d'estimer clairement de tels report. Il est probable que l'augmentation de la disponibilité de poisson produit par l'aquaculture au cours des dernières décennies perturbe l'effet des relations offre (débarquement) et demande sur les prix. Les détails de cette étude peuvent être trouvés en annexe 3 de ce rapport.

### 3. Déroulement du projet

Trois objectifs étaient définis dans le document de projet soumis à FFP en mars 2020 : i) Etude de la distribution géographique actuelle de la dorade rose sur la côte Atlantique; ii) Analyse de l'évolution et de l'état des pêcheries et du stock ; iii) Mise à jour du modèle d'évaluation de stock et simulation de sa dynamique selon la stratégie de gestion en tenant compte de l'hermaphrodisme protandre de la dorade rose. Le projet prévoyait de concrétiser ces objectifs par quatre livrables :

- (1) Manuscrit scientifique sur les aspects (i) Comparaison de la distribution géographique historique et actuelle de la dorade rose dans le golfe de Gascogne et (ii) Description de l'évolution des pêcheries et du stock de dorade rose du golfe de Gascogne
- (2) Manuscrit scientifique sur l'aspect (iii) Dynamique de reconstitution démographique en fonction de différentes stratégies de gestion et de l'incertitude sur les traits d'histoire de vie
- (3) Présentation des résultats à un colloque international
- (4) Présentation des résultats à la profession

Au cours du projet, il est apparu que les données disponibles, notamment les données d'acoustique, ne permettaient pas d'estimer une trajectoire de reconstitution suffisamment fiable pour faire des projections sous des scénarios de gestion. Une étude de cette dynamique serait donc restée sous une forme de simulation ou hypothétique sans amener de réponse d'intérêt pour la pêcherie en terme d'état du stock et d'options de gestion. Afin de produire un travail plus utile, un avenant au projet a

été signé pour le prolonger et remplacer le livrable 2 par un manuscrit sur une approche de la dynamique du budget énergétique (dynamic energy budget, DEB) de l'espèce. L'avenant au projet précisait que cette modélisation DEB ne serait pas finalisée pendant la durée du projet, mais sera poursuivie par IFREMER après la clôture du projet DynRose. Ceci en raison de la complexité d'une modélisation DEB, en particulier sur une espèce migratrice.

Le livrable 1 a donné lieu à un article dans la revue Ecological modelling (Annexe 1). La seconde partie de ce livrable "Description de l'évolution des pêches et du stock de dorade rose du golfe de Gascogne" a été concrétisée par une analyse de l'effet de l'effondrement du stock de dorade rose dans les années 1980 sur son prix au débarquement. Cette étude porte sur les années 1973 à 2020 et traite donc aussi des variations de prix au cours de la période récente. Elle constitue un second manuscrit qui relève du livrable 1. L'étude est en cours de finalisation pour soumission à une revue scientifique et présentée en annexe 2.

Comme prévu par l'avenant au projet, un modèle DEB de la dorade rose a été paramétré et le rapport correspondant, est présenté en annexe 3. Cette modélisation requiert un travail additionnel pour rédiger un article à soumettre à une revue scientifique.

Les livrables 3 et 4 correspondent aux présentations dans des colloques internationaux et nationaux. Il s'agit de deux colloques scientifiques internationaux : ISOBAY 2021 (colloque golfe de Gascogne, avec une forte présence de scientifique français et espagnols) et conférence scientifique du CIEM 2021 (suivie par la communauté scientifique halieutique et environnement européenne) et d'un colloque français (Rencontres de l'ichtyologie en France, 2022). Le projet a donc donné lieu à des présentations dans trois colloques. Les travaux ont aussi été présentés à l'OP partenaire pêcheurs de Bretagne.

Enfin, l'échantillonnage par acoustique pour estimer l'abondance de la dorade rose qui avait été initiée avant le début du projet a été abandonnée suite aux analyses de données réalisées au cours du projet. En revanche, un échantillonnage de la zone de la pointe Bretagne par ADN environnemental (ADNe), dont l'objectif est d'estimer la distribution spatiale et l'abondance des poissons en échantillonnant les traces d'ADN qu'ils laissent dans l'eau a été mis en place. Cet échantillonnage requiert une campagne de trois à cinq jours de mer à bord d'un petit bateau de pêche. Une telle campagne a déjà été réalisée trois fois en 2020, 2021 et 2022 et sera poursuivi au moins quelques années dans le cadre d'une collaboration avec l'Université de Zurich (Suisse). Cette méthode permet d'étudier l'ensemble de la biodiversité à partir d'un type d'échantillonnage unique. Pour la zone étudiée, cette approche a été appliquée aux poissons. Le potentiel de l'ADNe pour suivre la distribution et l'abondance de la dorade rose à partir de l'ADNe sera évalué grâce aux travaux engagés lors du projet européen PANDORA et de Dynrose.

## 4. Conclusion

Le projet DynRose a produit des résultats nouveaux sur trois aspects du stock de dorade rose du golfe de Gascogne : la distribution spatiale et l'habitat du stock, le budget énergétique de l'espèce et l'évolution des pêches et des prix à la première vente. L'étude de l'habitat a abouti au résultat important que l'habitat potentiel de la dorade rose couvre l'essentiel du plateau continental dans le golfe de Gascogne et plus au nord en mer Celtique tandis que l'habitat réalisé est actuellement beaucoup plus réduit. Par conséquence, la dorade rose devrait pouvoir recoloniser plus largement son habitat potentiel, et ce malgré les changements environnementaux survenus depuis les années 1980. L'étude de la dynamique du budget énergétique (modèle Dynamic Energy Budget, DEB) a permis de compiler un grand nombre de données physio-écologiques de l'espèce et de paramétriser le modèle. La

poursuite de ce travail permettra d'étudier plusieurs aspects non compris de la biologie et la dynamique de la dorade rose dont les facteurs d'un changement observé de croissance. Les pêcheries qui débarquent de la dorade rose ont fortement changé avec un déclin des débarquements issus des engins actifs et des filets fixes. Les métiers de l'hameçons restent pratiquement les seuls à débarquer l'espèce ces dernières années. Parmi les espèces de poisson exploitées dans le golfe de Gascogne, la dorade rose est celle dont le prix moyen est le plus élevé. Bien que le quota et les débarquements français de dorade soient très faibles, le même type de relations prix-débarquements s'établit généralement pour la dorade rose et 17 autres espèces quelque soient leur caractéristiques (espèces principales en quantité débarquée, haute valeur, existence d'une production aquacole et proximité taxonomique avec la dorade rose). Les prix de ces espèces répondent en général à un système inverse de la demande (où les prix dépendent de la quantité mise sur le marché) plutôt que d'une classique loi de l'offre et de la demande. Enfin, le projet a ouvert de nouvelles perspectives, avec la mise en place d'un suivi de la zone de la pointe Bretagne par ADN environnemental, dans le cadre d'une collaboration avec l'Université de Zurich

## 5. Dissémination et communication

### 5.1 Revue de presse

Le projet DynRose fait l'objet d'une page dans le numéro spécial du Marin « Le Marin avec France Filière Pêche : 10 ans d'actions au service de la filière » paru le 01.09.2022 (<https://www.francefilierepesche.fr/le-marin-x-ffffp-10-ans-dactions-au-service-de-la-filiere/>).

### 5.2. Communication vers la communauté scientifique

Le projet a donné lieu à deux présentations dans des colloques internationaux ISOBAY 2021, ICES ASC 2021 et au colloque national RIF 2022 (Rencontre de l'Ichtyologie en France). Les diapositives de ces présentations sont incluses en annexe 4.

Un article est publié sur l'aspect distribution spatiale et habitat (annexe1), un second (impact de quantité débarquées sur les prix) est en cours de finalisation (annexe 2) et un troisième (annexe3) requiert des analyses complémentaires.

### 5.3. Communication avec la profession

La communication avec la profession a été faite tout au long du projet. Le projet a été monté en relation avec la profession, l'OP Les Pêcheurs de Bretagne. Cette communication était initiée avant le projet DynRose dans le cadre du projet H2020 PANDORA. Une campagne acoustique sur un bateau de pêche avait été faite en 2019 et financée par ce projet PANDORA. Les résultats des analyses ont été présentés lors de réunions. Cette collaboration sera poursuivie au-delà du projet, au moins à l'occasion de la poursuite de l'échantillonnage par ADNe.

## Annexes et supports de communications

Les résultats détaillés du projet sont présentés dans les annexes suivantes:

### Annexe 1

Version preprint de l'article publié, référence ci-dessous (online version disponible depuis le 06.01.2023) :

Lola De Cubber, L., Trenkel, V.M., Diez, A., Gil-Herrera, J., Novoa Pabone A.M., Em, D., Lorance, P. (2023). Robust identification of potential habitats of a rare demersal species (blackspot seabream) in the Northeast Atlantic. *Ecological modelling.* 477.

### Annexe 2

Article en préparation sur les relations entre prix et quantité débarquées de 1973 à 2020.

Effects of stock collapse on price dynamics of blackspot seabream in the Bay of Biscay, Lorance P; et Trenkel, V.M.

### Annexe 3

Rapport sur la paramétrisation d'un modèle DEB

DynRose : Paramétrisation d'un modèle *Dynamic Energy Budget* model sur la Dorade rose (*Pagellus bogaraveo*). Fabri-Ruiz, S., Lorance, P., Trenkel, V.

### Annexe 4

L'annexe 4 fournit une version imprimée des communications présentées lors de colloques. Les diaporamas correspondant sont fournis à FFP par fichier séparés.

XVII international Symposium on Oceanography of the Bay of Biscay (ISOBAY 17) [17ème symposium d'océanographie du golfe de Gascogne], 1-4 Juin 2021

ICES 2021 Annual Science Conference [Conférence Scientifique Annuelle du CIEM 2021], 6-10 Septembre 2021

Huitièmes Rencontres de l'Ichtyologie en France, Paris, 14-18 mars 2022

## Annexe 1

### Article publié

Lola De Cubber, L., Trenkel, V.M., Diez, A., Gil-Herrera, J., Novoa Pabone A.M., Em, D., Lorance, P. (2023). Robust identification of potential habitats of a rare demersal species (blackspot seabream) in the Northeast Atlantic. *Ecological modelling*. 477

1 Robust identification of potential habitats of a rare demersal  
2 species (blackspot seabream) in the Northeast Atlantic

3 Lola De Cubber<sup>a,b,\*</sup>, Verena M. Trenkel<sup>a</sup>, Guzman Diez<sup>c</sup>, Juan Gil-Herrera<sup>d</sup>, Ana  
4 Maria Novoa Pabon<sup>e</sup>, David Eme<sup>a,f</sup>, Pascal Lorance<sup>a</sup>

5 <sup>a</sup>DECOD (*Ecosystem Dynamics and Sustainability*), IFREMER, INRAE, Institut-Agro -  
6 Agrocampus Ouest, Nantes, France

7 <sup>b</sup>Institut de Recherche pour le Développement (IRD), MARBEC (IRD, Ifremer, CNRS, Univ  
8 Montpellier), Av. Jean Monnet - Sète, France

9 <sup>c</sup>AZTI, Marine Research, Basque Research and Technology Alliance (BRTA). Txatxarramendi  
10 ugartera z/g, 48395 Sukarrieta - Bizkaia, Spain

11 <sup>d</sup>Centro Oceanográfico de Cádiz (IEO-CSIC), Muelle de Levante s/n, 11006, Cádiz, Spain

12 <sup>e</sup>Departamento de Oceanografia e Pescas, Universidade dos Açores, 9901-862 Horta, Portugal

13 <sup>f</sup>RiverLY Research Unit, National Research Institute for Agriculture Food and Environment  
14 (INRAE), Villeurbanne, France

---

---

## 15 Abstract

16 Species distribution models (SDM) are commonly used to identify potential habitats.  
17 When fitting them to heterogeneous, opportunistically collated presence/absence data,  
18 imbalance in the number of presence and absence observations often occurs, which could  
19 influence results. To robustly identify potential habitats for blackspot seabream (*Pagellus*  
20 *bogaraveo*) throughout its distribution area in the Northeast Atlantic and the western  
21 Mediterranean Sea, we used an ensemble species distribution modelling (eSDM) approach,  
22 modelling gridded presence-absence data with environmental predictors for two types of  
23 occurrence data sets. The first data set displayed the observed unbalanced spatially het-  
24 erogeneous presence/absence ratio and the second a balanced presence/absence ratio. The  
25 data covered the full distribution area, including the European Atlantic shelf, the Azorean  
26 region and the Western Mediterranean Sea. Across these regions, populations display vari-  
27 able status. The main environmental predictors for potential habitats were bathymetry  
28 and annual maximum SST. The fitted ensemble compromise (eSDM) was projected over  
29 the whole grid to create a habitat suitability map. This map exhibited higher probabilities  
30 of presence for the balanced-ratio data set. A binary presence-absence map was then gen-  
31 erated using optimised presence probability thresholds for four validation indices. Using  
32 the true skill statistic to optimise the threshold, the surface areas of the binary presence-  
33 absence map was 53% smaller for the balanced data set than for the observed unbalanced  
34 data set. However, the choice of validation index had an even greater impact (up to 15  
35 000 %). This indicates that studies using opportunistic data for SDM fitting need to pay  
36 attention to the effects of presence/absence data imbalance and the choice of validation  
37 index to fully evaluate uncertainty.

## 38 Keywords

39 *Pagellus bogaraveo*, species distribution models, ensemble modelling, heterogeneous  
40 data set, presence-absence imbalance

---

\*Corresponding author: lola.decubber@gmail.com

41 **1. Introduction**

42 Actual and potential areas of species distribution can be investigated via eco-  
43 logical niche modeling (Soberon and Nakamura, 2009). A species' niche is defined  
44 as a subset of environmental conditions under which populations of a species have  
45 positive growth rates (Soberon and Nakamura, 2009). The habitat is then the ge-  
46ographical translation of these environmental conditions. The fundamental niche is  
47 the theoretical combination of environmental variable that allows for physiological  
48 processes (feeding, growth, reproduction) to take place (Hutchinson, 1978). Essen-  
49 tial fish habitats, defined as areas or volumes of water and bottom substrates that  
50 provide the most favourable habitats for fish populations to spawn, feed and mature  
51 throughout their full life cycle, are thus the geographical translation of the optimal  
52 part of the fundamental niche of a species (Helaouet and Beaugrand, 2009; Vala-  
53nis et al., 2008). The realised niche is the subset of environmental conditions the  
54 species is actually using (Soberon and Nakamura, 2009). Species may occur outside  
55 the fundamental niche during migrations. In contrast, the realised niche might be  
56 reduced when densities are low because of intensive predation or fishing (Helaouet  
57 and Beaugrand, 2009). The realised habitat of a species can then be defined as  
58 the geographical translation of the realised niche of a species. It differs from the  
59 species' distribution since all locations displaying the environmental conditions of  
60 the realised niche might not be occupied simultaneously, especially if the species'  
61 distribution is wide.

62 Species distribution models (SDMs) have been used in conservation biology to  
63 describe the habitat distribution of organisms in both marine and terrestrial sys-  
64 tems (Laman et al., 2018; Elith & Leathwick, 2009; Valanis et al., 2008). They are  
65 grounded in the concept of ecological niche (Hutchinson, 1957). They have been  
66 widely used since 2005 and have reached high statistical sophistication in recent  
67 years (Schickele et al., 2020; Jiménez & Soberón, 2020; Robinson et al., 2017). Eco-  
68logical assumptions implied when using SDMs are that there is niche conservatism  
69 (Crisp et al., 1981) and unlimited dispersal abilities (Wiens et al., 2009) and that  
70 biotic interactions do not influence large-scale distributions (Gleason, 1926; Guisan  
71 and Thuiller, 2005; Schickele et al., 2020). Among the numerous statistical SDMs

72 approaches developed to map fish habitats, ensemble species distribution modelling  
73 (eSDM), also referred to as ensemble niche modelling (Thuillier et al, 2016), which  
74 combines the use of several SDM categories, appears to be a good compromise in  
75 terms of programming skills required, computation time and consistency of the re-  
76 sults (Schickele et al., 2020; Mateo et al., 2019).

77 Data availability is often opportunistic, so that neither the fundamental habitat  
78 nor the realised species' habitat is entirely represented by SDMs. Indeed, the the-  
79 oretical entire range of fundamental environmental conditions of a species is never  
80 fully known and available presence records will never cover the full habitat. Ecol-  
81 ogists thus generally refer to SDM output as potential niche and habitat of the  
82 species of interest (Schickele et al., 2020; Helaouet and Beaugrand, 2009). Several  
83 data filtration and selection processes, as well as physiological prospects (for exam-  
84 ple, optimal environmental ranges for spawning or egg development) can then help  
85 approaching the species' realised or essential habitat (Schickele et al., 2020; Helaouet  
86 and Beaugrand, 2009).

87 Implementing SDMs, especially in the case of widely distributed species such as  
88 the blackspot seabream *Pagellus bogaraveo* (Brünnich, 1768), often requires combin-  
89 ing heterogeneous multiple data sets (Schickele et al., 2020; Fithian et al., 2015).  
90 In the case of presence/absence data, two types of biases have then to be taken  
91 into account. First, detectability might vary among sampling techniques used to  
92 collect data (Kellner and Swihart, 2014). Second, variations in prevalence (i.e. the  
93 number of presence records among sampled points) might reflect primarily varia-  
94 tions in abundance rather than habitat suitability. When data are missing on the  
95 detection probability of sampling techniques, taking into account detection might  
96 not always improve SDM performance (Welsh et al., 2013), and these two biasing  
97 effects (detectability and variations in prevalence) might be difficult to disentangle.  
98 In the case of presence-only data, a common practice is to generate pseudo-absence  
99 data (Schickele et al., 2020). In this case, the number of generated pseudo-absences  
100 is generally set equal to the number of presences (Montgomery, 2005). For actual  
101 presence-absence data, prevalence will vary in space, in particular for large study  
102 areas. This raises questions given spatial predictions from SDMs are known to be

103 sensitive to sample prevalence (Jimenez-Valverde et al., 2021).

104 The general aim of this study was to investigate the potential habitat of the  
105 blackspot seabream and its occupancy level in three regions in the Northeast At-  
106 lantic: Atlantic European shelf, the Azorean region and the Mediterranean Sea.  
107 Occupancy levels were presumed to differ between regions because of the contrasted  
108 population status and variable degree of fishery exploitation. To evaluate the im-  
109 pact of heterogeneous prevalence in the data and obtain robust results we compared  
110 eSDM models using 1) all available presence/absence records, i.e. prevalence varying  
111 over the distribution area of blackspot seabream; 2) the same number of presence  
112 and absence record, i.e. constant prevalence over the distribution area.

## 113 2. Material and methods

### 114 2.1. Case study

115 The blackspot seabream used to be a widely distributed and abundant species  
116 of the North Eastern Atlantic shelf from the Faroe Islands down to Gibraltar, the  
117 Azores and the Western Mediterranean Sea (Desbrosses, 1932; Sanz-Fernandez et  
118 al., 2019; Pinho et al., 2014; Erzini et al., 2006; Spedicato et al., 2002; D’Onglia et  
119 al., 2010; 2012). In fact, it was also referred to as "la dorade commune" (understand  
120 "the common seabream") by French authors in the early 1900s (Desbrosses, 1932;  
121 Olivier, 1928). Increase in fishing effort in the Bay of Biscay (North Eastern Atlantic  
122 shelf) in the 1960s linked to stock declines of other species of fisheries interest such  
123 as hake, associated to its susceptibility to overexploitation, led to a brutal collapse  
124 of this blackspot seabream stock 20 years later in 1975-1985 and low stock size ever  
125 since (see Fig.1a, Lorance, 2011; Guichet et al., 1971; Dardignac, 1988).

126 Blackspot seabream displays three characteristics that make it susceptible to  
127 over-exploitation (Francis and Clark, 2005). First, its biological productivity is low,  
128 individuals reaching 70 cm long in 25 to 30 years and females being mostly the  
129 older individuals since the species is hermaphroditic protandrous, with changing sex  
130 from male to female (Guéguen, 1969, Lorance, 2011). Second, blackspot seabream is  
131 easy to capture during its seasonal migrations because of its aggregative behaviour  
132 (Afonso et al., 2012; 2014).

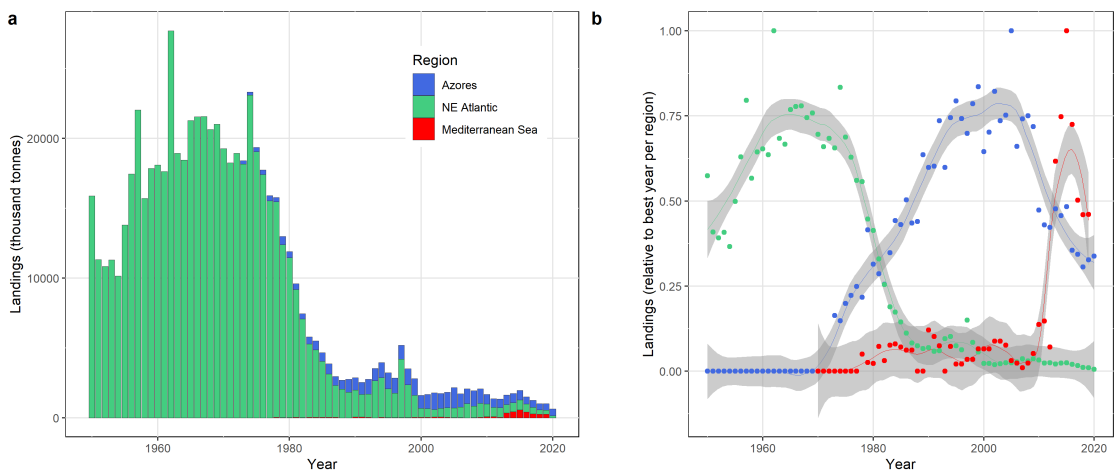


Figure 1: Commercial landings of blackspot seabream between 1950 and 2020 in the three regions investigated in this study as total catch (a) and relative to the highest year per region (b), where dots are individual values and lines are smoothed time trends with 95% confidence intervals. Data before 2000 from Lorance (2011) and from ICES and FAO catch statistics thereafter.

Indeed, adults carry out geographic and depth seasonal migrations from coastal waters, where they reproduce and where juveniles are found, down to 700 m and up to several hundreds of km away from the coast (Morato et al., 2001; Mytilineou et al., 2005). Accordingly, in the Bay of Biscay, individuals present to the West of Brittany ( $48^{\circ}\text{N}$ ) were found to overwinter in the Cantabrian Sea ( $43^{\circ}\text{N}$ ) (Guéguen, 1974). In Azorean waters, juveniles which are only found in coastal areas migrate to isolated seamounts when reaching adult stage, sometimes more than 400 km away (Hareide and Garnes, 2001). Lastly, the species has a high commercial value owing to its organoleptic quality, comparable to gilthead seabream and sea bass (Rincon et al. 2016).

Overall, available stock assessments and landings of commercial fisheries suggest that populations from the European shelf are at low level with small recent catches (2018-2021) compared to past levels (anterior to 1980), while populations from the Azorean region are in better condition with current fisheries being sustainable (ICES, 2021, Fig. 1). Historically (before 1980), catches from the Northeast Atlantic shelf constituted the bulk of landings, reaching up to more than 20000 t per year (Fig. 1a), with the Bay of Biscay being the main fishing area. In comparison, levels of gilthead seabream catches were similar back then, while cur-

151 recently, hake is the most fished species in the Bay of Biscay with around 30000 t  
152 landed per year, followed by monkfish (8000 t per year), sole (3000 t per year) and  
153 seabass (2000 t per year) (Official Nominal Catches 2006-2019. Version 15-10-2021.  
154 Accessed 05-05-2022 via <https://ices.dk/data/dataset-collections/Pages/Fish-catch-and-stock-assessment.aspx>, ICES). From the 1990s, catches from the Northern At-  
155 lantic came mostly from the Iberian coast and the Strait of Gibraltar and were at  
156 similar level than catches from the Azorean area (Fig. 1a). Reported catches from  
157 the Mediterranean Sea are probably not realistic, because in this region 5000 to  
158 10000 tonnes of fish have been landed as unidentified sparid fish or similar labelling  
159 and this might have comprised catch statistics of blackspot seabream (FAO-GFCM,  
160 2021). Therefore, the increased reported landings in recent years (Fig. 1b) may  
161 be due to improved reporting of landings by species. Quotas as well as other man-  
162 agement measures such as minimum landing size and closed fishing seasons are  
163 implemented in all areas (Pinho et al., 2014; Lorance, 2011). Indeed, fishing has  
164 been shown to be the main factor accounting for variations in the species' stock  
165 abundance, with values reaching up to 73% of the variations in stock abundance  
166 nowadays around Gibraltar (Sanz-Fernandez et al., 2019). In the case of poor stock  
167 status, the species distribution might contract within its essential habitats, that thus  
168 needs to be identified to enable targeted conservation management measures to be  
169 implemented.

171 *2.2. Data*

172 *2.2.1. Species observations*

173 Presence/absence records of blackspot seabream were compiled from trawling  
174 and longline scientific surveys (EVHOE, SP-NORTH, SP-ARSA, PT-IBTS, MED-  
175 ITS, ARQDAÇO) available on the DATRAS portal ([https://datras.ices.dk/Data\\_products/Download/Download\\_Data\\_public.aspx](https://datras.ices.dk/Data_products/Download/Download_Data_public.aspx)) or held by national research In-  
176 stitutes, from commercial fisheries data from the Voracera fleet in Gibraltar and from  
177 on-board observations of fishing activities in the Bay of Biscay and the Mediter-  
178 ranean Sea, as well as from the Global Biodiversity Information Facility (GBIF,  
179 <https://www.gbif.org/>) (see Fig.2).

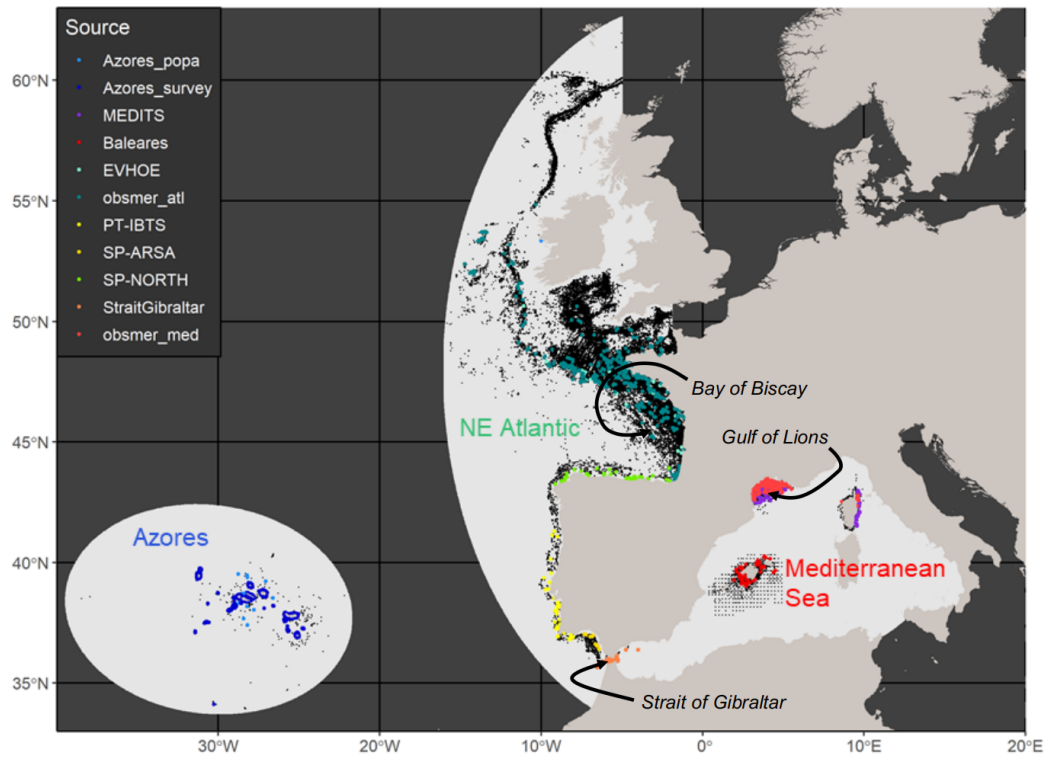


Figure 2: Presence-absence data for blackspot seabream compiled in this study. Black dots represent absence records. Coloured dots correspond to presence records from different data sets: Azores\_popa (Fisheries Observer Program, 1998-2013), Azores\_survey (ARQ-DAÇO longline survey, 1996-2013), Baleares (Marine Biodiversity Atlas of the Balearic Sea, GBIF, 2001-2008), EVHOE (scientific bottom-trawl survey, 1997-2019), MEDITS (scientific bottom-trawl survey, 2004-2019), obsmer\_atl and obsmer\_med (French onboard observation program), PT-IBTS (scientific bottom-trawl survey, 2002-2017), SP-ARSA (scientific bottom-trawl survey, 1996-2019), SP-NORTH (scientific bottom-trawl survey, 2001-2019), StraitGibraltar (Commercial fisheries data, 2009-2011). light grey area is the model domain composed of three regions: Azores, NE Atlantic region and Mediterranean Sea.

181     2.2.2. *Environmental data*

182     Environmental variables consisted of topographic data, sea bottom type and sea-  
 183     water parameters. We extracted bathymetry at a  $0.0003^{\circ}$  resolution from GEBCO  
 184     ([https://www.gebco.net/data\\_and\\_products/gridded\\_bathymetry\\_data](https://www.gebco.net/data_and_products/gridded_bathymetry_data)) and the  
 185     R terrain function (raster package, Hijmans et al., 2011) enabled the calculation of  
 186     bottom slope. Seabed habitat data were extracted from EMODnet (<https://www.emodnet.eu/en/seabed-habitats>) at a 250 m resolution. Homogenization of substrate  
 187     type according to EMODnet categories among all regions led to 14 sea bottom type  
 188     categories: unknown, rock or other hard substrata, coarse substrate, coarse and  
 189     hard substrata.

190 mixed sediment, mixed sediment, sediment, sand, sandy mud, muddy sand, sandy  
 191 mud or muddy sand, fine mud or sandy mud or muddy sand, fine mud, *Posidonia*  
 192 *oceanica*, and dead mattes of *Posidonia oceanica*. Monthly values of Sea Surface  
 193 Temperature (SST), bottom temperature, surface current velocity and salinity be-  
 194 tween January 1994 and December 2018 at a 0.083° resolution were extracted from  
 195 Copernicus Marine Service (GLOBAL\_REA\_NALYSIS\_PHY\_001\_030 product,  
 196 <https://resources.marine.copernicus.eu/>). An overview of environmental variables  
 197 investigated is provided in Sup. Mat. 1. The mean, maximum, minimum and stan-  
 198 dard deviation of environmental variables were computed for each grid cell ( $n =$   
 199 6465).

### 200 2.3. Methods

201 The general workflow used in this study is presented in Fig. 3. Model reporting  
 202 was done following recommendations by Zurell et al. (2020).

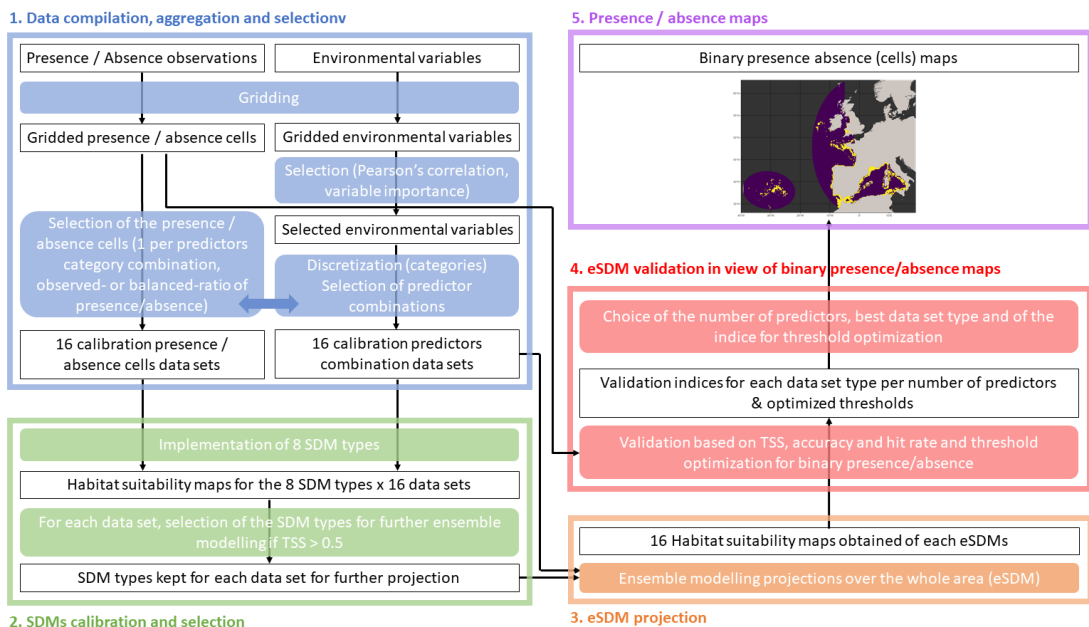


Figure 3: General workflow of the procedure used for identifying blackspot seabream habitats: (1) compilation, gridding and selection of environmental and occurrence data, (2) statistical Species Distribution Models (SDM) calibration (for each category) and selection, (3) Projection of the ensemble (eSDM) model (habitat suitability map), (4) Validation of projections based on maximization of various indices and determination of threshold value for (5) binary presence/absence mapping.

203    2.3.1. Study area

204    Three regions were modelled corresponding to the three main areas of distribution  
205    of the blackspot seabream: The Northeast Atlantic shelf, the Azorean region and the  
206    western Mediterranean basin (Fig. 2). A spatial grid of  $0.1^\circ \times 0.1^\circ$  cells (44851 in  
207    total) was created covering the three regions. This resolution was chosen accounting  
208    for the need for local and general overviews of species habitat, as well as computation  
209    time.

210    2.3.2. Occurrence data compilation, gridding and selection

211    For each grid cell with data ( $n = 6465$ ), the number of presence and absence  
212    records was counted. The occurrence data set displayed over- and under-sampled  
213    areas (Fig. 2). In order to take into account this heterogeneity, occurrence records  
214    were compiled into presence/absence records: cells with at least one presence were  
215    considered as presence cells, cells with only absence records were considered as ab-  
216    sence cells and the remaining cells were considered as non-sampled cells and were not  
217    used for model fitting. In order to maintain an homogeneous distributions of sam-  
218    pled cells along environmental gradients, continuous environmental variables were  
219    discretised into 60 classes each (which appeared to be a good compromise to create  
220    relevant classes for all environmental variables) over the whole grid domain. When  
221    a given combination of environmental variable classes corresponded to several pres-  
222    ence cells, only one presence cell was kept, similarly for absence cells. When a given  
223    combination corresponded to several presence and absence cells, one presence and  
224    one absence cell was kept. Thus the number of data points used for model fitting  
225    depended on the environmental predictors included in a particular model (Table 2).

226    Since the ratio between the number of presence and absence grid cells still varied  
227    among regions after the gridding process, two approaches were tested. In the first  
228    case (observed-ratio data set), all available presence / absence grid cells were kept  
229    in the next steps of the analysis. In the second case (balanced-ratio data set), the  
230    same number of absence and presence grid cells was used for all regions by randomly  
231    selecting absence grid cells among all available absence cells. The second approach  
232    corresponds to the common practice for presence-only data for which pseudo-absence

233 data are created (Montgomery, 2005)(See Fig. 3, step 1).

234 *2.3.3. Selection of environmental predictors*

235 Given the observation of heterogeneous responses to some of the environmental  
236 variables according to the region (Azores, Atlantic shelf and Mediterranean Sea, see  
237 Sup. Mat. 2), a categorical predictor was added for region. To identify the most par-  
238 simonious environmental data set explaining the blackspot seabream distribution,  
239 pairwise correlations between all environmental variables were investigated with a  
240 Pearson's correlation test using as correlation threshold  $r > 0.7$  (Schickele et al.,  
241 2020; Dormann et al. 2013). When several environmental variables were highly cor-  
242 related, we retained the environmental variable with the highest relative importance  
243 (Schickele et al., 2020; Leroy et al., 2014)(Sup. Mat. 3). As the previous selection  
244 step led to a high number (9) of remaining environmental predictors for both occur-  
245 rence data sets, multiple models were fitted with decreasing number of predictors  
246 (9 to 2 predictors), removing sequentially the predictor with the smallest relative  
247 importance to balance model fit and model complexity (Meynard et al., 2019) (See  
248 Fig. 3, step 1). Next, for each of the eight combinations of predictors and each  
249 occurrence data set type (observed-ratio and balanced-ratio), one occurrence data  
250 set was created for calibration (16 data sets).

251 *2.3.4. Species distribution model categories and settings*

252 The following eight SDM categories were implemented in R using the BIOMOD2  
253 package (Thuillier et al., 2003;2016) with default parameter settings: generalised lin-  
254 ear model (GLM), generalised boosting model (GBM), generalized additive model  
255 (GAM), artificial neural network (ANN) model, flexible discriminant analysis (FDA),  
256 random forest (RF), classification tree analysis (CTA) and surface range envelope  
257 (SRE) model (Valanis et al., 2008; Thuiller et al., 2009; Albouy et al., 2012; Clair-  
258 baux et al., 2019; Pecchi et al., 2019). For each SDM category and data set, a 3-fold  
259 cross validation procedure was performed.

260    2.3.5. *SDM category selection and compromise*

261    We used the True Skill Statistics index (TSS, Allouche et al., 2006) to quantify  
262    the performance of each of the eight fitted SDMs for each calibration data set (See  
263    Fig. 3, step 2). It was calculated as  $TSS = \text{sensitivity} + \text{specificity} - 1$ . A SDM was  
264    selected for ensemble modelling if it had  $TSS > 0.5$ . A compromise (the ensemble  
265    Species Distribution Model, eSDM) of the presence probability was then calculated  
266    as the mean of probabilities of retained SDMs weighted by their TSS value. Presence  
267    probability uncertainty was quantified using the coefficient of variation from cross-  
268    validation results. Individual SDM response curves to environmental predictors as  
269    well as the eSDM resulting presence probabilities according to the different predictors  
270    (Schickele et al., 2020) are presented in Sup. Mat. 4 and 5.

272    2.3.6. *Binary habitat maps and predictors selection*

273    To define habitat suitability maps, for each of the 16 calibrated ensemble models  
274    (2 data sets x 8 predictors combination with 2 to 9 predictors), presence probabilities  
275    were projected over the whole domain, including the cells not included in the cali-  
276    bration process (extrapolation for the non sampled cells). Then, in order to create  
277    binary presence/absence maps, the habitat suitability maps (presence probabilities)  
278    were compared to all observed presence and absence compiled cells (not only those  
279    used for model fitting). Threshold values for binary projections of presence and  
280    absence were calculated based on a set of indices as recommended by Robinson et  
281    al. (2017), namely the hit rate (proportion of correctly classified presence cells),  
282    the True Skill Statistics (TSS, Allouche et al., 2006), the CBI (computed with the  
283    ecospat.boyce function of the ecospat package on R, Hirzel et al. 2006), and the  
284    overall accuracy (sum of the proportion of correctly classified presence and absence  
285    cells, Allouche et al., 2006). More precisely, each validation index was maximized  
286    varying threshold values for binary projections of presence and absence (from 0 to 1  
287    with a 0.001 interval) with the optimize function in R. Each maximized index value  
288    thus corresponded to a distinct optimized threshold value.

289    For each data set type, the best calibrated eSDM was chosen as the one showing

the lowest number of predictors and the highest validation index values. To combine validation index values, their values were re-scaled between 0 (lowest index value obtained across eSDM outputs with 2-9 predictors) and 1 (highest index value). In the case of the balanced-ratio data set, as absence cells selection might have impacted ensemble model performance in the previous steps, 10 data sets with the chosen number of predictors and varying absence cells were randomly selected and the average of habitat suitability maps (re-calibration) was used for further validation. Lastly, for each data set type and validation index, the surface of potential habitat was calculated.

### 3. Results

#### 3.1. Data characteristics

In total, 106 457 occurrence records were compiled, among which 6465 presence records, corresponding to 782 cells where the species was present and 5683 cells where it was recorded as absent (Fig. 2, Table 1).

Table 1: Summary of blackspot seabream occurrence data by region. Domain per region as in Fig. 2. Records correspond to point observations of presence or absence of the species while cells correspond to grid cells of the domain where one or several presence or absence point observation was made. One presence observation was sufficient to qualify as presence cells.

	Total area records	Atlantic		Azores		Mediterranean		
	cells	rec./cell	records	cells	rec./cell	records	cells	rec./cell
N presence	6928	782	8.8	639	389	1.6	4872	165
Proportion		1.7 %			1.7 %		29.5	228
N absence	99529	5683	17.5	74556	4626	16.1	13906	376
Proportion		12.7 %			20 %		4%	5.6 %
N sampled	106457	6465	16.5	75196	5015	15	18778	541
Proportion		14.4 %			21.6 %		5.8 %	7.4%
N presence / N sampled	6.5 %	<b>12 %</b>	0.8 %	<b>7.8 %</b>		25.9 %	<b>30.5 %</b>	11.4 %
N cells per region		44851		23209			9392	12250

The proportion of presence cells among sampled cells was highly heterogeneous between regions, as well as the number of records per cell (respectively 7.8 to 30.5 % and 14 to 35 records per cell, see Table 1).

#### 3.2. eSDM outputs and habitat suitability maps

After predictor selection using pairwise correlation analysis, nine predictors were retained for the ensemble modelling procedure: region (NE Atlantic, Azores, Mediter-

310 ranean Sea), sea bottom type, mean and standard deviation of bathymetry (m), an-  
311 nual maximum Sea Surface Temperature (SST, °C), annual mean and minimum ab-  
312 solute current velocity ( $\text{m.s}^{-1}$ ), annual standard deviation of salinity (%) and annual  
313 standard deviation of bottom temperature (°C) (Sup. Mat. 3). Mean bathymetry  
314 and maximum SST had the highest explanatory power for both data sets, both vari-  
315 ables contributing equally (Table 2). The main difference between ensemble models  
316 for the two data set types was that for the observed-ratio data set (heterogeneous  
317 ratios of presence and absence over the model domain), the categorical predictor "re-  
318 gion" had a high relative importance, which was not the case for the balanced-ratio  
319 data set (balanced number of presence and absence grid cells in each region) (Table  
320 2, Sup. Mat. 6).

321 SDM categories ANN, GBM and RF were selected in most cases ( $\text{TSS} > 0.5$ ),  
322 while the selection of the other SDM categories varied according to the number of  
323 predictors and the data set type used (Table 2, Sup. Mat. 6). TSS values were higher  
324 for the observed-ratio data set for all models (two to nine predictors), with values  
325 around 0.7 for the balanced-ratio data set, and around 0.9 for the observed-ratio data  
326 set (Table 2, Sup. Mat. 6). As a result of the data selection procedure, the data set  
327 size decreased with decreasing number of predictors, leading to low data set sizes  
328 for models with less than five predictors (Table 2). Comparing projected habitat  
329 suitability maps (presence probabilities per grid cell over the whole domain) between  
330 data set types, it appeared that a balanced ratio between presence and absence  
331 data led to overall higher presence probabilities and hence a much wider potential  
332 habitat in the NE Atlantic region and in the Mediterranean Sea region compared to  
333 the results obtained with the observed-ratio data set, while the projected presence  
334 probabilities appeared rather similar for the Azores region (Figs. 4 and 5). The  
335 visual difference was confirmed by the mean projected presence probability over the  
336 whole domain being  $0.16 \pm 0.19$  for the balanced-ratio data set and only  $0.07 \pm 0.09$   
337 for the observed-ratio data set (Fig. 4).

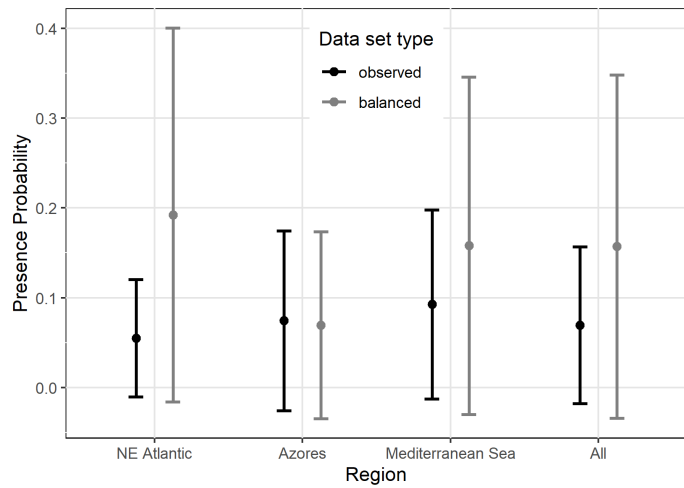


Figure 4: Presence probabilities (mean and sd) of the blackspot seabream per region and on the whole grid according to the data set type used for ensemble species distribution modelling with 6 predictors.

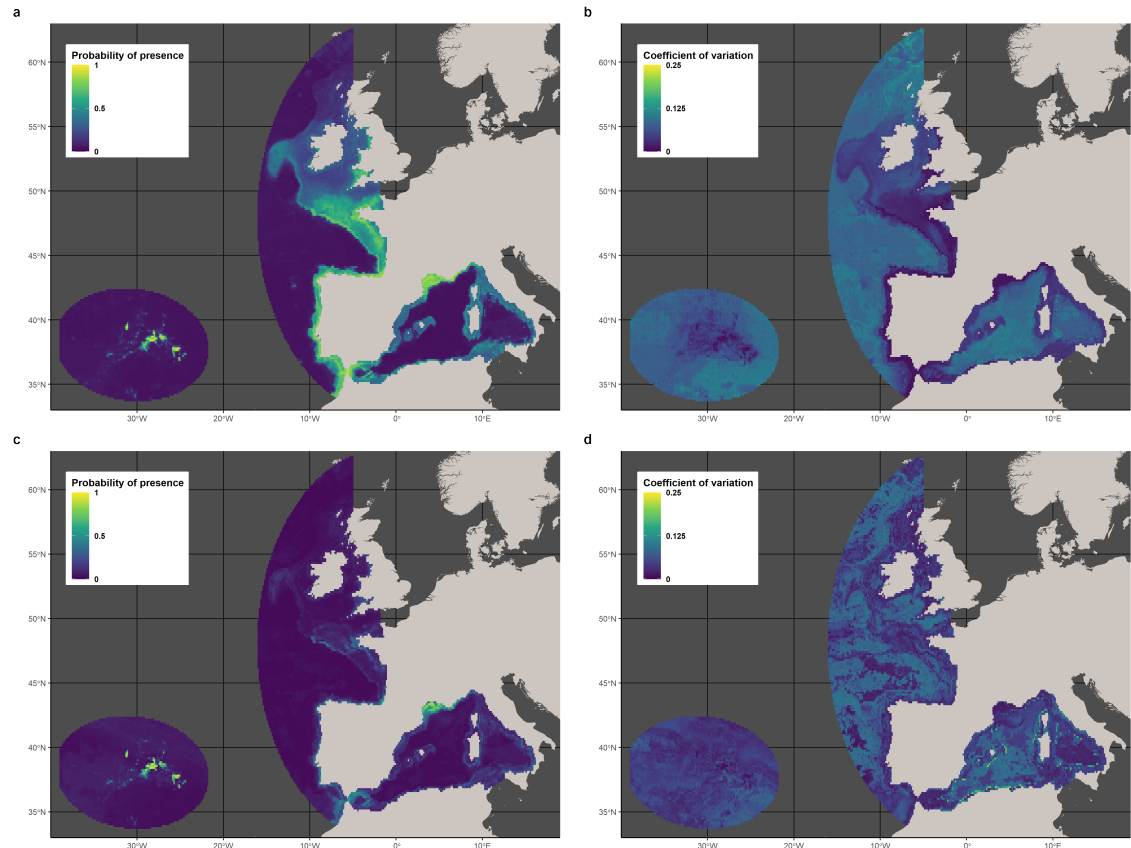


Figure 5: Habitat suitability maps for blackspot seabream for the main distribution area (a, c) and associated coefficients of variation (b, d) obtained with an ensemble species distribution model performed using a data set with a balanced number of presence and absence data (balanced-ratio, a, b) and a data set with the observed and heterogeneous number of presences and absences (observed-ratio, c, d), for models including six predictors (see Table 2 and Sup. Mat. 6).

Table 2: Summary of the 16 calibrated ensemble species distribution models implemented in this study with 8 different numbers of predictors for the observed-ratio data set type; predictors used and their relative importance (proportion of explained variance), characteristics of the data set used, SDMs included in eSDM and overall performance.

	2 predictors	3 predictors	4 predictors	5 predictor	6 predictors	7 predictors	8 predictors	9 predictors
<b>Environmental variables' importance</b>								
Mean bathymetry	50%	49 %	50%	37%	30%	31%	26%	27 %
Max SST	50%	34%	18%	25%	31%	25%	27%	26%
Sd bathymetry	-	17%	18%	20%	18%	16%	12%	11%
Sd bottom temperature	-	-	-	8%	8%	9%	7 %	8%
Sd salinity	-	-	-	-	5%	6 %	5 %	5 %
Min current velocity	-	-	-	-	-	3%	4%	2%
Mean current velocity	-	-	-	-	-	-	-	2 %
Sea bottom type	-	-	-	-	-	-	1%	1%
Region	-	-	11%	13 %	9%	10%	18%	17%
<b>Occurrence data set</b>								
Data set size	474	1510	1696	2620	3280	3357	3752	4163
Number of presence cells	8	161	161	372	470	475	536	576
Number of absence cells	466	1349	1535	2248	2810	2882	3216	3587
<b>SDM types and eSDM performance</b>								
Selected models (TSS > 0.5)	ANN, FDA, GAM, GBM, GLM, RF	ANN, CTA, FDA, GAM, GLM, RF	ANN, CTA, FDA, GBM, GLM, RF	ANN, GBM, GLM, RF	ANN, GBM, RF	ANN, GBM, RF	ANN, GBM, RF	ANN, GBM, RF
True Skill Statistic (mean $\pm$ sd across SDMs)	0.996 $\pm$ 0.003	0.791 $\pm$ 0.013	0.826 $\pm$ 0.013	0.867 $\pm$ 0.033	0.916 $\pm$ 0.030	0.895 $\pm$ 0.039	0.904 $\pm$ 0.043	0.894 $\pm$ 0.053

338 Differences between projected presence probabilities obtained with the balanced-  
 339 ratio data set and the observed-ratio data set were the highest in the NE Atlantic  
 340 (with respective values of  $0.19 \pm 0.21$  and  $0.06 \pm 0.07$ ) and the lowest in the Azores  
 341 (with both values equal to  $0.07 \pm 0.10$ ) (Fig. 4). For both data set types, coefficients  
 342 of variation of presence probabilities did not exceed 0.25 (Fig. 5).

343 Overall, the choice of data set type impacted presence probability values, but  
 344 did not impact consistently which predictors were selected, except for the region  
 345 predictor, nor the general shape of the response curve for each predictor, except for  
 346 maximum annual SST for which the relationship was dome-shaped for balanced-  
 347 ratio data set and more flat for the observed-ratio data set (Table 2 and Sup. Mat.  
 348 4).

### 349 3.3. Binary habitat maps

#### 350 3.3.1. Predictors

351 Comparison of the three validation index values between eSDMs using 2 to 9  
 352 predictors normalized between 0 and 1 (0 being the smallest index value across the  
 353 set of predictors and 1 being the highest) led to select the eSDM with six predictors  
 354 for both data set types. Indeed, these models displayed among the best index values  
 355 for the smallest number of predictors (Fig. 6).

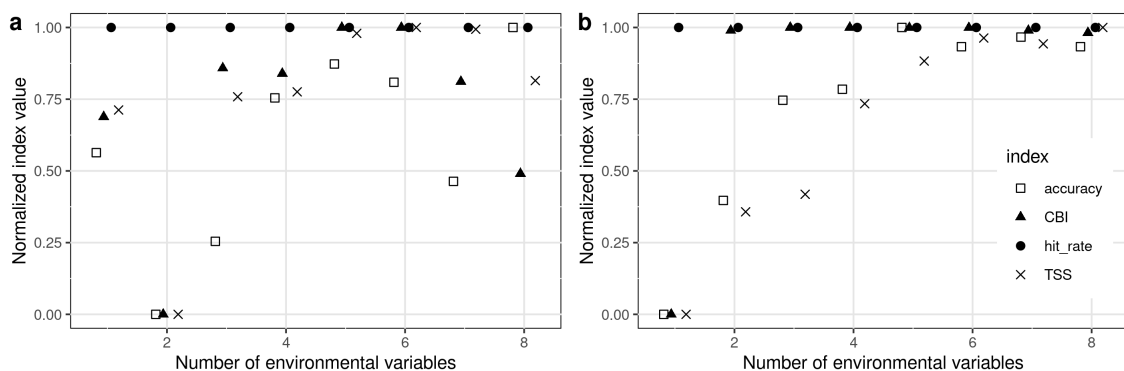


Figure 6: Normalized values of validation indices (accuracy, Allouche et al., 2006; hit rate, Allouche et al., 2006; True Skill Statistics, Allouche et al., 2006, Continuous Boyce Index, Hirzel et al. 2006) of the models according to the number of predictors used, for the balanced-ratio data set type (same number of absences and presences cells) (a) and the observed-ratio data set type (all records) (b).

356 The best predictors for the balanced-ratio data set were mean bathymetry, annual  
 357 maximum SST, standard deviation (sd) of bathymetry, sd of mean annual bottom

358 temperature, sd of mean annual bottom salinity and minimum annual absolute cur-  
 359 rent velocity. For the observed-ratio data set, predictor region was selected instead  
 360 of minimum annual absolute current velocity (Table 2, Sup. Mat. 6). The region  
 361 predictor had a 9% contribution to the explained variance and, compared to the  
 362 balanced-ratio data set, contribution of other variables was lower for bathymetry  
 363 and higher for all other variables.

364 *3.3.2. Indices and threshold optimization*

365 Validation index values (accuracy, hit rate, CBI and TSS) were slightly higher  
 366 for the observed-ratio data set than for the balanced-ratio data set (Sup. Mat. 8).  
 367 Variations in estimated habitat area between validation indices were higher than  
 368 between data set types (Fig. 7). Overall, the choice of threshold value used for  
 369 transforming presence probabilities into binary habitat maps strongly influenced  
 370 results for the whole area and for each of the regions (Fig. 8). For regional habitat  
 371 area estimation, separate threshold values were obtained by maximising index values  
 372 regionally. Maximizing the hit rate led to the lowest threshold values for the whole  
 373 area and each region, and subsequently the largest habitat areas.

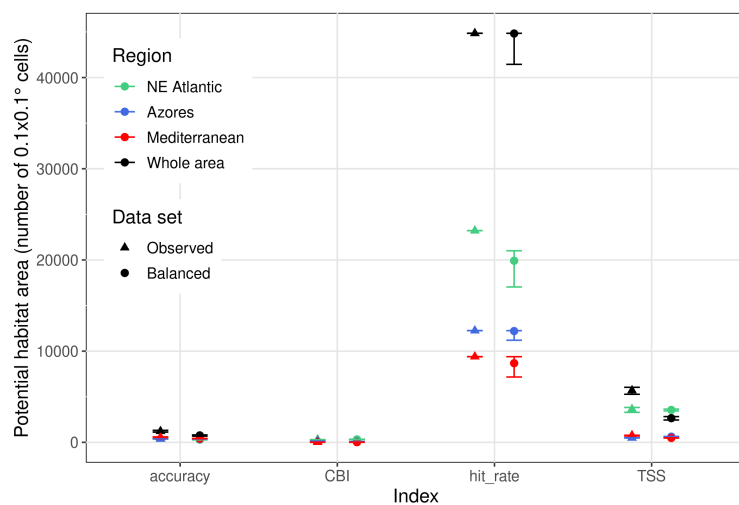


Figure 7: Blackspot seabream potential habitat area using the best model (6 predictors) and different validation indices for setting the presence/absence threshold value: accuracy, hit rate, Continuous Boyce Index and True Skill Statistics. Results for observed- and balanced-ratio data sets, when models were optimized for the whole model domain (black), the NE Atlantic region (green), the Azores region (blue), the Mediterranean Sea region (red).

374 CBI and accuracy led to the smallest habitat areas, especially for the NE Atlantic

375 region for which the observed presence / absence ratio was low. For the whole area,  
 376 averaged across the two data types, the habitat areas for hit rate and TSS were  
 377 14849% and 1280% larger than for CBI respectively. Comparing results between the  
 378 two data sets showed that the balanced data set led to smaller habitat areas for the  
 379 majority of indices for the whole area and each of the three regions (Figs. 7 and 8).  
 380 For the whole area, the difference ((balanced-observed)/observed) ranged between  
 381 -53% for TSS and 4% for CBI. For the Azores the difference ranged between -3% for  
 382 accuracy and 27% for TSS, for the Mediterranean Sea between -36% for TSS and  
 383 0% for CBI, and for the NE Atlantic region between -28% for accuracy and 23 %  
 384 for CBI. Thus, the choice of validation index had a much greater impact than the  
 385 data set type, though the later was also important for certain indices.

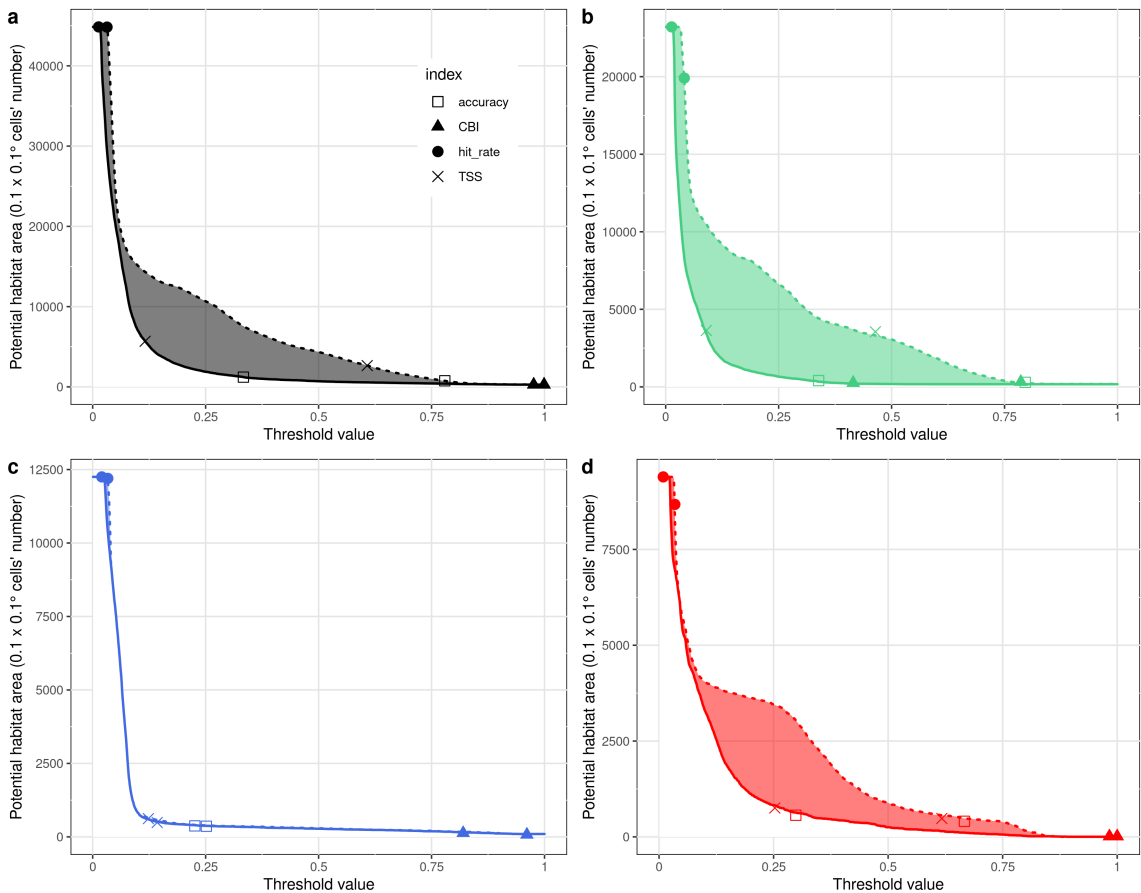


Figure 8: Area of the potential habitat of the blackspot seabream as a function of the threshold value used for binary presence/absence predictions for the balanced-ratio data set (dotted line) and the observed-ratio data set (solid line) and results obtained using different validation indices (accuracy, hit rate, CBI and TSS) for the whole area (a), NE Atlantic region (b), Azores region (c) and Mediterranean Sea region (d).

386    3.3.3. *Binary habitat maps*

387    Visual comparison of binary (presence / absence) habitat maps (threshold opti-  
388    mized according to TSS index) between data set types showed that for the balanced-  
389    ratio data set some locations from which the species had been reported were missed,  
390    particularly to the West of Ireland and along the Mediterranean coast (Figs. 2 and  
391    9). Overall, it appears that the potential habitat of the species covers a large area  
392    around seamounts in the Azores region, a wide area on the NE Atlantic shelf and a  
393    narrower are on the Mediterranean shelf (Fig. 9).

394    **4. Discussion**

395    In this study, to obtain robust estimates of the potential habitat of blackspot  
396    seabream across its wide distribution area exhibiting varying exploitation status, an  
397    ensemble species distribution modelling approach and two data sets with different  
398    prevalence levels were used. The identified potential habitats included islands con-  
399    tours and seamounts in the Azores region, the NE Atlantic shelf south of 48°N, with  
400    smaller areas further North, and the Northern shores of the western Mediterranean  
401    Sea, with more extended areas in the Strait of Gibraltar, in the Gulf of Lions and  
402    along the Italian coast.

403    Potential habitats of blackspot seabream were best explained by bathymetry  
404    (down to 700 - 1000 m) and SST (annual maximum SST generally greater than  
405    16°C), as well as bottom temperature, salinity and region as secondary predictors,  
406    independent of the prevalence level in the data set except for region. Further, the  
407    general shape of the response curves for each predictor were similar for the two data  
408    sets except for max SST (see response curves in Sup. Mat. 4). Other studies have  
409    reported the same main factors influencing the species' distribution and abundance,  
410    with occurrences reported in areas with bottom depths between 100 m and 700 m  
411    (Mytilineou et al., 2014; Burgos et al., 2013; Menezes et al., 2013; D'Onghia et  
412    al., 2010; Gueguen, 1974) and environmental conditions linked to temperature and  
413    salinity influencing stock variations (Sanz-Fernandez et al., 2019).

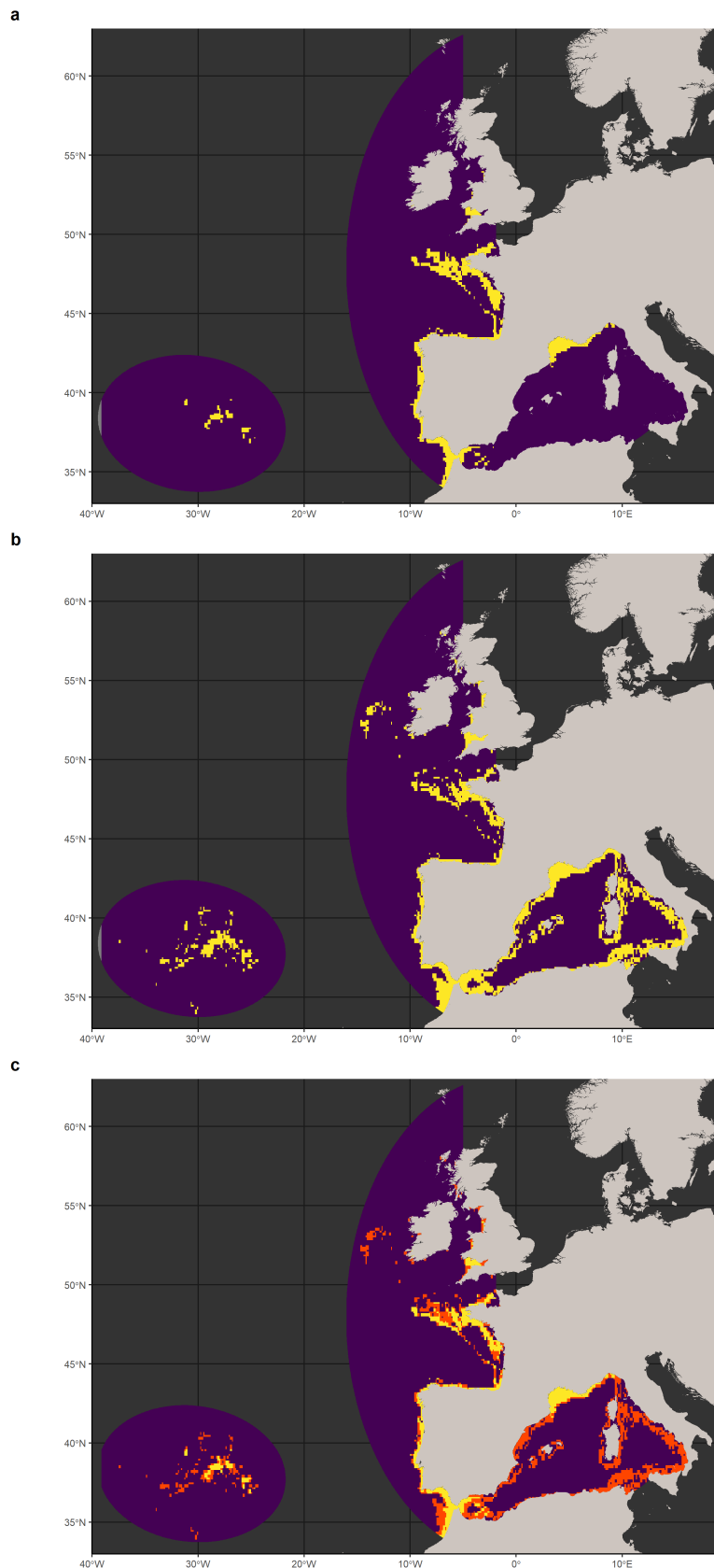


Figure 9: Map of estimated potential habitats with six predictors (yellow) for blackspot seabream over its whole area of distribution using the balanced-ratio data (a) or the observed-ratio data set (b) maximizing the TSS index for presence threshold estimation, and difference between the two potential habitat maps (c, red).

414 The general importance of the region predictor can be explained by regional  
415 differences in biophysical conditions while the difference in importance of this pre-  
416 dictor for the two prevalence data sets is most likely caused by differences in the  
417 prevalence in the observed-ratio data sets (Table 2). These regional discrepancies  
418 in prevalence might be explained by the differences in population status, with the  
419 Northeast Atlantic population being most depleted. It is less likely caused by dif-  
420 ferences in detectability by the employed sampling methods, which could however  
421 be explored by comparing several methods for the same area and using models in-  
422 tegrating detectability (Fithian et al., 2015; Fletcher et al., 2016; 2019).

423 In the Bay of Biscay, which is in the center of the Northeast Atlantic region, the  
424 eSDM suggested that the potential habitat covered a large part of the continental  
425 shelf. Indeed, the species used to occur over most of this shelf before the population  
426 collapsed in the late 1970s. In the Azorean region, which has been termed an  
427 oceanic seamount ecosystem (Silva and Pinho, 2007), the species occurs around  
428 islands, with juveniles distributed in near coast habitats as in the Bay of Biscay  
429 and adults spread from the coast to island slopes and isolated seamounts; juveniles  
430 never occur at sea mounts (Pinho et al., 2014). Depth was identified as the main  
431 factor for explaining blackspot seabream abundance and size composition on Azorean  
432 seamounts (Santos et al., 2021). In the same area, Morato et al. (2001) showed that  
433 the species feeds on both pelagic and benthic preys and suggested that its food supply  
434 on seamounts may depend upon oceanic production that drifts past seamounts,  
435 which in turn makes bottom slope a factor for the species distribution as current  
436 strength and therefore the amount of prey advected increase with slope. At the scale  
437 of the environment perceived by individual fish, similar hydrological conditions,  
438 in particular strong and variable tidal currents resulting from the interaction of  
439 oceanic water masses (Koslow, 1996; Lorance et al. 2002) prevail at seamounts  
440 and along the continental slope, where blackspot seabream also occurs. At this fine  
441 scale, the species shows diel vertical migrations (Afonso et al., 2012), which may  
442 suggest a behavior similar to that of deeper living "seamount aggregators" which  
443 share with blackspot seabream a high lipid content and strong swimming abilities,  
444 which are both related to high metabolism (Koslow, 1996). Overall, the habitat

characteristics of fish displaying this type of behavior include sloping sea bottom and related variations in current speed, which generate also temperature variations and is in-line with habitats variables found to be predictors of *blackspot seabream* presence-absence in this study.

The ratio between presence and absence cells in the data impacted strongly the projected probabilities of presence. Imposing a balanced-ratio between the number of presence and absence cells for model calibration led to higher presence probabilities on average compared to using the observed-ratio data set with a large majority of absence cells ( $0.16 \pm 0.19$  and  $0.07 \pm 0.09$  respectively). Thus, including primarily absence cells in model calibration reduced estimated presence probabilities.

The habitat suitability map for the balanced-ratio data set indicated wide potential habitats over the NE Atlantic shelf and along the western Mediterranean and Azores coasts, while potential habitats were smaller using the observed-ratio data set. The habitat size was reversed between the two data sets for the corresponding presence/absence maps, with larger binary habitats for the observed-ratio data set due to a smaller optimized threshold value. These binary maps obtained by applying a optimized presence probability threshold are probably closer to the realised habitat of the species as it involved the full presence/absence data to set the threshold values. The binary presence habitat was notably smaller over the European shelf, where one regional population is depleted. The past high abundance of the species throughout the Bay of Biscay (Olivier, 1928; Desbrosses, 1932; Guichet et al., 1971) indicates that this area was suitable for the species 100 to 50 years ago. The increase of fishing effort on the species at the same period (Lorance, 2011) must indeed have been the main trigger for the species' decreased abundance, leading to a concentration of the remaining individuals into the most suitable habitats in this region (along the coast around isobath -100m and on the continental slope). The present study suggests that current environmental factors remain suitable for the species, although environmental changes have occurred since, notably a temperature rise of  $0.2^{\circ}\text{C}/\text{decade}$  for the period 1965 - 2004 in the 0 - 200 m water column layer (Michel et al., 2009, Valencia et al., 2019). The observed presence-absence ratio data set had higher validation indices for the fitted model compared to the

balanced ratio data set. Further, the corresponding binary habitat map included more areas outside the sampled area. For example, it predicted the species' presence close to the West of Ireland, where the species did indeed occur in the past (Guégen, 1974) and more widely along the western Mediterranean coast where it is present nowadays (Spedicato et al., 2002).

The use of different validation indices (hit rate, TSS, CBI and accuracy) led to different threshold values for transforming the probability of presence into binary habitat and subsequently different habitat surface areas. Overall, the difference in the size of estimated habitat area was larger between validation indices when between data set types. Differences in predicted habitat areas according to the selected thresholding method have been reported by various authors (Nenzen and Araujo, 2011; Jimenez-Valverde and Lobo, 2007; Liu et al., 2005; 2016). In our case, given the species' low prevalence, absence cell records had a large impact on the estimated threshold when maximizing using the accuracy index, leading to habitats mostly restrained to the cells where species observations had been made, hence being closer to the (only partial) observed distribution. Although its use has been recommended in the case of unbalanced prevalence (Leroy et al., 2018), the use of the CBI index led to the same effect. In contrast, using the TSS index for setting the probability threshold value involved balancing correct predictions of both presence and absence cells, and hence seemed more likely to lead to binary habitats closer to the species' potential habitats.

The difference between habitat areas derived using TSS optimized threshold values for balanced and observed unbalanced data sets depended strongly on the region used for optimization. The largest negative difference was observed for the whole area (-53%), while it was negligible (-2%) for the NE Atlantic region and positive (27%) for the Azores. Unbalanced prevalence has been reported to artificially increase the TSS value (Leroy et al., 2018), which implies that the balanced data set should have provided a better understanding of blackspot seabream potential habitats. Contrary to this expectation it seems that in our case using a bigger data set with unbalanced presence/absence cells was more informative than using a smaller data set with a selected number of balanced presence/absence cells.

507 Several studies have shown that the use of presence-true absence data are gen-  
508 erally better than presence-only data with or without using pseudo absences, and  
509 that presence-only models generally under-estimate the species' presence in loca-  
510 tions where it has not been sampled (Dorazio, 2014; Meynard et al., 2019; Wisz  
511 and Guisan, 2009). Our study is in accordance with this general result. In addition  
512 it showed that the proportion of absences data matters. The difference between  
513 the estimated area of the blackspot seabream potential habitat obtained with the  
514 observed-ratio data set and the balanced-ratio data set for the same threshold value  
515 increased with the decreasing proportion of presence data in the observed data, from  
516 the Azores to the NE Atlantic, which in turn corresponds to decreasing stock status  
517 of blackspot seabream. In summary, the results of this study provided evidence that  
518 when using opportunistic data for SDM fitting attention needs to be paid to the  
519 effects of presence/absence data imbalance as well as the choice of validation indices  
520 to fully evaluate uncertainty of estimated habitat maps.

## 521 Acknowledgement

522 The study received financial support from France Filière Pêche (project DynRose)  
523 and the European Union's Horizon 2020 research and innovation programme under  
524 Grant Agreement No 773713 (PANDORA).

## 525 References

- 526 Afonso, P., Graça, G., Berke, G., Fontes, J., 2012. First observations on seamount  
527 habitat use of blackspot seabream (*Pagellus bogaraveo*) using acoustic telemetry. *J.  
528 Exp. Mar. Bio. Ecol.* 436–437, 1–10. <https://doi.org/10.1016/j.jembe.2012.08.003>
- 529 Afonso, P., McGinty, N., Graça, G., Fontes, J., Inácio, M., Totland, A., Menezes, G.,  
530 2014. Vertical migrations of a deep-sea fish and its prey. *PLoS One* 9. <https://doi.org/10.1371/journal.pone.0097884>
- 531 Albouy, C., Guilhaumon, F., Araújo, M.B., Mouillot, D., Leprieur, F., 2012. Com-  
532 bining projected changes in species richness and composition reveals climate change  
533 impacts on coastal Mediterranean fish assemblages. *Glob. Chang. Biol.* 18,  
534 2995–3003. <https://doi.org/10.1111/j.1365-2486.2012.02772.x>

- 536 Allouche, O., Tsoar, A., Kadmon, R., 2006. Assessing the accuracy of species distri-  
537 bution models: Prevalence, kappa and the true skill statistic (TSS). *J. Appl. Ecol.*  
538 43, 1223–1232. <https://doi.org/10.1111/j.1365-2664.2006.01214.x>
- 539 Burgos, C., Gil, J., Del Olmo, L.A., 2013. The Spanish blackspot seabream (*Pagellus*  
540 *bogaraveo*) fishery in the Strait of Gibraltar: Spatial distribution and fishing effort  
541 derived from a small-scale GPRS/GSM based fisheries vessel monitoring system.  
542 *Aquat. Living Resour.* 26, 399–407. <https://doi.org/10.1051/alr/2013068>
- 543 Clairbault, M., Fort, J., Mathewson, P., Porter, W., Strøm, H., Grémillet, D., 2019.  
544 Climate change could overturn bird migration: Transarctic flights and high-latitude  
545 residency in a sea ice free Arctic. *Sci. Rep.* 9. [https://doi.org/10.1038/s41598-019-54228-5](https://doi.org/10.1038/s41598-019-<br/>546 54228-5)
- 547 Crisp D.J., Southward A.J., Southward E.C., 1981. On the distribution of the inter-  
548 tidal barnacles *Chthamalus stellatus*, *Chthamalus montagui* and *Euraphia depressa*.  
549 *J Mar Biol Assoc UK* 61:359–380
- 550 D’Onghia, G., Maiorano, P., Carlucci, R., Capezzuto, F., Carluccio, A., Tursi, A.,  
551 Sion, L., 2012. Comparing Deep-Sea Fish Fauna between Coral and Non-Coral  
552 “Megahabitats” in the Santa Maria di Leuca Cold-Water Coral Province (Mediterranean  
553 Sea). *PLoS One* 7. <https://doi.org/10.1371/journal.pone.0044509>
- 554 D’Onghia, G., Maiorano, P., Sion, L., Giove, A., Capezzuto, F., Carlucci, R., Tursi,  
555 A., 2010. Effects of deep-water coral banks on the abundance and size structure of  
556 the megafauna in the Mediterranean Sea. *Deep. Res. Part II Top. Stud. Oceanogr.*  
557 57, 397–411. <https://doi.org/10.1016/j.dsr2.2009.08.022>
- 558 Dardignac, J., 1988. Les pêcheries du Golfe de Gascogne, bilan des connaissances.  
559 Plouzané, IFREMER, 204 pp.
- 560 Desbrosses, P., 1932. Poissons de chalut - la dorade commune (*Pagellus centrodonthus*  
561 Delaroche) et sa pêche. *Rev. des Trav. l’Office des Pêches Marit.* 5, 167–222.
- 562 Dorazio, R.M., 2014. Accounting for imperfect detection and survey bias in sta-  
563 tistical analysis of presence-only data. *Glob. Ecol. Biogeogr.* 23, 1472–1484.  
564 <https://doi.org/10.1111/geb.12216>

- 565 Dormann, C.F., Elith, J., Bacher, S., Buchmann, C., Carl, G., Carré, G., Marquéz,  
566 J.R.G., Gruber, B., Lafourcade, B., Leitão, P.J., Münkemüller, T., McClean, C., Os-  
567 borne, P.E., Reineking, B., Schröder, B., Skidmore, A.K., Zurell, D., Lautenbach, S.,  
568 2013. Collinearity: A review of methods to deal with it and a simulation study eval-  
569 uating their performance. *Ecography* (Cop.). 36, 27–46. <https://doi.org/10.1111/j.1600-0587.2012.07348.x>
- 571 Elith, J., Leathwick, J.R., 2009. Species distribution models: Ecological explanation  
572 and prediction across space and time. *Annu. Rev. Ecol. Evol. Syst.* 40, 677–697.  
573 <https://doi.org/10.1146/annurev.ecolsys.110308.120159>
- 574 Erzini, K., Salgado, M., Castro, M., 2006. Dynamics of black spot sea bream (*Pag-*  
575 *ellus bogaraveo*) mean length: Evaluating the influence of life history parameters,  
576 recruitment, size selectivity and exploitation rates. *J. Appl. Ichthyol.* 22, 183–188.  
577 <https://doi.org/10.1111/j.1439-0426.2006.00702.x>
- 578 FAO-GFCM, 2021. Fisheries and aquaculture statistics. GFCM Catches 1970–2019  
579 (FishstatJ). In: FAO Fisheries Division [on-line]. Rome. 2021 update. <https://www.fao.org/fishery/statistics/software/fishstatj/en>
- 581 Fithian, W., Elith, J., Hastie, T., Keith, D.A., 2015. Bias correction in species dis-  
582 tribution models: Pooling survey and collection data for multiple species. *Methods*  
583 *Ecol. Evol.* 6, 424–438. <https://doi.org/10.1111/2041-210X.12242>
- 584 Fletcher, R.J., Hefley, T.J., Robertson, E.P., Zuckerberg, B., McCleery, R.A., Dor-  
585 razio, R.M., 2019. A practical guide for combining data to model species distribu-  
586 tions. *Ecology* 100, 1–15. <https://doi.org/10.1002/ecy.2710>
- 587 Fletcher, R.J., McCleery, R.A., Greene, D.U., Tye, C.A., 2016. Integrated models  
588 that unite local and regional data reveal larger-scale environmental relationships  
589 and improve predictions of species distributions. *Landsc. Ecol.* 31, 1369–1382.  
590 <https://doi.org/10.1007/s10980-015-0327-9>
- 591 Francis, R.I.C.C., Clark, M.R., 2005. Sustainability issues for orange roughy fish-  
592 eries. *Bull. Mar. Sci.* 76, 337–351.
- 593 Gleason, H.A., 1926. The individualistic concept of plant association. *Bull. Torrey*  
594 *Bot. Club* 53, 7–26.

- 595 Guéguen, J. 1969. Croissance de la dorade, *Pagellus centrodontus* Delaroche. Revue  
596 des Travaux de l'Institut des Pêches Maritimes, 33: 251–264.
- 597 Gueguen, J., 1974. Précisions sur les migrations de la dorade rose *Pagellus Bogaraveo*  
598 (Brannich 1768). Sci. Pêche 237, 1–10.
- 599 Guichet, R., Guéguen, J., Guillou, A., 1971. La pêche du merlu et de la dorade à  
600 La Rochelle, analyse des statistiques d'effort de pêche et de production des années  
601 1966, 1967 et 1968. Rev. Trav. Inst. Pêches marit. 35, 239–286.
- 602 Guisan, A., Thuiller, W., 2005. Predicting species distribution: Offering more than  
603 simple habitat models. Ecology Letters 8 (9), pp. 993–1009. <https://doi.org/10.1111/j.1461-0248.2005.00792.x>
- 605 Hareide, N.R., Garnes, G., 2001. The distribution and catch rates of deep wa-  
606 ter fish along the Mid-Atlantic ridge from 43 to 61 °N. Fish. Res. 51, 297–310.  
607 [https://doi.org/10.1016/S0165-7836\(01\)00253-3](https://doi.org/10.1016/S0165-7836(01)00253-3)
- 608 Helaouët, P., Beaugrand, G., 2009. Physiology, ecological niches and species distri-  
609 bution. Ecosystems, 12(8), 1235–1245. <https://doi.org/10.1007/s10021-009-9261-5>
- 610 Hijmans, R.J., Etten, J.V., 2012. Raster: Geographic Analysis and Modeling With  
611 Raster Data. R Package Version 2.0–12.
- 612 Hirzel, A.H., Le Lay, G., Helfer, V., Randin, C., Guisan, A., 2006. Evaluating the  
613 ability of habitat suitability models to predict species presences. Ecol. Modell. 199,  
614 142–152. <https://doi.org/10.1016/j.ecolmodel.2006.05.017>
- 615 Hutchinson, G.E., 1957. Concluding remarks. Cold Spring Harb. Symp. Quant.  
616 Biol. 22, 415–427
- 617 Hutchinson, G.E., 1978. An Introduction to Population Ecology. Yale University  
618 Press, New Haven.
- 619 ICES. 2021. Working Group on the Biology and Assessment of Deep-sea Fisheries  
620 Resources (WGDEEP). ICES Scientific Reports. 3:47. 944 pp. <http://doi.org/10.17895/ices.pub.8108>

- 622 Jiménez-Valverde, A., 2021. Prevalence affects the evaluation of discrimination ca-  
623 pacity in presence-absence species distribution models. *Biodivers. Conserv.* 30,  
624 1331–1340. <https://doi.org/10.1007/s10531-021-02144-4>
- 625 Jiménez-Valverde, A., Lobo, J.M., 2007. Threshold criteria for conversion of proba-  
626 bility of species presence to either-or presence-absence. *Acta Oecologica* 31, 361–369.  
627 <https://doi.org/10.1016/j.actao.2007.02.001>
- 628 Jiménez, L., Soberón, J., 2020. Leaving the area under the receiving operating  
629 characteristic curve behind: An evaluation method for species distribution mod-  
630 elling applications based on presence-only data. *Methods Ecol. Evol.* 2020, 1–16.  
631 <https://doi.org/10.1111/2041-210X.13479>
- 632 Kellner, K.F., Swihart, R.K., 2014. Accounting for imperfect detection in ecology:  
633 A quantitative review. *PLoS One* 9. <https://doi.org/10.1371/journal.pone.0111436>
- 634 Koslow, J. A. 1996. Energetic and life-history patterns of deep-sea benthic, ben-  
635 thopelagic and seamount-associated fish. *J. Fish Biol.* 49:54–74.
- 636 Laman, E.A., Rooper, C.N., Turner, K., Rooney, S., Cooper, W., Zimmermann, M.,  
637 2018. Using species distribution models to describe essential fish habitat in Alaska.  
638 *Can. J. Fish. Aquat. Sci.*
- 639 Leroy, B., Bellard, C., Dubos, N., Colliot, A., Vasseur, M., Courtial, C., Bakkenes,  
640 M., Canard, A., Ysnel, F., 2014. Forecasted climate and land use changes, and  
641 protected areas: The contrasting case of spiders. *Divers. Distrib.* 20, 686–697.  
642 <https://doi.org/10.1111/ddi.12191>
- 643 Leroy, B., Delsol, R., Hugueny, B., Meynard, C.N., Barhoumi, C., Barbet-Massin,  
644 M., Bellard, C., 2018. Without quality presence–absence data, discrimination met-  
645 rics such as TSS can be misleading measures of model performance. *J. Biogeogr.*  
646 45, 1994–2002. <https://doi.org/10.1111/jbi.13402>.
- 647 Liu, C., Berry, P.M., Dawson, T.P., Pearson, R.G., 2005. Selecting thresholds of  
648 occurrence in the prediction of species distributions. *Ecography (Cop.)* 28, 385–393.  
649 <https://doi.org/10.1111/j.0906-7590.2005.03957.x>

- 650 Liu, C., Newell, G., White, M., 2016. On the selection of thresholds for predicting  
651 species occurrence with presence-only data. *Ecol. Evol.* 6, 337–348. <https://doi.org/10.1002/ece3.1878>
- 653 Lorance, P., 2011. History and dynamics of the overexploitation of the blackspot sea  
654 bream (*Pagellus bogaraveo*) in the Bay of Biscay. *ICES J. Mar. Sci.* 68, 290–301.  
655 <https://doi.org/10.1093/icesjms/fsq072>
- 656 Lorance, P., F. Uiblein, and D. Latrouite. 2002. Habitat, behaviour and colour  
657 patterns of orange roughy *Hoplostethus atlanticus* (Pisces: Trachichthyidae) in the  
658 Bay of Biscay. *J. Mar. Biolog. Assoc.* 82:321–331.
- 659 Mateo, R., Aroca-Fernández, M.J., Gastón, A., Gómez-Rubio, V., Saura, S., García-  
660 Viñas, J.I., 2019. Looking for an optimal hierarchical approach for ecologically  
661 meaningful niche modelling. *Ecol. Modell.* 409. <https://doi.org/10.1016/j.ecolmodel.2019.108735>
- 663 Menezes, G. M., Giacomello, E., 2013. Spatial and temporal variability of demersal  
664 fishes at Condor seamount (Northeast Atlantic). *Deep-Sea Research Part II: Topical*  
665 *Studies in Oceanography*, 98(PA), 101–113. <https://doi.org/10.1016/j.dsr2.2013.08.010>
- 666 Meynard, C.N., Leroy, B., Kaplan, D.M., 2019. Testing methods in species distribution  
667 modelling using virtual species: what have we learnt and what are we missing?  
668 *Ecography (Cop.)*. 42, 2021–2036. <https://doi.org/10.1111/ecog.04385>
- 669 Michel, S., Vandermeirsch, F., Lorance, P., 2009. Evolution of upper layer tem-  
670 perature in the bay of biscay during the last 40 years. *Aquat. Living Resour.* 22,  
671 447–461. <https://doi.org/10.1051/alar/2009054>
- 672 Montgomery, D.C., 2005. *Design and Analysis of Experiments*. Wiley
- 673 Morato, T., Solà, E., Grós, M.P., Menezes, G., 2001. Feeding habits of two congener  
674 species of seabreams, *Pagellus bogaraveo* and *Pagellus acarne*, off the Azores (north-  
675 eastern Atlantic) during spring of 1996 and 1997. *Bull. Mar. Sci.* 69, 1073–1087.
- 676 Mytilineou, C., Politou, C.Y., Papaconstantinou, C., Kavadas, S., D’Onghia, G.,  
677 Sion, L., 2005. Deep-water fish fauna in the Eastern Ionian Sea. *Belgian J. Zool.*  
678 135, 229–233.

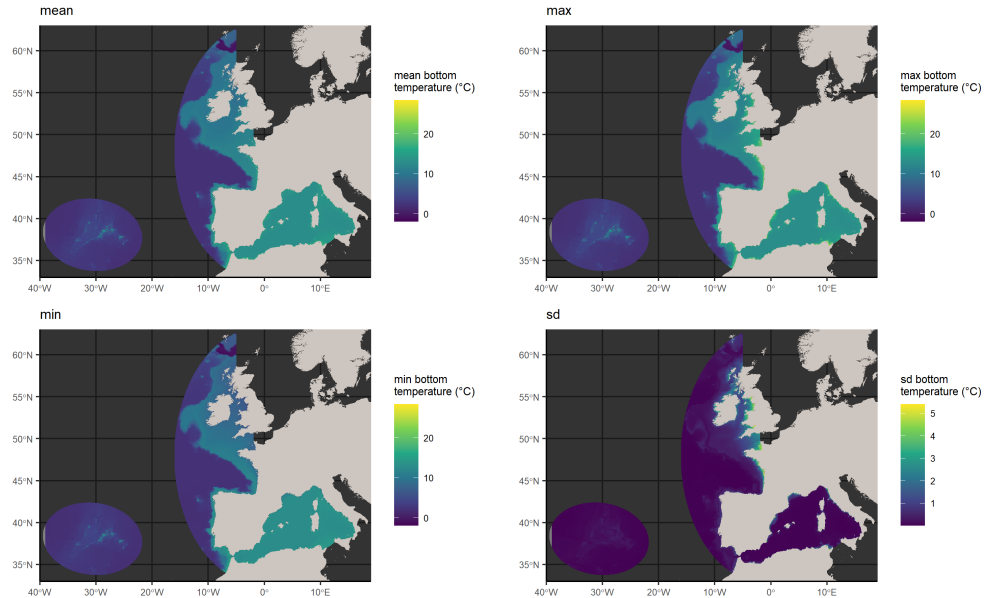
- 679 Mytilineou, C., Smith, C.J., Anastasopoulou, A., Papadopoulou, K.N., Christidis,  
680 G., Bekas, P., Kavadas, S., Dokos, J., 2014. New cold-water coral occurrences in the  
681 Eastern Ionian Sea: Results from experimental long line fishing. Deep. Res. Part  
682 II Top. Stud. Oceanogr. 99, 146–157. <https://doi.org/10.1016/j.dsr2.2013.07.007>
- 683 Nenzén, H.K., Araújo, M.B., 2011. Choice of threshold alters projections of species  
684 range shifts under climate change. Ecol. Modell. 222, 3346–3354. <https://doi.org/10.1016/j.ecolmodel.2011.07.011>
- 686 Olivier, R., 1928. Poissons de chalut, la dorade (*Pagellus centrodontus*). Rev. des  
687 Trav. l'Office des Pêches Marit. 1, 5–32.
- 688 Pecchi, M., Marchi, M., Burton, V., Giannetti, F., Moriondo, M., Bernetti, I., Bindi,  
689 M., Chirici, G., 2019. Species distribution modelling to support forest management.  
690 A literature review. Ecol. Modell. 411, 108817. <https://doi.org/10.1016/j.ecolmod.2019.108817>
- 692 Pinho, M., Diogo, H., Carvalho, J., J., P.G., 2014. Harvesting juveniles of blackspot  
693 sea bream (*Pagellus bogaraveo*) in the Azores (Northeast Atlantic): biological im-  
694 plications, management, and life cycle considerations. ICES J. Mar. Sci. 71,  
695 2448–2456. <https://doi.org/10.4135/9781412953924.n678>
- 696 Rincón, L., Castro, P.L., Álvarez, B., Hernández, M.D., Álvarez, A., Claret, A.,  
697 Guerrero, L., Ginés, R., 2016. Differences in proximal and fatty acid profiles, sen-  
698 sory characteristics, texture, colour and muscle cellularity between wild and farmed  
699 blackspot seabream (*Pagellus bogaraveo*). Aquaculture 451, 195–204. <https://doi.org/10.1016/j.aquaculture.2015.09.016>
- 701 Robinson, N.M., Nelson, W.A., Costello, M.J., Sutherland, J.E., Lundquist, C.J.,  
702 2017. A systematic review of marine-based Species Distribution Models (SDMs)  
703 with recommendations for best practice. Front. Mar. Sci. 4, 1–11. <https://doi.org/10.3389/fmars.2017.00421>
- 705 Santos, R., W. Medeiros-Leal, A. Novoa-Pabon, H. Silva, and M. Pinho. 2021.  
706 Demersal fish assemblages on seamounts exploited by fishing in the Azores (NE  
707 Atlantic). J. Appl. Ichthyol. 37:198-215.

- 708 Sanz-Fernández, V., Gutiérrez-Estrada, J.C., Pulido-Calvo, I., Gil-Herrera, J., Ben-  
709 choucha, S., el Arraf, S., 2019. Environment or catches? Assessment of the decline  
710 in blackspot seabream (*Pagellus bogaraveo*) abundance in the Strait of Gibraltar. *J.*  
711 *Mar. Syst.* 190, 15–24. <https://doi.org/10.1016/j.jmarsys.2018.08.005>
- 712 Schickele, A., Leroy, B., Beaugrand, G., Goberville, E., Hattab, T., Francour, P.,  
713 Raybaud, V., 2020. Modelling European small pelagic fish distribution: Method-  
714 ological insights. *Ecol. Modell.* 416, 108902. <https://doi.org/10.1016/j.ecolmodel.2019.108902>
- 716 Silva, H. M., Pinho, M. R. (2007). Small-Scale Fishing on Seamounts. In T. J.  
717 Pitcher, T. Morato, P. J. B. Hart, M. R. Clark, N. Haggan, and R. S. Santos  
718 (Eds.), *Seamounts: Ecology, Fisheries and Conservation* (pp. 335–360). Blackwell  
719 Publishing.
- 720 Soberón, J., Nakamura, M., 2009. Niches and distributional areas: Concepts, meth-  
721 ods, and assumptions. *Proceedings of the National Academy of Sciences of the*  
722 *United States of America*, 106 (SUPPL. 2), 19644–19650. <https://doi.org/10.1073/pnas.0901637106>
- 724 Spedicato, M.T., Greco, S., Sophronidis, K., Lembo, G., Giordano, D., Argyri, A.,  
725 2002. Geographical distribution, abundance and some population characteristics of  
726 the species of the genus *Pagellus* (Osteichthyes: Perciformes) in different areas of the  
727 Mediterranean. *Sci. Mar.* 66, 65–82. <https://doi.org/10.3989/scimar.2002.66s265>
- 728 Thuiller, W., Lafourcade, B., Engler, R., Araújo, M.B., 2009. BIOMOD - A platform  
729 for ensemble forecasting of species distributions. *Ecography (Cop.)*. 32, 369–373.  
730 <https://doi.org/10.1111/j.1600-0587.2008.05742.x>
- 731 Thuillier, W., Georges, D., Gueguen, M., Engler, R., Breiner, F., 2016. Biomod2:  
732 Ensemble platform for species distribution modeling. *R Packag.* version 3.3-7.
- 733 Valanis, D. V., Pierce, J.P., Zuur, A.F., Palialexis, A., Saveliev, A., Katara, I.,  
734 Wang, J., 2008. Modelling of essential fish habitat based on remote sensing, spatial  
735 analysis and GIS. *Hydrobiologia* 612, 5–20.
- 736 Valencia, V., Fontán, A., Goikoetxea, N., Chifflet, M., González, M., López, A.,  
737 2019. Long-term evolution of the stratification, winter mixing and Θ-S signature

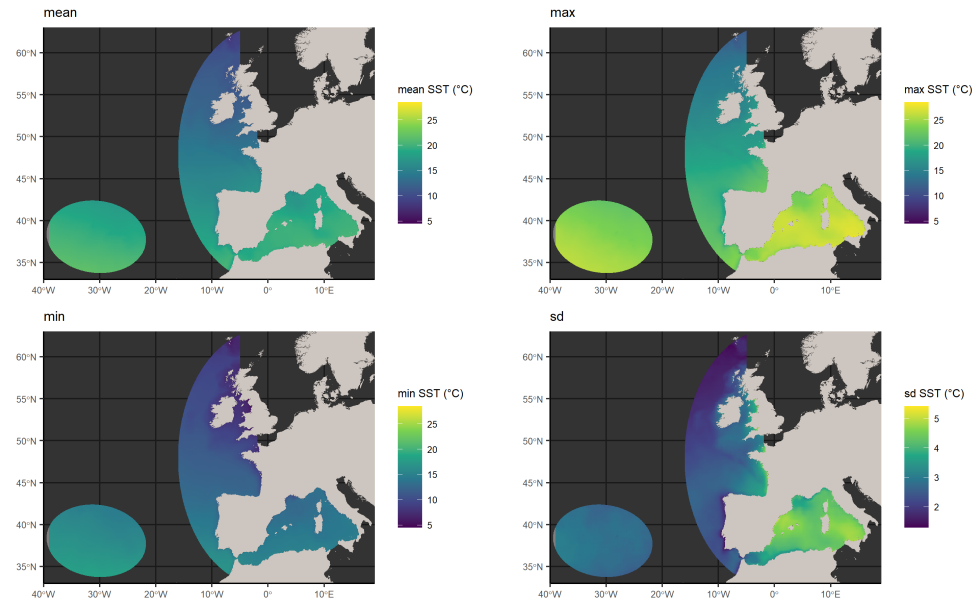
- 738 of upper water masses in the southeastern Bay of Biscay. *Cont. Shelf Res.* 181,  
739 124–134. <https://doi.org/10.1016/j.csr.2019.05.010>
- 740 Welsh, A.H., Lindenmayer, D.B., Donnelly, C.F., 2013. Fitting and Interpreting  
741 Occupancy Models. *PLoS One* 8. <https://doi.org/10.1371/journal.pone.0052015>
- 742 Wiens, J.J., Sukumaran, J., Pyron, R.A., Brown, R.M., 2009. Evolutionary and  
743 biogeographic origins of high tropical diversity in Old World frogs (Ranidae). *Evo-*  
744 *lution*, 63, 1217-1231.
- 745 Wisz, M.S., Guisan, A., 2009. Do pseudo-absence selection strategies influence  
746 species distribution models and their predictions? An information-theoretic ap-  
747 proach based on simulated data. *BMC Ecol.* 9, 1–13. <https://doi.org/10.1186/1472-6785-9-8>
- 749 Zurell, D., Franklin, J., König, C., Bouchet, P.J., Dormann, C.F., Elith, J., Fandos,  
750 G., Feng, X., Guillera-Arroita, G., Guisan, A., Lahoz-Monfort, J.J., Leitão, P.J.,  
751 Park, D.S., Peterson, A.T., Rapacciulo, G., Schmatz, D.R., Schröder, B., Serra-  
752 Diaz, J.M., Thuiller, W., Yates, K.L., Zimmermann, N.E., Merow, C., 2020. A  
753 standard protocol for reporting species distribution models. *Ecography (Cop.)*. 43,  
754 1261–1277. <https://doi.org/10.1111/ecog.04960>

755 **Supplementary Material**

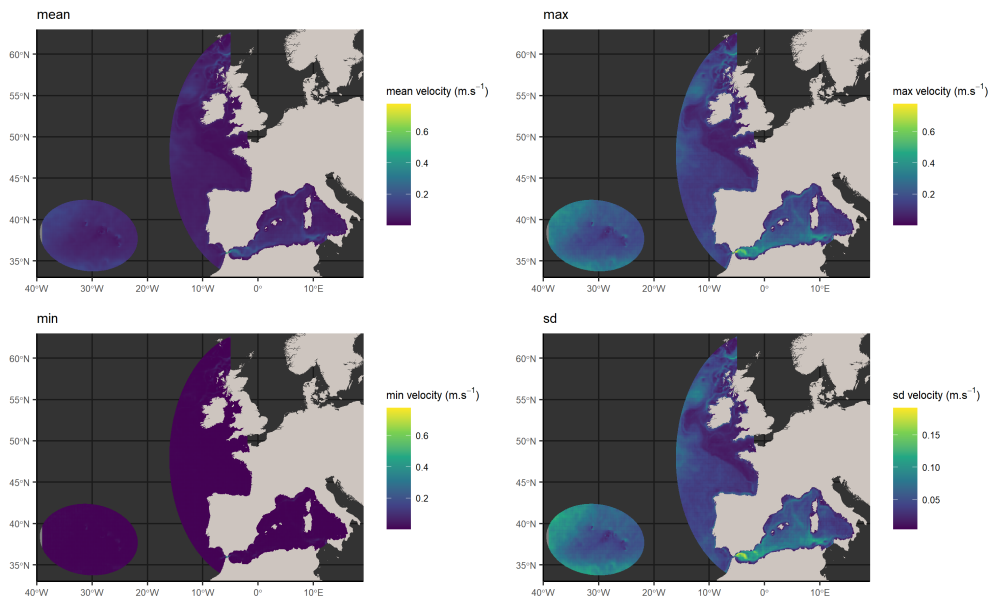
756 *Supplementary Material 1: Environmental variables extracted*



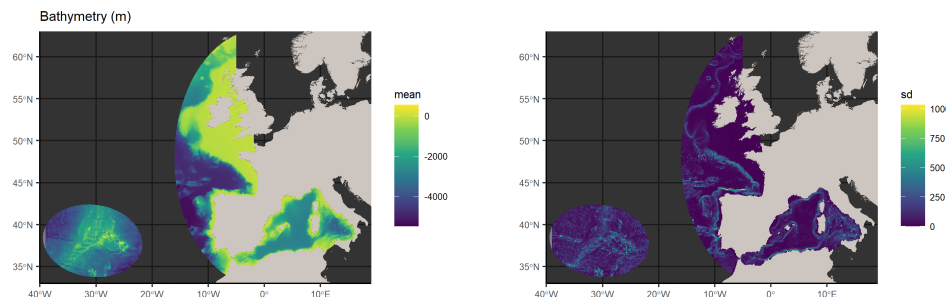
757 Sup. Mat. 1.1: Annual mean, maximum, minimum, and standard deviation of the bottom  
758 temperature over the blackspot sea bream main area of distribution between January 1994 and  
759 December 2018 extracted from Copernicus.



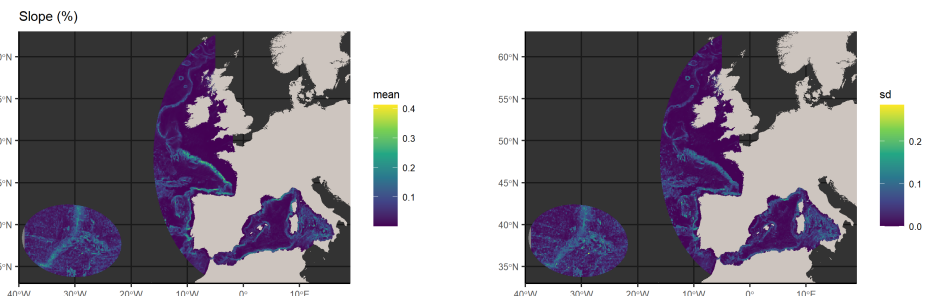
760 Sup. Mat. 1.2: Annual mean, maximum, minimum, and standard deviation of the sea surface  
761 temperature (SST) over the blackspot sea bream main area of distribution between January 1994  
762 and December 2018 extracted from Copernicus.



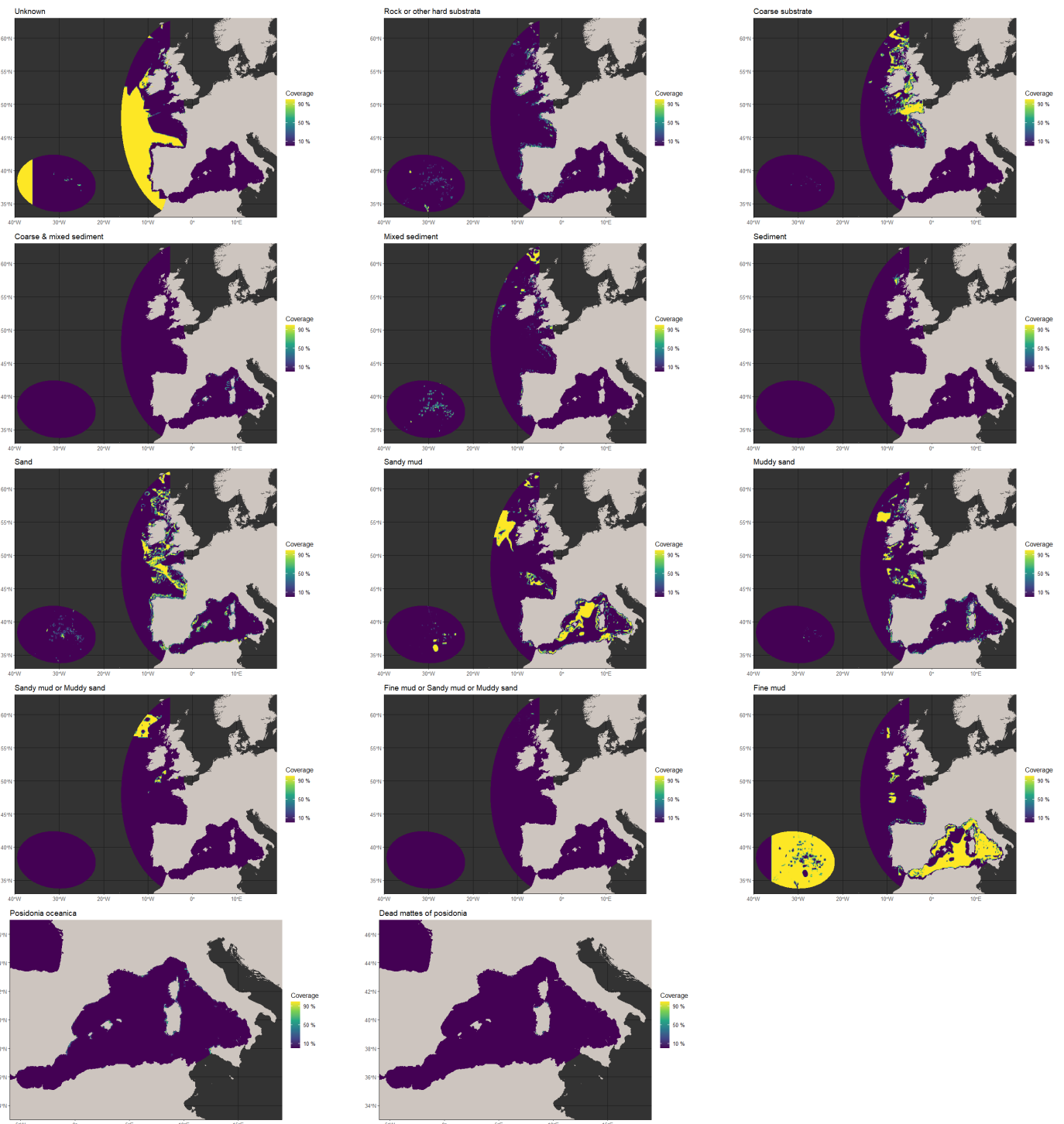
763 Sup. Mat. 1.3: Annual mean, maximum, minimum, and standard deviation of the absolute  
 764 currents velocity over the blackspot sea bream main area of distribution between January 1994 and  
 765 December 2018 extracted from Copernicus.



766 Sup. Mat. 1.4: Mean and standard deviation of the bathymetry over the blackspot seabream  
 767 main area of distribution extracted from GEBCO.

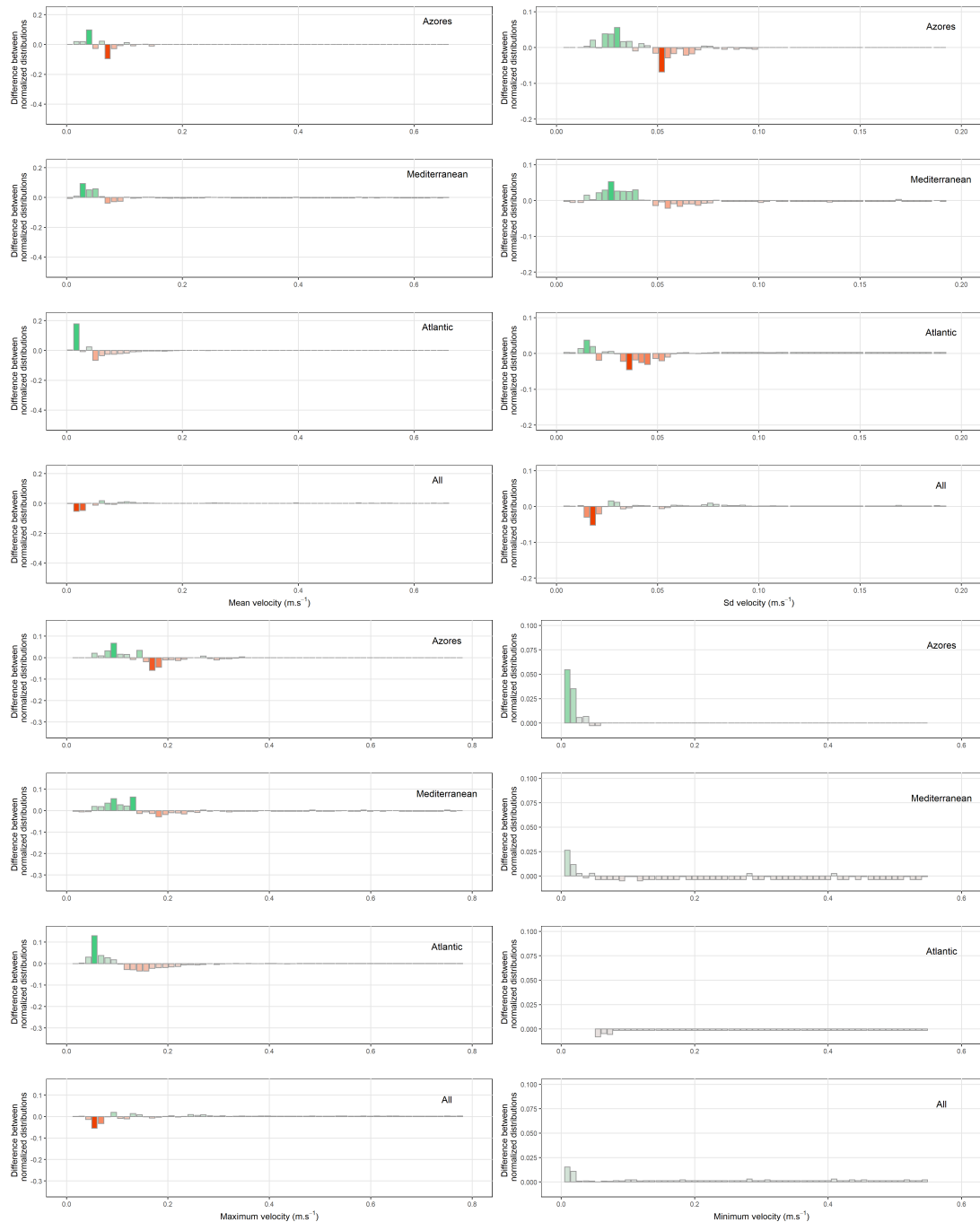


768 Sup. Mat. 1.5: Mean and standard deviation of the slope over the blackspot seabream main  
 769 area of distribution extracted from GEBCO.

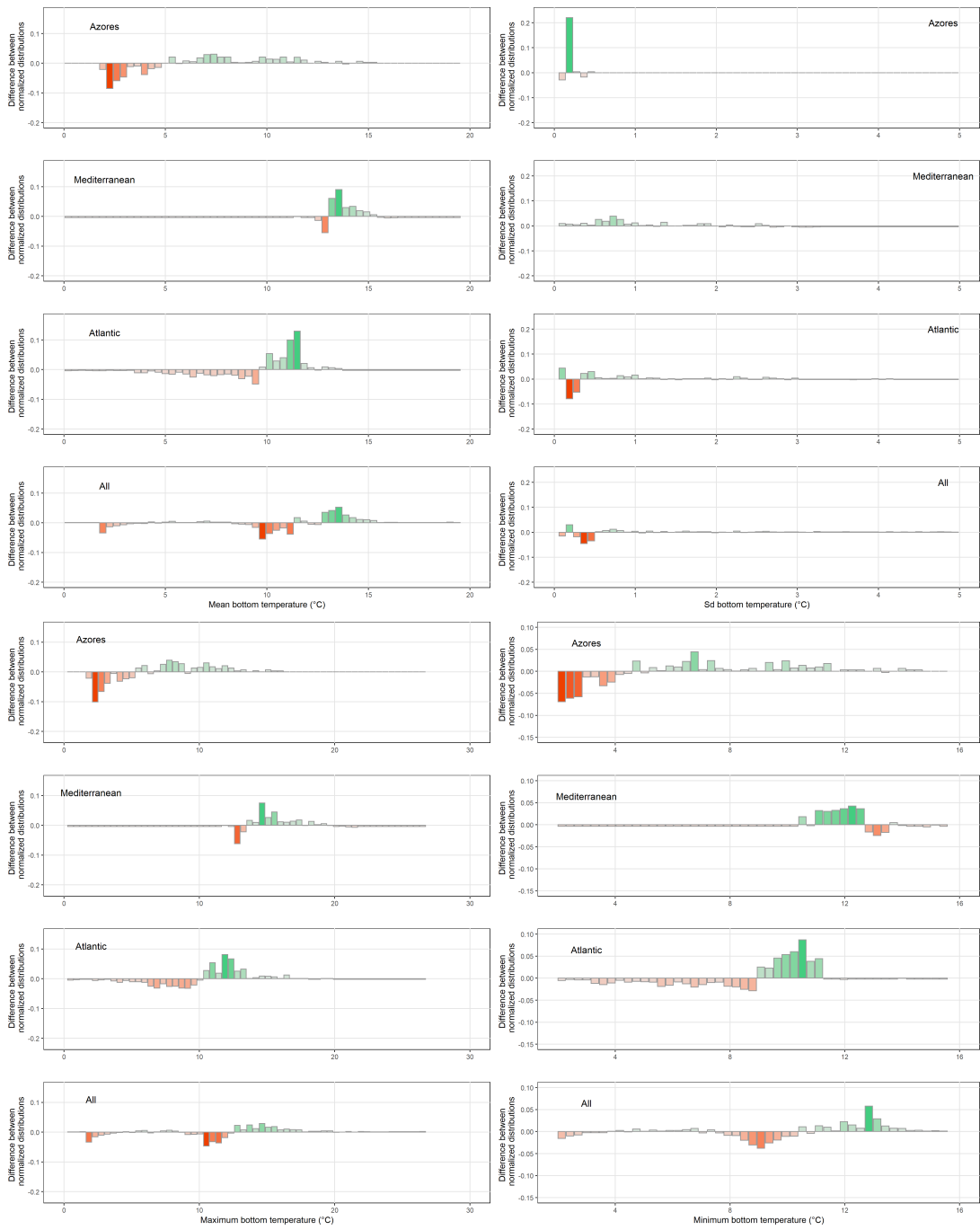


770 Sup. Mat. 1.6: Percentage of cell occupied by each of the 14 Emnet sea bottom categories:  
 771 unknown, rock or other hard substrata, coarse substrate, coarse and mixed sediment, mixed  
 772 sediment, sediment, sand, sandy mud, muddy sand, sandy mud or muddy sand, fine mud or sandy  
 773 mud or muddy sand, fine mud, *Posidonia oceanica*, dead mattes of *Posidonia oceanica*. Each cell  
 774 was attributed the value corresponding to the most present category.

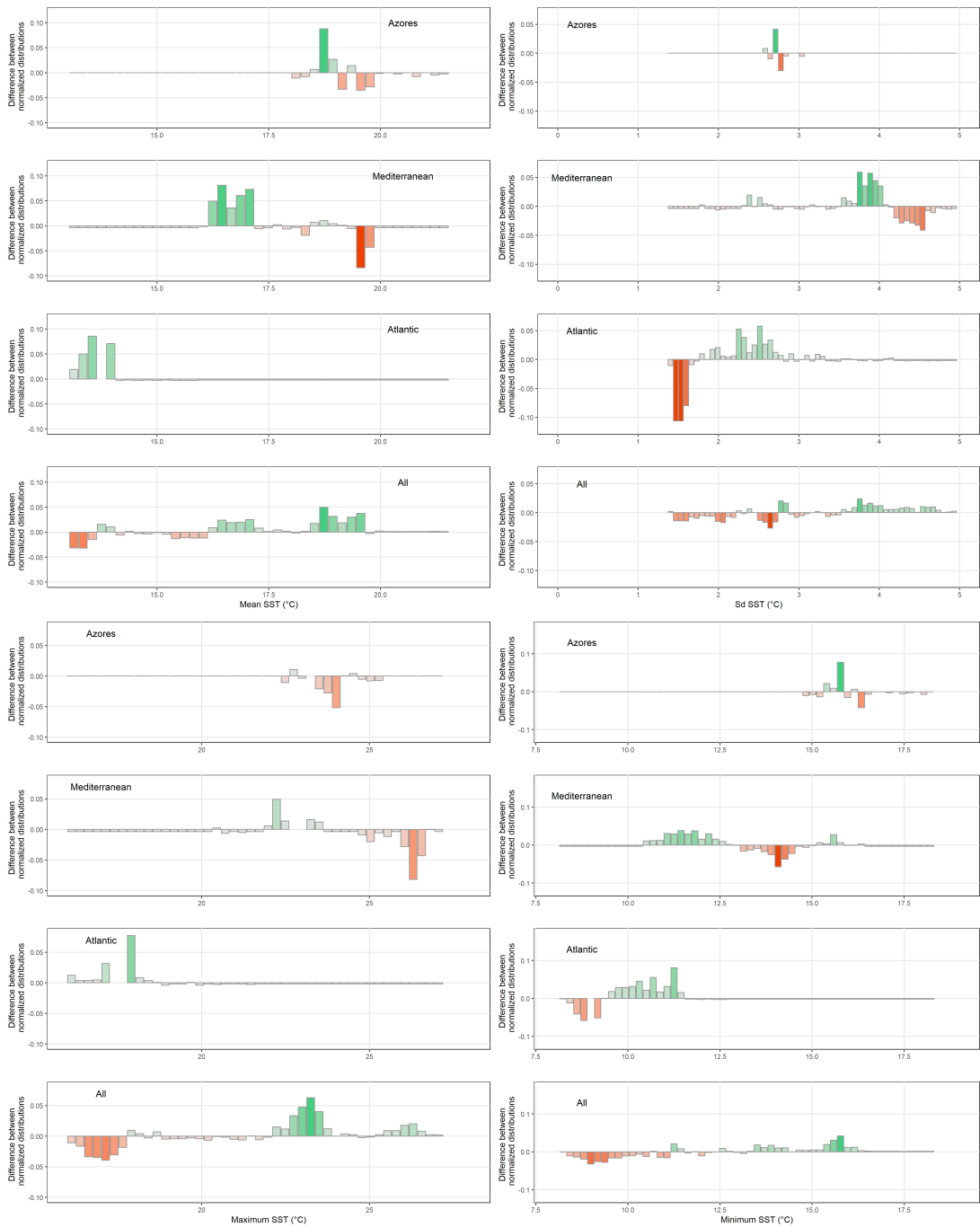
775 *Supplementary Material 2: Data exploration*



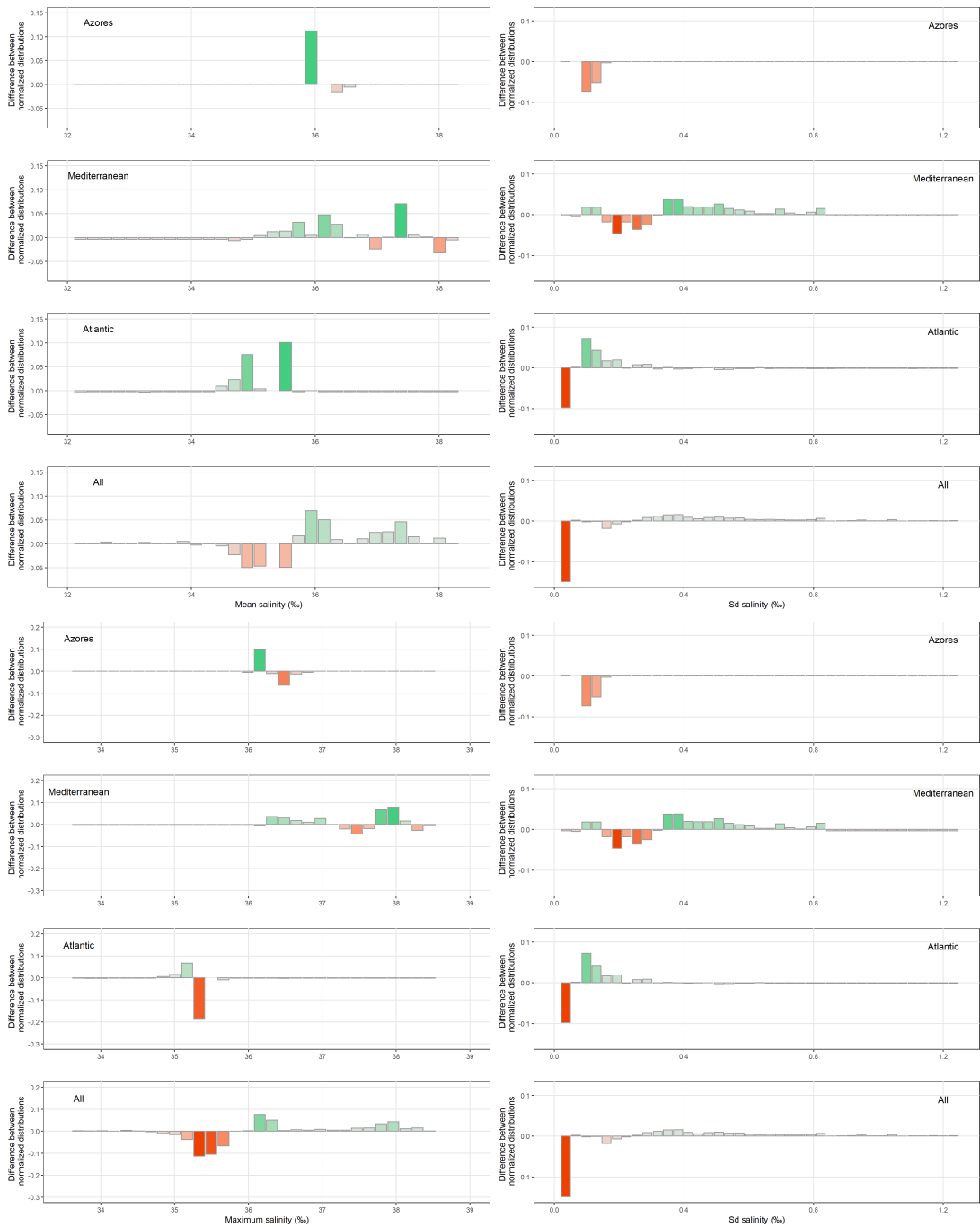
776 Sup. Mat. 2.1: Comparison of the distributions in mean, sd, maximum and minimum annual  
 777 currents velocity of presence records over sampling cells in the whole area and in Azorean region,  
 778 Mediterranean Sea, and Atlantic shelf.



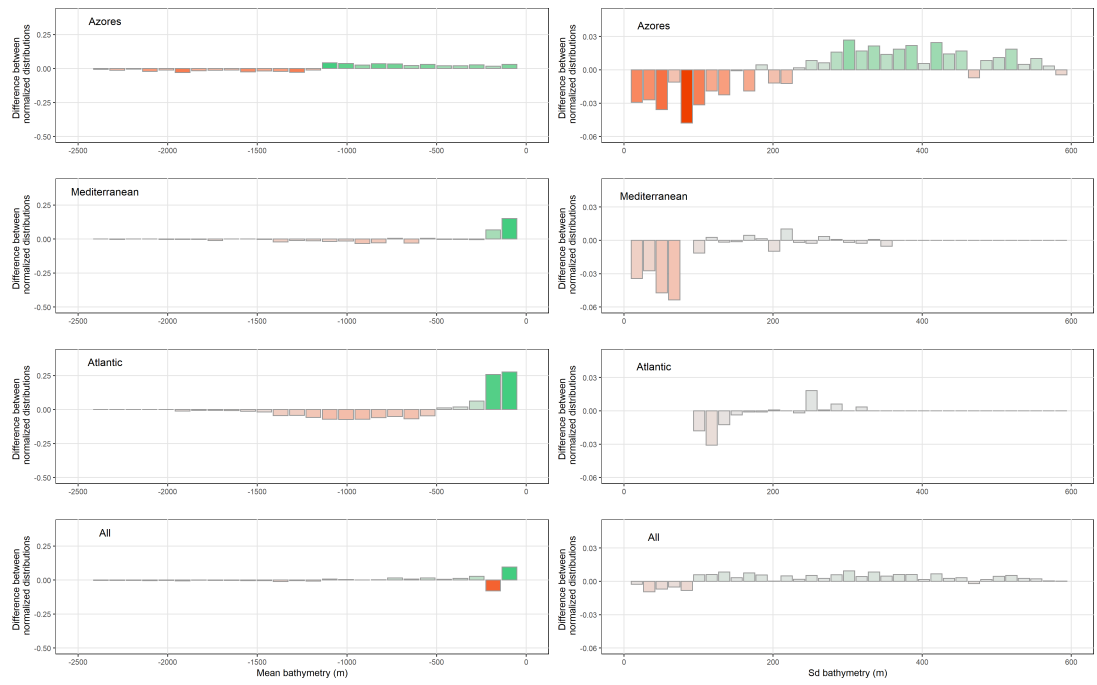
Sup. Mat. 2.2: Comparison of the distributions in mean, sd, maximum and minimum annual bottom temperature of presence records over sampling cells in the whole area and in Azorean region, Mediterranean Sea, and Atlantic shelf.



782 Sup. Mat. 2.3: Comparison of the distributions in mean, sd, maximum annual  
 783 sea surface temperature (SST) of presence records over sampling cells in the whole area and by  
 784 region (Azores, Mediterranean Sea, and Atlantic shelf).

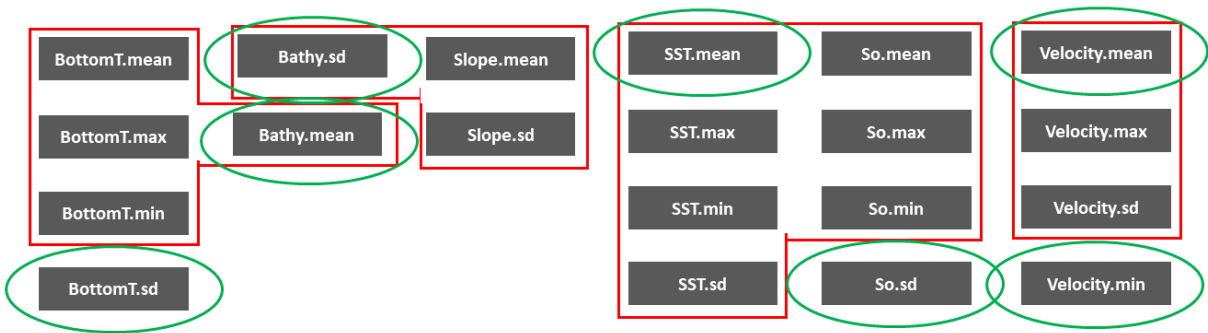


Sup. Mat. 2.4: Comparison of the distributions in mean, sd, maximum and minimum annual salinity of presence records over sampling cells in the whole area and in Azorean region, Mediterranean Sea, and Atlantic shelf.



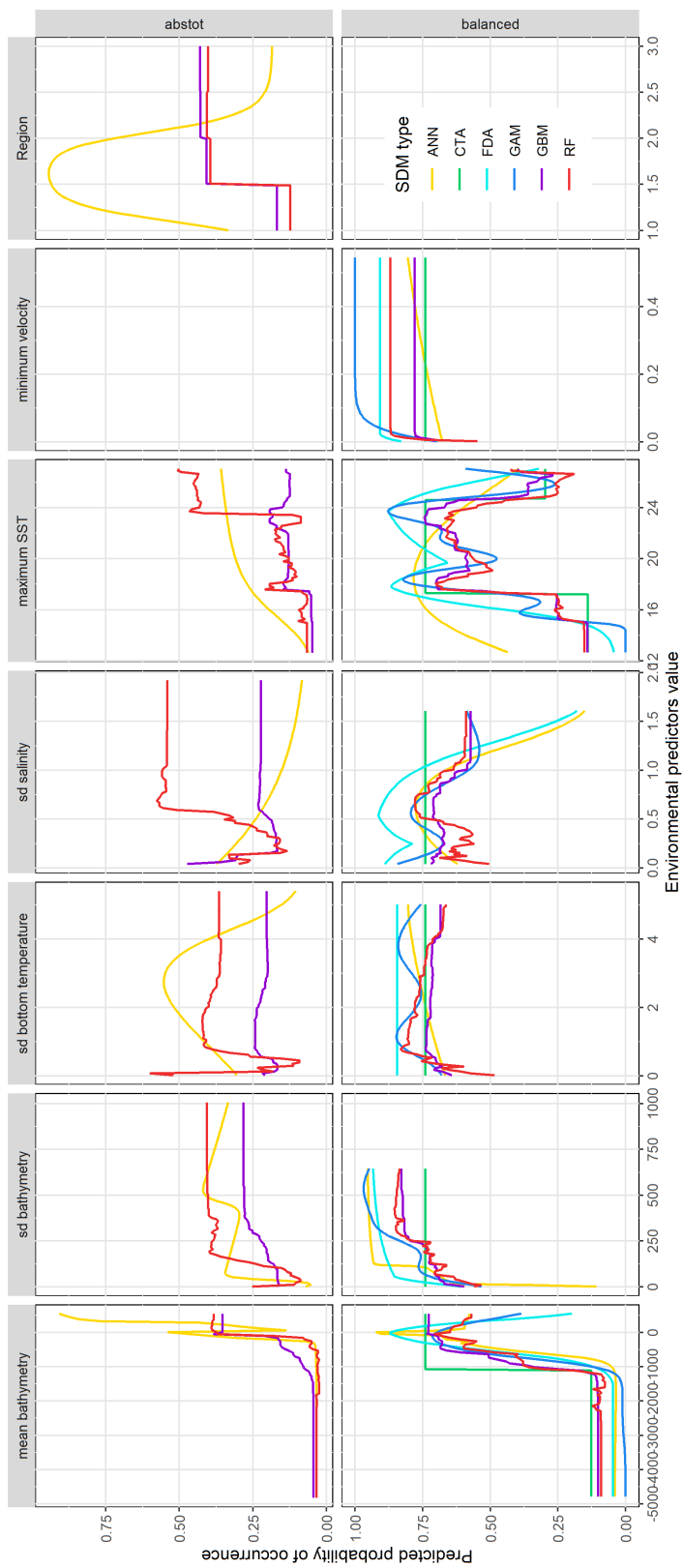
788      Sup. Mat. 2.5: Comparison of the distributions in mean and sd bathymetry of presence records  
 789      over sampling cells in the whole area and in Azorean region, Mediterranean Sea, and Atlantic shelf.

790 *Supplementary Material 3: Groups of correlated environmental variables*



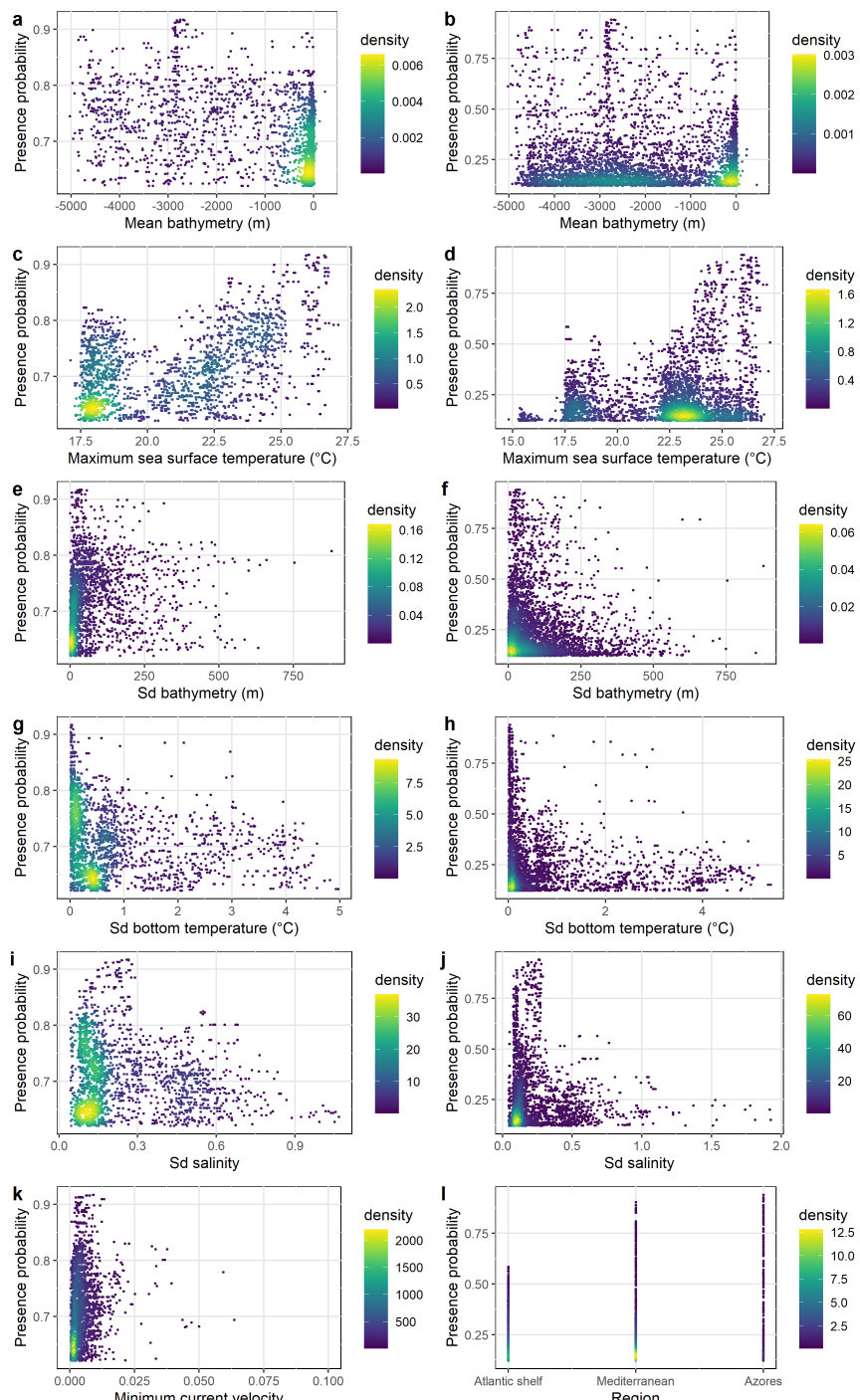
791 Sup. Mat. 3.1: Groups of correlated variables (Pearson's correlation,  $r > 0.7$ ) in red, and vari-  
792 able selected among each group, in green, selected according the percentage of explained variance.  
793 BottomT is bottom temperature, Bathy is bathymetry, SST sea surface temperature, So salinity  
794 and Velocity surface current velocity.

795      *Supplementary Material 4: Response curves of the various selected SDMs used in the ensemble model procedure using 6 environmental  
 796      variables with the observed- (top) and balanced-ratio (bottom) data sets.*





797     *Supplementary Material 5: Distribution of presence cells of the blackspot sea  
 798 bream in the model domain of distribution (based on the presence threshold obtained  
 799 with TSS indices: presence respectively for a presence probability  $p > 0.62$  for the  
 800 balanced-ratio data set and  $p > 0.12$  for the observed-ratio data set) according to  
 801 the predictors values when using 6 predictors with the balanced- (a, c, e, g, i, k) and  
 802 observed-ratio (b, d, f, h, j, l) data sets. High densities of values appear yellow on  
 803 the scatter plots.*

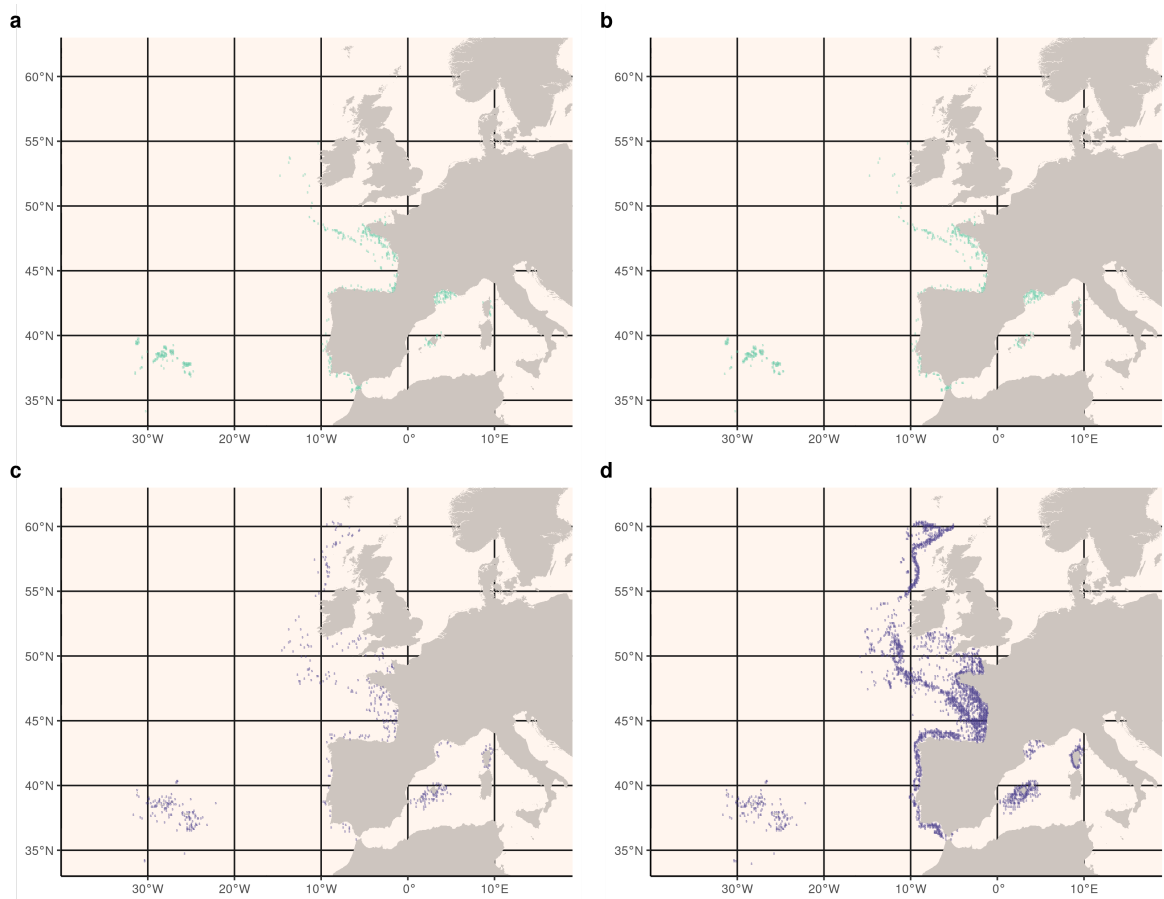




804      *Supplementary Material 6: Summary of the 16 ensemble species distribution models implemented in this study with 8 different*  
 805      *numbers of predictors and two different kinds of data sets (balanced- / observed-ratio): predictors used and their relative importance*  
 806      *(proportion of variance explained), characteristics of the data set used, used SDMs and overall performance.*

		Data set	2 predictors	3 predictors	4 predictors	5 predictor	6 predictors	7 predictors	8 predictors	9 predictors
<b>Environmental variables' importance</b>										
Mean bathymetry	balanced	64%	69%	60%	59%	55%	55 %	53%	58%	58%
	observed	50%	49 %	50%	37%	30%	31%	26%	27 %	27 %
Max SST	balanced	36%	22%	23 %	28%	28%	22%	28%	22%	22%
	observed	50%	34%	18%	25%	31%	25%	27%	26%	26%
Sd bathymetry	balanced	-	9%	12 %	7%	9%	12%	9%	10%	10%
	observed	-	17%	18%	20%	18%	16%	12%	11%	11%
Sd bottom temperature	balanced	-	-	5%	7%	3%	2%	3%	3%	3%
	observed	-	-	-	8%	8%	9%	7 %	7 %	8%
Sd salinity	balanced	-	-	-	2 %	3%	3%	3%	2%	2%
	observed	-	-	-	-	5%	6 %	5 %	5 %	5 %
Min current velocity	balanced	-	-	-	-	2%	2%	2%	1%	1%
	observed	-	-	-	-	-	3%	4%	2%	2%
Mean current velocity	balanced	-	-	-	-	-	2 %	1%	1%	1%
	observed	-	-	-	-	-	-	-	2 %	2 %
Sea bottom type	balanced	-	-	-	-	-	-	-	1%	1%
	observed	-	-	-	-	-	-	-	1%	1%
Region	balanced	-	-	-	-	-	-	-	-	1%
	observed	-	-	11%	13 %	9%	10%	18%	17%	17%
<b>Occurrence data set</b>										
Data set size	balanced	16	322	322	744	940	950	1072	1152	1152
	observed	474	1510	1696	2620	3280	3357	3752	4163	4163
Number of presences	balanced	8	161	161	372	470	475	536	576	576
	observed	8	161	161	372	470	475	536	576	576
Number of absences	balanced	8	161	161	372	470	475	536	576	576
	observed	466	1349	1535	2248	2810	2882	3216	3587	3587
<b>Models' selection and performance</b>										
Selected models (TSS > 0.5)	balanced	CTA, FDA, ANN, CTA, FDA, ANN, CTA, FDA, GAM, GLM, GBM, RF	ANN, CTA, FDA, GAM, GLM, GBM, RF							
	observed	ANN, FDA, ANN, CTA, FDA, GAM, GLM, GBM, RF	ANN, CTA, FDA, GAM, GLM, GBM, RF	ANN, CTA, FDA, GAM, GLM, GBM, RF	ANN, CTA, FDA, GAM, GLM, GBM, RF	ANN, CTA, FDA, GAM, GLM, GBM, RF	ANN, CTA, FDA, GAM, GLM, GBM, RF	ANN, CTA, FDA, GAM, GLM, GBM, RF	ANN, CTA, FDA, GAM, GLM, GBM, RF	ANN, CTA, FDA, GAM, GLM, GBM, RF
True Skill Statistic	balanced	0.711 ± 0.010	0.767 ± 0.004	0.712 ± 0.011	0.711 ± 0.006	0.716 ± 0.003	0.730 ± 0.001	0.7155 ± 0.014	0.725 ± 0.025	0.725 ± 0.025
	observed	0.996 ± 0.003	0.791 ± 0.13	0.826 ± 0.013	0.867 ± 0.033	0.916 ± 0.030	0.895 ± 0.039	0.904 ± 0.043	0.894 ± 0.053	0.894 ± 0.053

807   Supplementary Material 7: Maps of the presence (a,b, green) and absence (c,d,  
808   blue) data cells used for calibrating eSDMs with the balanced-ratio (a,c) and the  
809   observed-ratio (b,d) of presence and absence.



810    *Supplementary Material 8: Maximized index values when comparing the blackspot*  
 811    *seabream eSDM habitat estimates for best model (6 predictors) to occurrence data and*  
 812    *corresponding probability threshold values for presence/absence for building binary*  
 813    *habitat maps.*

Validation index	Region	Data set	Maximized index	Optimised threshold
TSS	all	balanced	0.45	0.62
	all	observed	0.57	0.12
	Azores	balanced	0.57	0.12
	Azores	observed	0.56	0.14
	Atlantic	balanced	0.45	0.46
	Atlantic	observed	0.53	0.09
	Mediterranean	balanced	0.54	0.62
	Mediterranean	observed	0.62	0.25
accuracy	all	balanced	0.90	0.77
	all	observed	0.91	0.33
	Azores	balanced	0.78	0.25
	Azores	observed	0.79	0.23
	Atlantic	balanced	0.93	0.80
	Atlantic	observed	0.93	0.34
	Mediterranean	balanced	0.82	0.67
	Mediterranean	observed	0.84	0.3
CBI	all	balanced	0.98	1
	all	observed	1	0.98
	Azores	balanced	0.75	0.96
	Azores	observed	0.97	0.82
	Atlantic	balanced	0.97	0.79
	Atlantic	observed	0.65	0.42
	Mediterranean	balanced	0.89	1
	Mediterranean	observed	0.93	0.98
hit rate	all	balanced	1	0.04
	all	observed	1	0.01
	Azores	balanced	1	0.03
	Azores	observed	1	0.02
	Atlantic	balanced	1	0.04
	Atlantic	observed	1	0.01
	Mediterranean	balanced	1	0.03
	Mediterranean	observed	1	0.01

## Annexe 2

Article en préparation sur les relations entre prix et quantité débarquées de 1973 à 2020.

## **Effects of stock collapse on price dynamics of blackspot seabream in the Bay of Biscay**

Pascal Lorance and Verena M. Trenkel

DECOD (Ecosystem Dynamics and Sustainability), IFREMER, INRAe, Institut-Agro - Agrocampus Ouest, France, Nantes, France

Corresponding author: Pascal Lorance pascal.lorance@ifremer.fr

### **Abstract**

The blackspot seabream stock in the Bay of Biscay collapsed in the late 1970s due to overexploitation. The resulting drastic decrease in landings drove ex-vessel prices up sharply, making it the most valuable species landed by French fleets in Atlantic French harbours in recent years. The overall relationship between prices and landings was negative for blackspot seabream during two considered time periods, 1973-2003 and 2000-2020, indicative of an inverse demand system. A similar negative relationship was found for around half of species among a list of 17 teleost marine species selected for comparison based on price and stock abundance criteria and taxonomic relatedness. Negative relationships between interannual variations in blackspot price and landings were only found for the first period, while such a relationship occurred for more than half of the compared species during both periods, indicating rapid adjustments to market availability. Potential for consumer switch from blackspot seabream to the other species was studied considering correlations in prices and landings. Positive correlations of prices were found during the first time period and some negative correlations during the second period.

### **Introduction**

Blackspot seabream is one of the higher priced demersal fish species in France, Spain and Portugal owing to its firm and flavourful flesh (Rincon et al., 2016). Although no study on the market of this fish species has been published, there is anecdotal evidence that in recent years it has been sold to gourmet restaurants and retailed in wealthier areas in France. Until the mid 1970s, blackspot seabream was an abundant species in the Bay of Biscay (Lorance, 2011) and available all year round on French fish markets. Considering the period posterior to the stock collapse, international landings (Spain and France) of blackspot seabream from the Bay of Biscay (ICES Subarea 8) from 1990 to 2020 varied between 500 tonnes in some years in the early 1990s to less than 200 in the past decade (ICES catch data downloaded on 18.10.2022. Compared to more than 20 000 in some years in the 1960s-1970s (Lorance, 2011).

The size distribution of marketed fish changed over time as a result of reduced consumer demand for portion-sized fish and legislation changes. In the late 1960s before the stock collapse, a commercial category for blackspot seabream <100 g existed (Lorance, 2011). Individuals <500 g might have represented 20–24% of the landings in 1966–1968 (Guichet et al., 1971). Smaller blackspot seabream were marketed under specific commercial names (pirono and pelon). In addition to changes in consumption habits increasing the size of landed blackspot seabream in recent years, legislative measures have also been put into place. A TAC for ICES subareas 6-8 was set to 350 tonnes in 2003 and gradually reduced to 105 tonnes in 2020. Since 2017, the

species has been subject to a Minimum Conservation Reference Size (MCRS) of 33 cm both in the Atlantic and the Mediterranean Sea (regulation (EU) 2019/1241 of the European Parliament and of the Council). This MCRS corresponds to a weight of 475 g. A larger minimum landing size of 35 cm applied between 2010 and 2012. In France, to the best of our knowledge, the species has always been sold as whole fresh fish. In recent years, the small quantities landed have been mostly sold to markets for high-quality products such as used by gourmet restaurants. These restaurants serve fish fillets, which are prepared in the restaurant and not at a distant fishmonger workshop.

In several studies, fish ex-vessel sale prices have been found to decrease with increasing landed volume (Barten and Bettendorf, 1989; Lesur-Irichabeau et al., 2016; Burgess et al., 2017), though the opposite, that is higher landings and higher prices have also been reported (Magnusson and Dekker, 2021). A negative relationship between quantity sold and price corresponds to an inverse demand system (Barten and Bettendorf, 1989), which might occur on different temporal scales, from the daily (Lesur-Irichabeau et al., 2016; Maynou, 2022) to the annual level (Fryxell et al., 2017). Fryxell et al. (2017) identified a negative relationship between total annual landings and mean annual price of North American cod and pollock as the fishery degraded. In addition to a global negative relationship between prices and landed quantities found for many species, price changes in time have been found to be driven by temporal changes in landings (Pincinato et al., 2020).

This study aimed at investigating trends in ex-vessel prices of blackspot seabream starting before the stock crash and compared these trends to selected fish species to appraise the effects of the decreasing abundance and decreasing landings driven by regulation of blackspot seabream on its price and the potential for consumer switch to other species. The species selected for comparison were teleost marine fishes, mostly demersal species, based on price and stock abundance criteria, as well as taxonomic relatedness. All selected species were sold fresh in French auction markets of Atlantic harbours.

## Material and Methods

### *Species selection*

The price of blackspot seabream and its relationship with landings was compared to selected species caught by French fleets in the Bay of Biscay and which are mostly consumed fresh by households (FranceAgrimer, 2021). The list excluded all small pelagic fishes, for which a large proportion of landings goes through the fish processing industry, as well as lower value species, which may also be distributed through catering companies. For the comparison, three species categories were created: (1) the main benthic and demersal fish species in terms of quantities landed, referred to as **major species**: hake (*Merluccius merluccius*), sole (*Solea solea*) and two species of anglerfish sold together (*Lophius piscatorius* and *L. budegassa*). (2) Teleost species fetching high prices, ( $\geq 5$  €/kg in 2020) and which are regularly landed in French ports of the Bay of Biscay, referred to as **high-value species**. These species are of similar or larger size than blackspot seabream. The list included European seabass (*Dicentrarchus labrax*), John Dory (*Zeus faber*), gilthead seabream (*Sparus aurata*), red porgy (*Pagrus pagrus*), and meagre (*Argyrosomus regius*), the two high price flatfishes turbot (*Scophthalmus maximus*) and brill (*S. rhombus*), pollack (*Pollachius pollachius*), and red mullet (*Mullus surmuletus*). The large pelagic bluefin tuna (*Thunnus thynnus*) was also included in the list. Only half of these high-value species are

currently managed by a TAC. (3) Species taxonomically related to the blackspot seabream, referred to as **related species**. These species included the axillary seabream (*Pagellus acarne*) of flesh quality similar to that of blackspot seabream but of smaller size, the lesser priced black seabream (*Spondylisoma cantharus*) and white seabream (*Diplodus sargus*), and the common pandora (*Pagellus erythrinus*). The species in this group fetched lower prices (< 5 €/kg in 2020) and are not subject to a TAC. Though related to blackspot seabream, gilthead seabream and red porgy were included in the group of high-value species due their higher sale prices. However, they had the lowest landings in this group (Table 1).

### Data

Two data sets for ex-vessel prices and landings were used with different resolutions. For the years 1973-2002, a data set from the French national committee of marine fisheries (CNPM) was available. For this data, meagre was missing and the axillary seabream and the common pandora were combined and it is unclear whether data reported under this combination did not also include some red porgy. The three species were therefore not considered for this data set. Further, the data set contained only mean annual prices across all French ports for all studied species except for bluefin tuna and hake for which mean overall prices and prices for landings in Bay of Biscay ports were available and the later were used. For the period 2000-2020, data were extracted from the French national database of fisheries statistics and prices refer to Atlantic landing ports only. Mean annual prices were calculated as the sum of landed value divided by the sum of landings.

Prices in both data sets were standardised to 2001 values using the consumer price index of French fresh food products extracted from the French institute for statistical and economical studies ([www.insee.fr](http://www.insee.fr); value 100 in 2001). Due to the structural differences, the data sets for the two time periods were analysed separately.

### Analyses

The relationship between inflation corrected mean annual prices and total annual landings was investigated on two levels for each species and compared to group-specific hypotheses detailed below. First, for each species and period, the overall relationship between prices and landings was investigated using Pearson's correlation coefficient. Second, the interannual relative variation in price  $\Delta P_{i,t}$  for species  $i$  was related to the interannual relative variation in its landings  $\Delta L_{i,t}$  fitting the linear model:

$$\Delta P_{i,t} = a_i + b_i \Delta L_{i,t} \quad \text{where } \Delta P_{i,t} = \frac{P_{i,t} - P_{i,t-1}}{P_{i,t-1}}; \Delta L_{i,t} = \frac{L_{i,t} - L_{i,t-1}}{L_{i,t-1}}.$$

The slope  $b_i$  was used to quantify relative price changes with respect to relative changes in landings. We hypothesised that price of the highly sought after blackspot seabream increased with decreasing landings following an inverse demand system (negative value for  $b_i$ ). Similarly, we expected a negative slope for all high-value species, except for gilthead seabream. Gilthead seabream is also produced by aquaculture in larger quantities than fisheries landings (FAO, 2022) In the Northeast Atlantic aquaculture production in recent years was 3 to 5 times as much as fisheries landings whilst aquaculture production from the Mediterranean and Black Sea was about 50 times more than fisheries landings. This is expected to lead to fisheries landings not playing an important role in price formation as these are driven by aquaculture production as observed in Australia in a similar situation (Pascoe et al., 2022). In contrast, for three major

species we assumed demand being able to adjust to changes in landings, which means prices would fluctuate independent of landings ( $b_1$  close to zero). Lastly, for the group of related species, we expected price also to be unrelated to landings, because they are of lesser flesh quality (black seabream, white seabream) or smaller size (axillary seabream, common pandora) and hence less demanded by consumers.

To investigate the potential for consumer switch from blackspot seabream to the other selected species, we calculated the Pearson correlation between blackspot seabream prices and the price time series of the selected species, similarly for landings. Incentives for consumer switch could come from both prices and landings. Price has been identified as a barrier to fish consumption and availability was found to impact the frequency of fish consumption (see review in Carlucci et al., 2015). Thus, we hypothesized that negative correlation between prices or landings with those of blackspot seabream could indicate the existence of an incentive for consumer switch to the given species in years blackspot seabream landings were low and/or prices high. Further, for switching, the perception of the degree of similarity of the species to blackspot seabream was expected to play a role. In a consumer survey on factors affecting the decision to purchase different fish species, taste was one of the major factors (Nauman et al., 1995). Hence, negative correlations of landings with one of the high-value species as well as with axillary seabream because of similar flesh quality were interpreted as signs of potential for consumer switching. All calculations were carried out using the R programming language.

For the last 15 years (2006-2020) landings data by size category were available. Size category of fish catches landed in the European Union are defined by regulation for 38 species or groups of species (COUNCIL REGULATION(EC) No 2406/96 of 26 November 1996 laying down common marketing standards for certain fishery products) allowing to analyse the relationship between inflation corrected prices and landings at different levels. The correlation between price per landings event and quantity landed was estimated for every species. As all blackspot seabream was landed as whole fresh fish, only fish sold in the same state was considered for all species.

## Results

Mean inflation corrected ex-vessel prices for blackspot seabream during 1973 and 2002 were similar to the prices fetched for the most valuable major species (European hake), while they were average compared to the list of high-value species (top row in Figure 1). For the period 2000 to 2020, price information for a larger number of species was available and the data were considered much more reliable than for the previous period. During this period, the ex-vessel price fetched by blackspot seabream was comparable to those of the highest priced species in the three considered species groups (bottom row in Figure 1). Since 2010, blackspot seabream has become the highest priced species landed by French vessels from the Bay of Biscay. This position might be due to its small availability on markets despite continuous high demand as French landings of blackspot seabream from the Bay of Biscay were typically less than 100 tonnes per year. Blackspot seabream becoming the most expensive species is an important change from the previous three decades during which most of the species in the high-value group fetched higher prices than blackspot seabream.

Annual landings for the period 1973-2002 reflected the well known rapid collapse of the blackspot seabream stock in the late 1970s (Figure 2). The collapse led to an increase in price of

blackspot seabream up to 1990 (0.47 €/year). European hake, pollock and white seabream landings also showed a strong decrease around fifteen years later than blackspot seabream in the mid 1980s. However, contrary to blackspot seabream, prices decreased parallel to landings for hake and white seabream. Several species in all species groups showed increasing landings during the period while prices increased, decreased or fluctuated with no clear trend depending on species. A notable case is common sole for which price increased steadily until the mid 1980s while landings remained more or less stable.

Considering the period 2000 to 2020, blackspot seabream landings first increased and then decreased again from the mid 2000s, following the introduction of a TAC in 2003, which was subsequently reduced. Since 2003, inflation corrected blackspot seabream prices increased steadily by 0.42 € per year (Figure 3). This is the strongest increase among all studied species for this period during which on average prices decreased slightly (mean -0.02 €/year). Decreasing landings in parallel to those of blackspot seabream were observed for the major species common sole and several of the high-value species (brill, pollock, red mullet, Atlantic bluefin tuna). Only for Atlantic bluefin tuna and pollock did prices increase however (0.16 €/year and 0.06 €/year respectively) while they decreased slightly for brill (0.05 €/year) and red mullet (0.03 €/year). The landings of related species, except black seabream, were increasing other the whole period while prices decreased (maximum -0.46 €/year for common pandora).

During the period 1973 to 2002, an overall significant negative relationship between prices and landings as seen for blackspot seabream was only found for three high-value species, while the correlation was positive for two species (brill and turbot) and not significant for the three remaining species (Figure 4a). Thus the results did not provide much evidence for our hypotheses for this period. The results were similar for the three major species, with one significant negative correlation, one positive and one species without correlation between prices and landings, not providing much evidence for the hypothesis of no relationship for this species group. The related species black seabream had a negative relationship between prices and landings, while white seabream showed a positive relationship (Figure 4a). Thus, the prices for these two species were not independent of landings as hypothesised, showing a classical price demand relationship for the white seabream and an inverse demand for black seabream. In summary, only five out of the 13 (38%) considered species showed evidence for an inverse demand system, independent of species group.

During the two decades 2000 to 2020, ex-vessel prices and landings were negatively correlated for most species (59%), including blackspot seabream, and irrespective of group (Figure 4b). This provides evidence for an overall inverse demand system during this period and contradicts the hypotheses for major and related species, for which no relationship was hypothesized. No relationship between price and landings was only found for common sole, axillary seabream and white seabream. For brill, the relationship was significantly positive during this period; it had also been positive during the first study period. Note that brill prices and landings both increased during the first study period and decreased during the second period (Figure 2 and 3).

The slope for the linear relationships between interannual relative changes in prices and interannual relative changes in landings was significantly negative for ten species (71%) during 1973 to 2002 and again ten species (58%) between 2000 and 2020, with seven species in common for the two periods (Table 1). Thus, for these species, years with higher interannual relative decrease in landings had lower relative increase in prices. For blackspot seabream, the

relationship was significantly negative only during the first study period. During the first period, the strongest negative relationship was found for angler and black seabream with price increases around 50% of landing decreases, i.e. a 1% landings decrease led to a 0.5% price increase on average (slopes -0.49 and -0.51). During the second period, the strongest negative relationships were found for common sole, red mullet and again black seabream, similarly with a smaller relative change in price compared to landings (slopes -0.56, -0.55, -0.53 respectively).

The correlations between blackspot seabream price and the price of other species during the period 1973-2002 was positive for most species, irrespective of species group (Figure 5a). Thus, there might not have been much price incentive for consumers to switch from blackspot seabream to these other species. In contrast, during the later period (2000-2020), blackspot seabream prices were significantly negatively correlated with all three major species, three high-value species out of ten (brill, red porgy and turbot), as well as the related axillary seabream and common pandora (Figure 5c). Hence, there might have been price incentives to switch to these species for consumers looking for alternatives to blackspot seabream. Considering correlations in landings, a change in the sign of relationships was observed between the two study periods, similarly to prices. During the first period, the correlation between blackspot seabream landings and those of the selected species were primarily negative for high-value species as well as two major species (Figure 5b). This means higher landings of these other species coincided with lower landings of blackspot seabream, in particular during the second half of the period, and hence might have provided scope for consumer switch. During the second period, correlations of blackspot seabream landings with those of high-values species were primarily positive for high-value species and two major species, except red porgy (Figure 5d). With relatively lower prices and higher landings during the period 2010-2020, the high-value related red porgy might have offered an alternative to blackspot seabream for consumers looking for a similar product. However, its price was above that of blackspot seabream from 2000 to around 2010 (Figure 1). Further, the average annual landings of red porgy during the second period were only 29 t, which is even less for than blackspot seabream for which it was 54 t (Table 1). Hence, taken together, these facts probably reduced the likelihood of red porgy having been a relevant alternative.

## Discussion

In this study, the inflation corrected ex-vessel price for the currently small stock of blackspot seabream was compared to three groups of species also landed by French vessels from the Bay of Biscay, including the three major demersal species in terms of volume, ten high-value species and four less valuable taxonomically related species. Several of the selected species, though landed in moderate quantities, are of high importance, if not vital, to some local fisheries (Daurès et al., 2009). Indeed, European small-scale fisheries depend economically on fewer species than large scale fisheries (Guyader et al., 2013). Separate analyses were carried out for two time series (1973-2002 and 2000-2020) as the databases differed in resolution and structure. For the former period, landings and price data were more aggregated and less reliable, with some species being probably confounded. Some species were therefore removed from the first data set.

In recent years, blackspot seabream was among the few higher priced species landed in French Atlantic ports. Until the 2000s, the decline in blackspot seabream stock abundance had a direct effect by reducing landings (Lorance, 2011). In more recent years, landings were constrained by TACs and hence most likely less directly linked to availability to fisheries. As the stock trend since 2000 is not known, the variation of price during this period can be considered an effect of management on landings rather than directly driven by stock abundance as in the early period.

Surprisingly, the inflation corrected price of blackspot seabream increased in recent years in a general context of overall stable or decreasing fish prices, considering all major commercial, high-value and taxonomically related species landed from the Bay of Biscay. Part of this may come from change in the size of blackspot seabream caught, as the proportion of larger individuals in landings increased in recent years.

Overall, we found that for blackspot seabream sale prices were higher in years with lower landings as expected in an inverse demand system often observed for fish (e.g. Barten and Bettendorf, 1989) but also bivalves (Lesur-Irichabeau et al., 2016). The same pattern was found for the majority of species selected for comparison during the second study period, irrespective of species group and in contradiction to our hypotheses. No dominant pattern emerged for the first study period, possibly due to the data being less reliable. Data from the historic period might have shown fluctuations which did not represent actual price variations. In particular, at the time, the same commercial name may have been used for different species, blurring any relationships between prices and landings. We tried to account for this by not analysing certain species, but the problem might have remained to some degree.

On the time scale of interannual changes, blackspot seabream prices did only increase between years when landings decreased during the period 1973-2002, but not after 2000. In contrast, such a relationship was found for the majority of other selected species, independent of species group. Thus, this provides some evidence for an inverse demand system operating in the Bay of Biscay also at the annual scale.

We also investigated the potential for consumer switch from the rarefying blackspot seabream to the other selected species by looking at the correlations between their prices and their landings. We interpreted negative correlations in prices or landings as potential for switching as price can be a barrier to fish consumption and lack of availability impact fish consumption (Carlucci et al., 2015). The negative correlations between blackspot seabream prices and those of some of the other species during the second study period might indicate the existence of price incentives. However, interpretation is hampered by the fact that no study evaluating the similarity in terms of consumer preference for the different studied species in comparison to blackspot seabream exists. In an older Scottish study, participants did not express any preference among nine common white fish species (Hamilton and Bennett, 1983). In this study, flavour was the most significant positive determinant of acceptability, while texture was neutral. Rickertsen et al. (2017) studied consumer attitudes and preferences of 276 French consumers using questionnaires and sensorial trials for farmed salmon and pangasius, and wild cod and anglerfish. In terms of taste, the participants' first preference was for salmon, followed by anglerfish. In terms of willingness-to-pay, anglerfish received the highest value, followed by cod. Thus, the negative correlation of anglerfish price with blackspot seabream, as well as the generally lower price, might have provided purchase incentives in recent decades. However, given blackspot seabream has fetched the highest prices of all species since 2010, price sensitive consumers will have had ample alternative choices cheaper than blackspot seabream.

Given the lower data quality for the first study period, attempts to compare prices presented here with other estimates of ex-vessel prices were made. The Sea around us (SAU) project has published reconstructed landings and prices (Pauly et al., 2020). Estimated landings of blackspot seabream for the Bay of Biscay from SAU were in the same range as landings reconstructed by Lorance (2011) but prices were very different from those estimated here because SAU estimated prices of groups of species where all seabream were included in. No explanation for this

difference could be found. The attempt to compare our data with the data made available by the Food and Agricultural Organisation (FAO) (Melnychuk et al., 2017) was not anymore successful, because numerous demersal species were attributed the same price in this database, while they clearly fetched very different prices in French Atlantic harbours. Given these results, we stuck to the data for which we knew the source despite the shortcomings for the earlier period.

### Acknowledgement

This study received funding from France Filière Pêche (DynRose project) and the European Union's Horizon 2020 research and innovation programme under Grant Agreement No 773713 (PANDORA).

### References

- Barten, A. P., and Bettendorf, L. J. 1989. Price formation of fish. An application of an inverse demand system. *European Economic Review*, 33: 1509-1525.
- Burgess, M. G., Costello, C., Fredston-Hermann, A., Pinsky, M. L., Gaines, S. D., Tilman, D., and Polasky, S. 2017. Range contraction enables harvesting to extinction. *Proceedings of the National Academy of Sciences of the United States of America*, 114: 3945-3950.
- Carlucci, D., Nocella, G., De Devitiis, B., Visceccchia, R., Bimbo, F., and Nardone, G. 2015. Consumer purchasing behaviour towards fish and seafood products. Patterns and insights from a sample of international studies. *Appetite*, 84: 212-227.
- Daurès, F., Rochet, M.-J., Van Iseghem, S., and Trenkel, V. M. 2009. Fishing fleet typology, economic dependence, and species landing profiles of the French fleets in the Bay of Biscay, 2000-2006. *Aquatic Living Resources*, 22: 535-547.
- FAO. 2022. Fishery and Aquaculture Statistics. Global production by production source 1950-2020 (FishStatJ). In: FAO Fisheries and Aquaculture Division [online]. Rome. Updated 2022. [www.fao.org/fishery/statistics/software/fishstatj/en](http://www.fao.org/fishery/statistics/software/fishstatj/en)
- FranceAgrimer. 2021. Consommation des produits de la pêche et de l'aquaculture 2020. <https://www.franceagrimer.fr/Actualite/Filieres/Peché-et-aquaculture/2021/Consommation-des-produits-de-la-peche-et-de-l-aquaculture-Donnees-2020>.
- Fryxell, J. M., Hilborn, R., Bieg, C., Turgeon, K., Caskenette, A., and McCann, K. S. 2017. Supply and demand drive a critical transition to dysfunctional fisheries. *Proceedings of the National Academy of Sciences of the United States of America*, 114: 12333-12337.
- Guichet, R., Gueguen , J., and Guillou, A. 1971. La peche du merlu et de la dorade à la Rochelle analyse des statistiques d'effort de peche et de production des années 1966, 1967 et 1968. *Revue des travaux de l'institut des pêches maritimes*, 35: 239-286.
- Guyader, O., Berthou, P., Koutsikopoulos, C., Alban, F., Demaneche, S., Gaspar, M. B., Eschbaum, R., et al. 2013. Small scale fisheries in Europe: A comparative analysis based on a selection of case studies. *Fisheries Research*, 140: 1-13.
- Hamilton, M., and Bennett, R. 1983. An investigation into consumer preferences for 9 fresh white fish species and the sensory attributes which determine acceptability. *Journal of Food Technology*, 18: 75-84.
- Lesur-Irichabeau, G., Guyader, O., Fresard, M., Leroy, C., Latouche, K., and Le Grel, L. 2016. Information on sellers and buyers characteristics: added value to explain price formation

- at primary fish markets in managed French scallop fisheries. *Applied Economics*, 48: 2078-2092.
- Lorance, P. 2011. History and dynamics of the overexploitation of the blackspot sea bream (*Pagellus bogaraveo*) in the Bay of Biscay *ICES Journal of Marine Science*, 68: 290–301.
- Magnusson, A. K., and Dekker, W. 2021. Economic development in times of population decline—a century of European eel fishing on the Swedish west coast. *ICES Journal of Marine Science*, 78: 185-198.
- Maynou, F. 2022. Sale price flexibilities of Mediterranean hake and red shrimp. *Marine Policy*, 136.
- Melnichuk, M. C., Clavelle, T., Owashi, B., and Strauss, K. 2017. Reconstruction of global ex-vessel prices of fished species. *ICES Journal of Marine Science*, 74: 121-133.
- Nauman, F. A., Gempesaw, C. M., and Bacon, J. R. 1995. Consumer choice for fresh fish: factors affecting purchase decisions. *Marine Resource Economics*, 10: 117-142.
- Pascoe, S., Schrobbback, P., Hoshino, E., and Curtotti, R. 2022. Impact of changes in imports and farmed salmon on wild-caught fish prices in Australia. *European Review of Agricultural Economics*, jbac003.
- Pauly, D., Zeller, D., and Palomares, M. L. D. E. 2020. Sea Around Us Concepts, Design and Data ([seaaroundus.org](http://seaaroundus.org)).
- Pincinato, R. B. M., Asche, F., and Oglend, A. 2020. Climate change and small pelagic fish price volatility. *Climatic Change*.
- Rickertsen, K., Alfnes, F., Combris, P., Enderli, G., Issanchou, S., and Shogren, J. F. 2017. French Consumers' Attitudes and Preferences toward Wild and Farmed Fish. *Marine Resource Economics*, 32: 59-81.
- Rincon, L., Luis Castro, P., Alvarez, B., Dolores Hernandez, M., Alvarez, A., Claret, A., Guerrero, L., et al. 2016. Differences in proximal and fatty acid profiles, sensory characteristics, texture, colour and muscle cellularity between wild and farmed blackspot seabream (*Pagellus bogaraveo*). *Aquaculture*, 451: 195-204.

Table 1 Mean landings (t) and results for linear relationships between interannual relative changes in landings and interannual relative changes in ex-vessel prices for selected species in the Bay of Biscay. Negative slopes mean prices decreased as landings increased. Species groups: 1 major species; 2 high-value species; 3 related species.

Name	Group	TAC	1973-2002			2000-2020		
			Landings	Slope	Pval vue	r <sup>2</sup>	Landings	Slope
<b>Blackspot</b>		2003						
<b>seabream</b>			1054	-0.24	0.03	0.17	54	-0.11
<b>Angler</b>	1		14536	-0.49	0	0.41	20213	-0.37
<b>Common sole</b>	1		6386	-0.11	0.38	0.03	7914	-0.56
<b>European hake</b>	1		15242	-0.25	0.03	0.16	24984	-0.16
<b>Atlantic bluefin</b>	2							
<b>tuna</b>			496	-0.15	0.01	0.31	639	-0.3
<b>Brill</b>	2		363	0.04	0.75	0	522	0.02
<b>European</b>	2							
<b>seabass</b>			2438	-0.21	0.03	0.17	4568	-0.42
<b>Gilthead</b>	2	none						
<b>seabream</b>			143	-0.06	0.45	0.02	409	-0.25
<b>John dory</b>	2	none	634	-0.19	0.04	0.15	1606	-0.31
<b>Meagre</b>	2	none					807	-0.18
<b>Pollack</b>	2		4903	-0.27	<0.01	0.32	3337	-0.36
<b>Red mullet</b>	2		1746	-0.37	<0.01	0.8	3110	-0.55
<b>Red porgy</b>	2	none					29	-0.01
<b>Turbot</b>	2		707	-0.11	0.13	0.08	728	-0.03
<b>Axillary</b>	3	none						
<b>seabream</b>							46	0.08
<b>Black seabream</b>	3	none	2767	-0.51	<0.01	0.54	3506	-0.53
<b>Common</b>	3	none						
<b>pandora</b>							29	-0.04
<b>White seabream</b>	3	none	161	-0.22	0.04	0.19	202	0.01

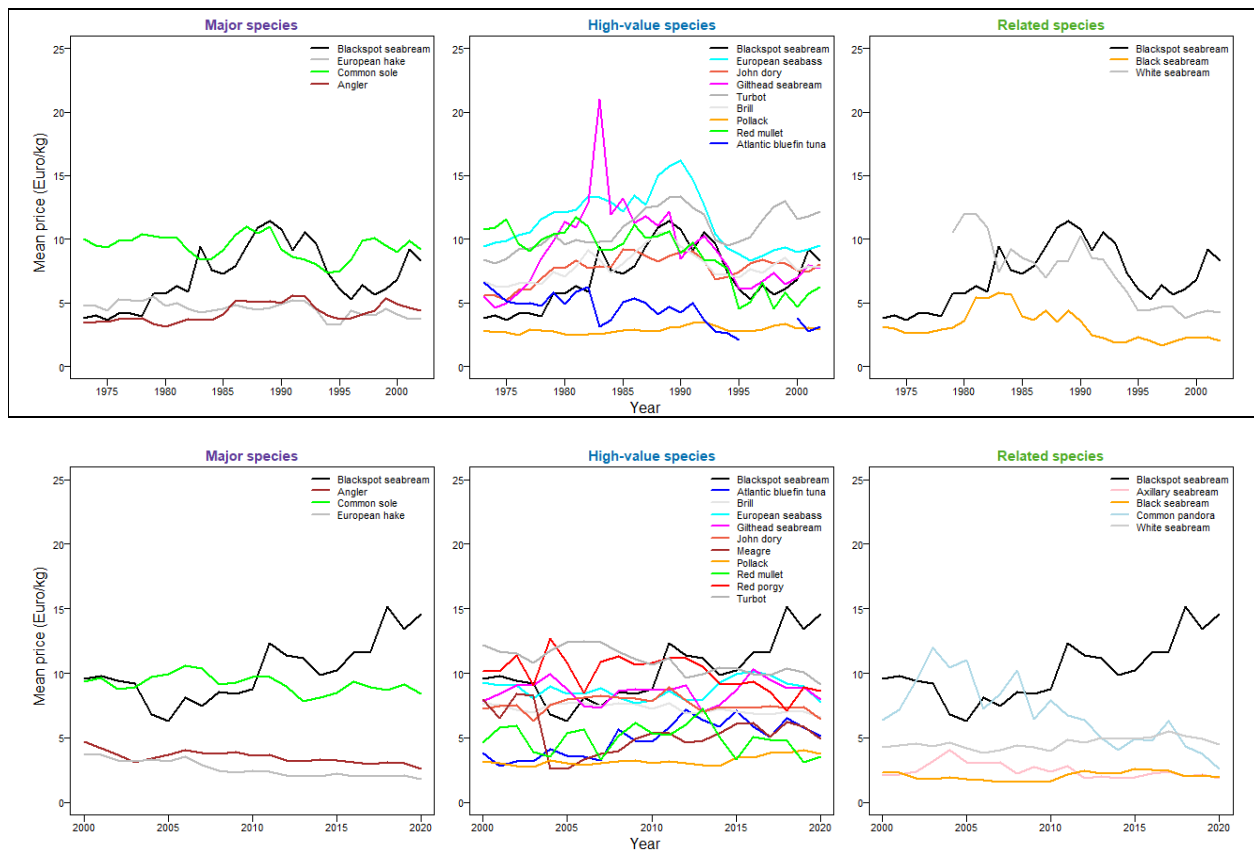


Figure 1: Time series of mean inflation corrected ex-vessel prices for blackspot seabream and selected species from the Bay of Biscay for the period 1973 to 2002 (top row) and 2000 to 2020 (bottom row).

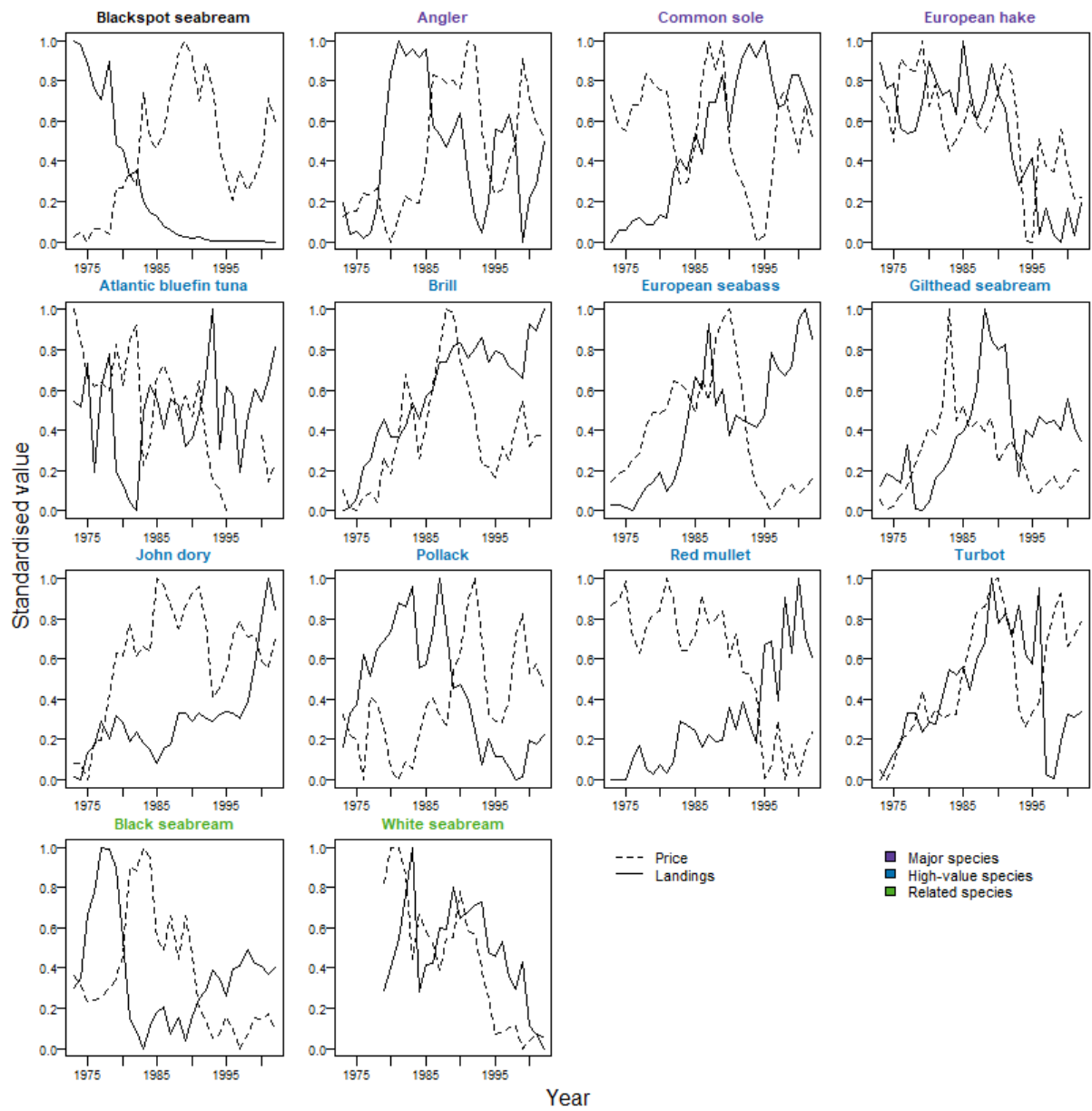


Figure 2: Time series of standardised annual French landings and mean ex-vessel prices for selected species in the Bay of Biscay for the period 1973 to 2002.

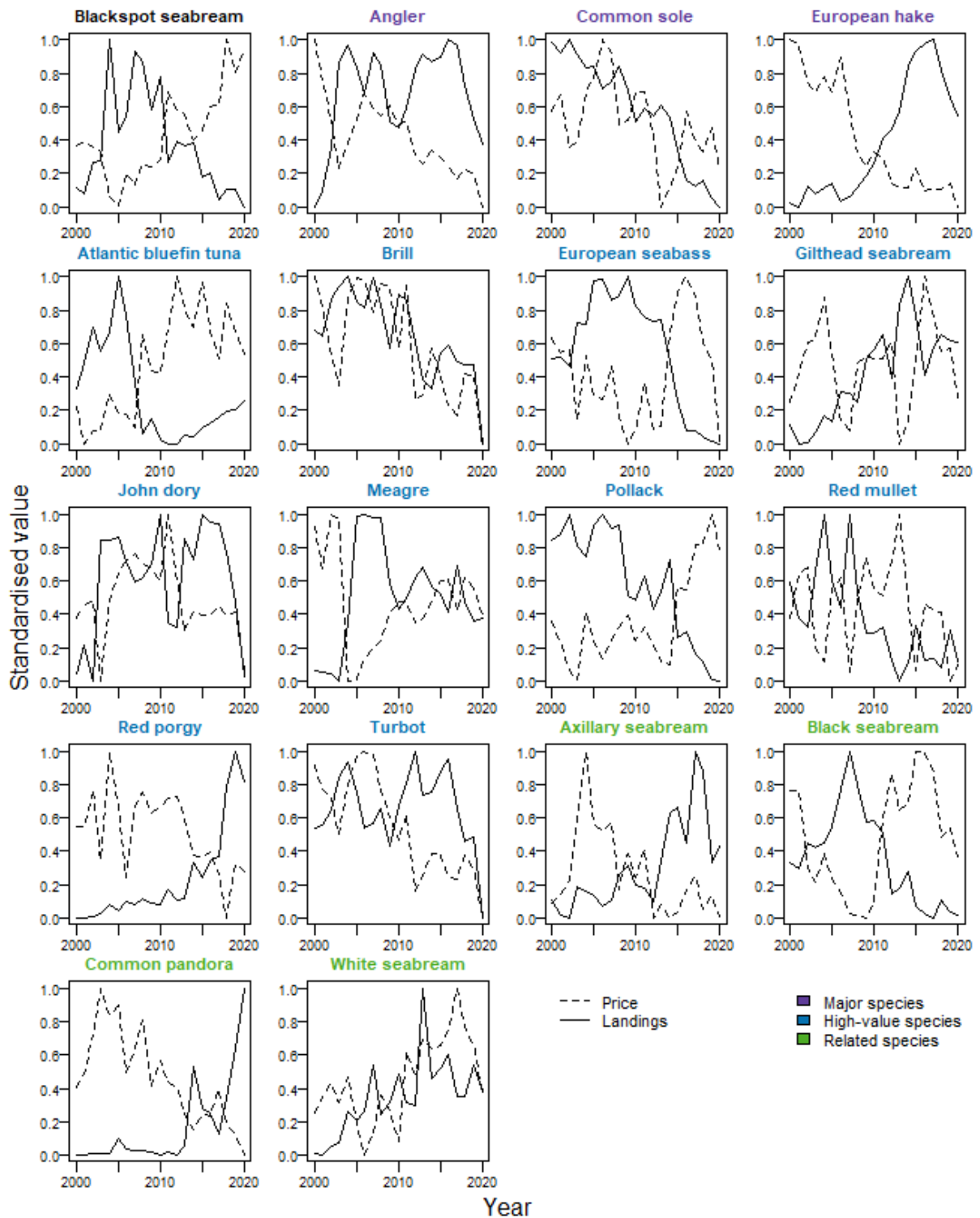


Figure 3: Time series of standardised annual French landings and mean ex-vessel prices for selected species in the Bay of Biscay for the period 2000 to 2020.

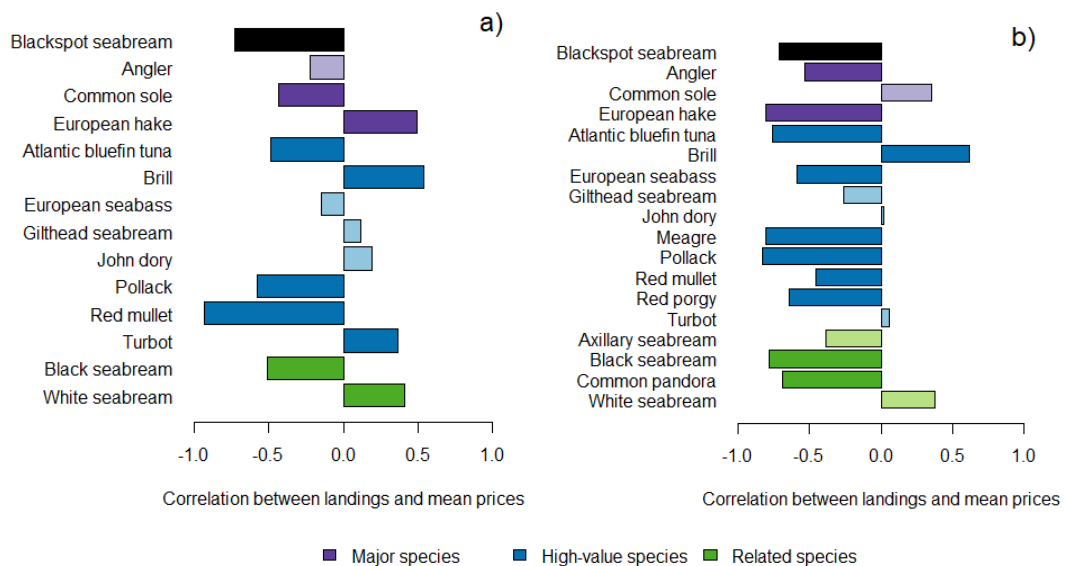


Figure 4: Pearson correlation coefficients between mean prices and landings in the Bay of Biscay for blackspot seabream and selected species from three species groups. a) 1973 to 2002. b) 2000-2020. Significant correlations ( $p < 0.05$ ) in darker colour.

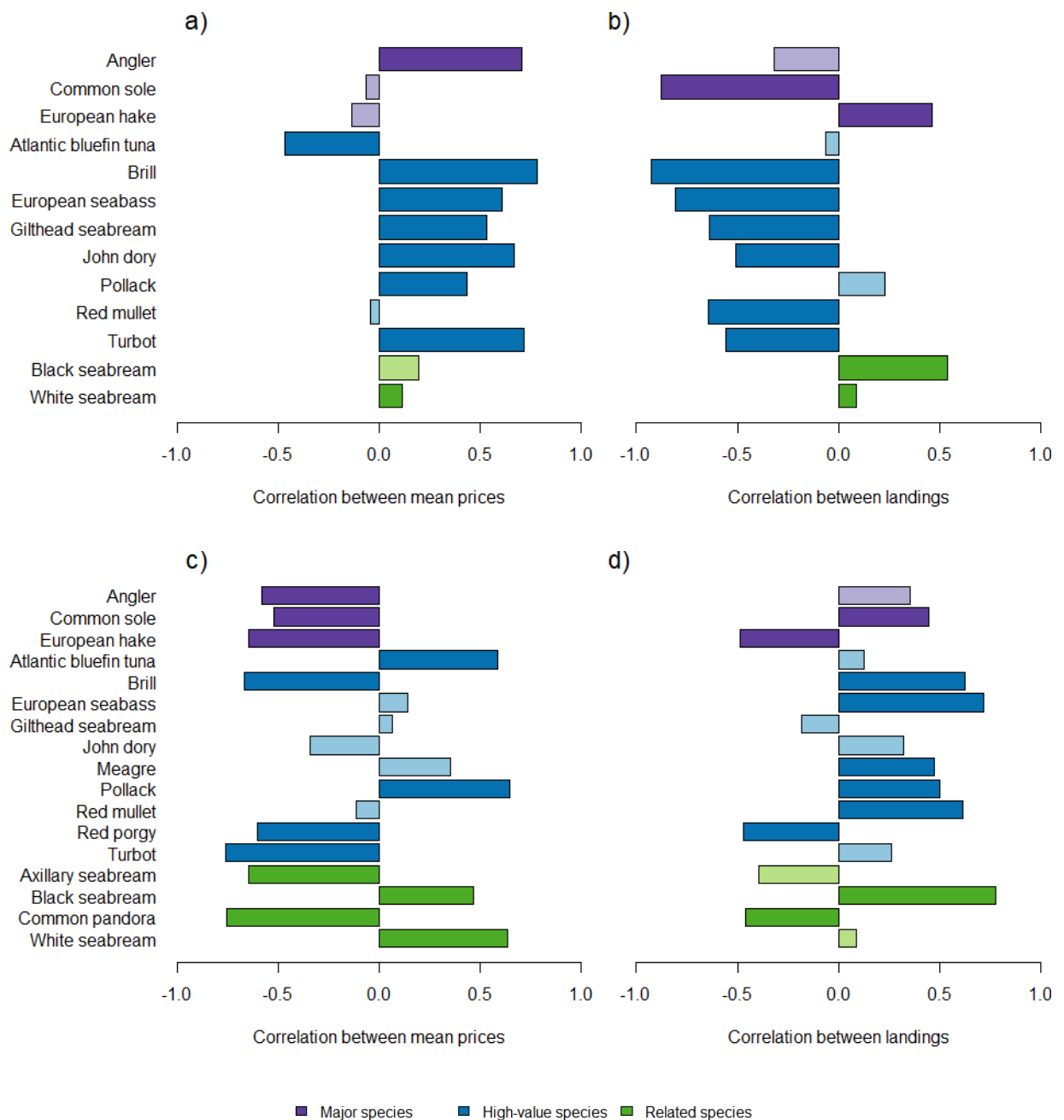


Figure 5: Pearson correlation coefficients between blackspot seabream mean prices and those of selected species (a and c) and blackspot seabream landings and those of selected species (b and d) in the Bay of Biscay. a) & b) 1973 to 2002. c) & d) 2000-2020. Significant correlations ( $p < 0.05$ ) in darker colour.

Annexe3  
Rapport sur la paramétrisation d'un modèle DEB

# **DynRose : Paramétrisation d'un modèle *Dynamic Energy Budget* model sur la Dorade rose (*Pagellus bogaraveo*)**

Fabri-Ruiz, S., Lorance, P., Trenkel, V

## **Introduction**

Le modèle DEB fournit une description mécanistique et quantitative des flux d'énergie dans un organisme qui assimile et utilise l'énergie pour sa maintenance, sa croissance et sa reproduction tout au long de son cycle de vie (Kooijman, 2009). La théorie DEB vise à décrire comment les flux d'énergie des espèces changent en fonction des conditions environnementales (ici la disponibilité en nourriture et la température). Elle s'appuie sur des hypothèses tirées des principes de la thermodynamique et plus spécifiquement des lois de la conservation de la masse et de l'énergie (Jusup et al., 2017). Le modèle DEB a été appliqué à de nombreux taxons aussi bien marins que terrestres ainsi qu'à des espèces présentant de vastes distributions géographiques (van der Meer, 2006). L'un des principaux avantages d'un modèle DEB est qu'il est basé sur une théorie générique, ce qui signifie que la même structure de modèle peut être appliquée à différentes espèces, où seules les valeurs des paramètres diffèrent (Marques et al., 2018). Compte tenu de sa non-spécificité, la théorie DEB a été largement appliquée et testée avec succès pour un grand nombre d'espèces de poissons pour répondre à des questions de recherches variées. Parmi les applications, on pourra citer la simulation de la croissance et de la reproduction des poissons plats (van der Veer et al., 2009, 2003) et de l'anchois (Pecquerie et al., 2009) dans des conditions environnementales variables, la prévision des effets métaboliques des radionucléides (uranium) sur des individus de poissons zèbres (Augustine et al., 2012), la description des facteurs biologiques influençant la bioaccumulation des polluants organiques persistants (PCBs) dans le merlu européen (Bodiguel et al., 2009) et la sole commune (Eichinger et al., 2010) à travers l'ontogénèse des poissons et, la description du cycle de vie complet des espèces de poissons migrateurs écologiquement et économiquement importants tels que le saumon du Pacifique (Pecquerie et al., 2011) et le thon rouge du Pacifique (Jusup et al., 2011).

Il n'existe aucun modèle paramétré pour la Dorade rose (*Pagellus bogaraveo*) à l'heure actuelle or ce type de modèle permettrait de comprendre quelles sont les mécanismes qui occasionnent une migration depuis la zone côtière vers la zone mésopélagique lors du passage à l'âge adulte ou encore d'explorer les raisons du changement de sexe ou non qui se produisent au cours du cycle de vie des individus. Une étape préalable pour explorer ces questions de recherche est la paramétrisation du modèle DEB. Dans ce rapport technique, une première estimation des paramètres du modèle DEB pour l'espèce *Pagellus bogaraveo* est présentée.

## **Matériel et méthodes**

### **1) Description du modèle**

Le modèle DEB établit les flux d'énergie entre quatre variables d'état : la réserve ( $E$ ), la structure ( $V$ ), la maturation ( $E_H$ ) et le tampon reproducteur ( $E_R$ ).  $E$ ,  $V$  et  $E_R$  sont les variables d'état qui constituent la biomasse de l'organisme (Figure 1).

L'énergie pénètre dans l'organisme sous la forme de nourriture (X) par ingestion à un taux (Eq.1)

$$\dot{p}_X = \{\dot{p}_{Xm}\}fL^2 \text{ [Eq. 1]}$$

Avec  $f = \frac{X}{X+X_K}$  correspondant à la réponse fonctionnelle de type II de Hollings comprise entre [0,1], où 0 correspond à des conditions dites de « famine » and 1 des conditions de nourriture *ad libitum*. L'ingestion dépend donc de la nourriture ( $f$ ), de la surface ( $L^2$ ) et du taux d'ingestion maximale spécifique à la surface ( $\{\dot{p}_{Xm}\}$ ). L'énergie est ensuite assimilée dans la réserve à un taux ( $\dot{p}_A$ ). Cette transformation entraîne la production de fèces et de minéraux. L'énergie sortant de la réserve ( $\dot{p}_C$ ) est subdivisée selon la "règle de kappa" (règle  $\kappa$ ). Une fraction  $\kappa$  est allouée et répartie entre la maintenance somatique ( $\dot{p}_M$ ), et la croissance, tandis qu'une fraction  $1-\kappa$  est utilisée pour la maintenance de la maturité ( $\dot{p}_J$ ) et la maturation ( $\dot{p}_R$ ). Il n'y a pas de compétition entre les deux branches, c'est-à-dire qu'un organisme peut continuer de grandir et se reproduire en même temps. L'énergie est néanmoins toujours prioritairement allouée à la maintenance (maintenance somatique et maintenance de la maturité) de telle sorte que, si le taux d'utilisation de l'énergie issue des réserves  $E$  n'est pas suffisant pour «payer» le coût de la maintenance somatique, l'individu puise alors l'énergie dans son compartiment de reproduction  $E_R$  puis dans celle allouée à sa structure  $V$ .

Dans le modèle DEB, le cycle de vie est caractérisé par trois étapes qui se distinguent par leur flux d'énergie : Embryon, Juvénile et Adulte. L'embryon n'assimile pas de nourriture ( $E_H=E_H^h$ ). La deuxième étape est la phase juvénile qui a lieu après la naissance ( $E_H=E_H^b$ ). La transition entre l'embryon et le stade juvénile se produit une fois que l'individu a atteint un seuil particulier d'énergie investie dans le développement. A ce moment, l'individu est suffisamment complexe pour commencer à se nourrir et utiliser l'énergie acquise dans les aliments pour continuer son développement, sa croissance et sa maintenance, mais il n'accorde pas d'énergie à la reproduction. Un investissement supplémentaire dans le développement conduit à une deuxième transition qui est la transition entre le stade juvénile et adulte, appelée puberté. Lorsque l'organisme devient adulte, il cesse d'attribuer de l'énergie au développement et redirige l'énergie vers la reproduction et donc la formation de gamètes ( $E_H>E_H^p$ ). Le niveau de maturité contrôle les transitions des phases du cycle de vie complet de l'organisme. La représentation schématique et la description du modèle sont données dans la Figure 1, et la spécification et la dynamique des variables d'état et des flux d'énergie sont énumérées dans la Table 1, avec les paramètres donnés dans la Table 2.

Le cycle de vie de certains poissons comprend une phase larvaire et une métamorphose en forme juvénile. La phase larvaire et la métamorphose qui s'ensuit coïncident souvent avec une accélération métabolique, c'est-à-dire une augmentation progressive des valeurs de certains paramètres entre la naissance et la métamorphose (Kooijman et al., 2011). Une telle transition nécessite généralement une extension du modèle DEB standard (Marques et al., 2018) en modèle ici abj.

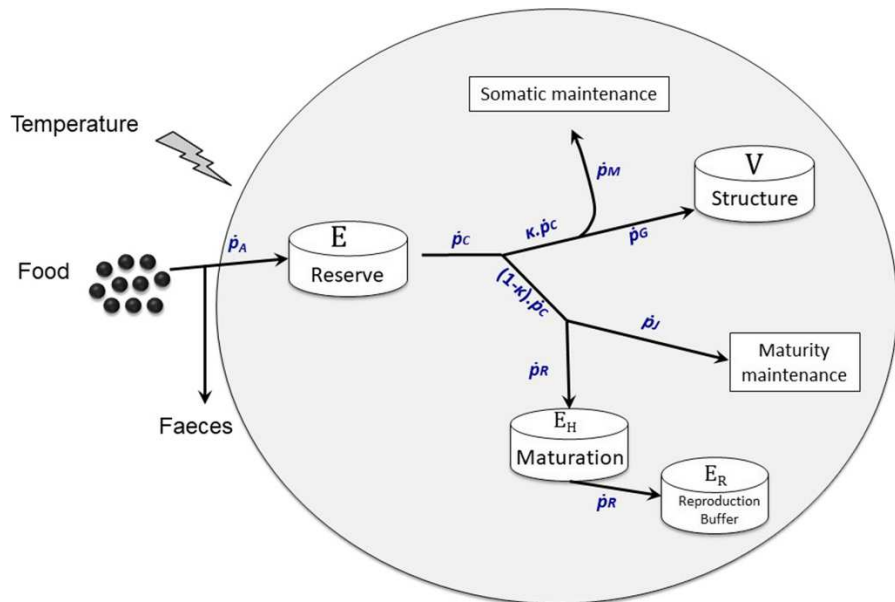


**Figure 1** : Représentation conceptuelle des processus métaboliques. Les flèches pleines représentent les flux d'énergie standard, et les cases marquent les variables d'état. L'énergie est assimilée de la nourriture dans la réserve et ensuite allouée pour alimenter les processus métaboliques : une fraction fixe  $\kappa$  du flux mobilisé est allouée à la maintenance somatique et à la croissance, et la fraction restante ( $1-\kappa$ ) à l'augmentation et au maintien de la maturité, ou vers la reproduction.

### 1) Estimation des paramètres du modèle DEB

Un modèle DEB se compose de paramètres primaires et de paramètres composés. Les paramètres primaires sont intimement liés à un seul processus sous-jacent, tandis que les paramètres composés dépendent généralement de plusieurs processus sous-jacents. Les paramètres composés peuvent être dérivés des paramètres primaires en utilisant les formulations de la théorie (Kooijman, 2009). Les paramètres primaires de la théorie DEB peuvent être divisés en paramètres principaux et paramètres auxiliaires (Lika et al., 2011a). Ces paramètres contrôlent directement les variables d'état (à l'exception de l'efficacité de la défécation) (Figure 2, Table 2). La théorie DEB suppose que les variables d'état ne sont pas directement mesurables (empiriquement), mais elle décrit pleinement leur dynamique par un ensemble d'équations qui caractérisent l'état physiologique de l'individu à l'aide des paramètres du modèle. Les paramètres auxiliaires permettent de relier les variables d'état à des quantités mesurables comme la taille, le poids, la respiration, etc. Tous ces paramètres ne sont pas fournis par le modèle et doivent donc être estimés grâce aux données « réelles ». C'est ce qu'on appelle l'estimation.

**Table 1** : Variables d'état et dynamique pour un individu

Variables d'états (unités)	Description	Dynamiques
$E (J)$	Energie de la réserve	$\frac{dE}{dt} = \dot{p}_A - \dot{p}_C$
$V (cm^3)$	Volume structurel	$\frac{dV}{dt} = \frac{\dot{p}_C}{[E_G]}$
$E_H (J)$	Energie investie dans la maturation	$\frac{dE_H}{dt} = \dot{p}_R (E_H < E_H^P)$
$E_R (J)$	Energie investie dans la reproduction	$\frac{dE_R}{dt} = \dot{p}_R (E_H = E_H^P)$
Processus	Flux d'énergie ( $J \cdot d^{-1}$ )	
Assimilation :	$\dot{p}_A = \{\dot{p}_{Am}\} f L^2 (E_H > E_H^b)$	
Mobilisation :	$\dot{p}_C = E \frac{\dot{v}[E_G]L^2 + \dot{p}_S}{[E_G]L^3 + \kappa E}$	
Maintenance somatique :	$\dot{p}_S = [p_M]L^3$	
Maintenance de la maturité :	$\dot{p}_J = k_J E_H$	
Croissance :	$\dot{p}_G = \kappa \dot{p}_C - \dot{p}_S$	
Maturité/reproduction :	$\dot{p}_R = (1 - \kappa) \dot{p}_C - \dot{p}_J$	

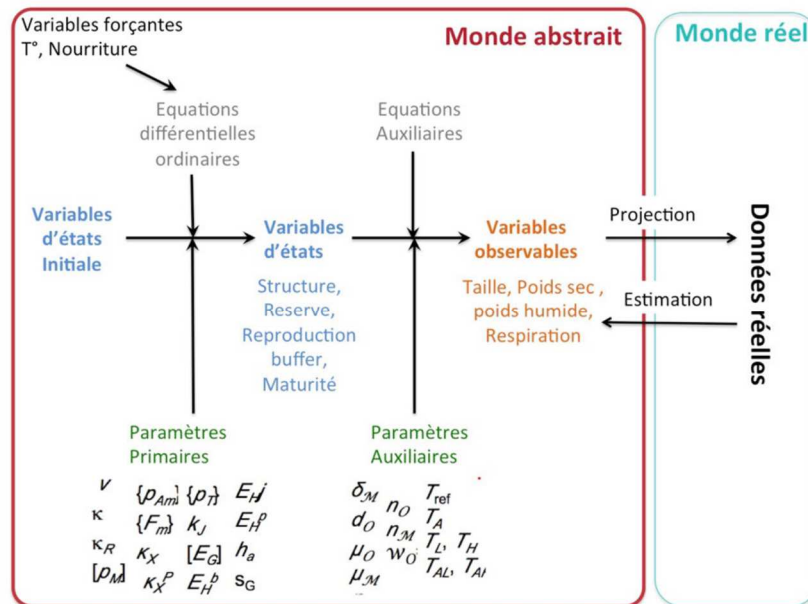


**Figure 2** : Schématisation de la relation entre le monde abstrait, c'est-à-dire le modèle de la théorie DEB, et le monde réel où les données proviennent d'études expérimentales, de la littérature ou de données de terrain (Fabri-Ruiz (2018) modifié de © L. Pecquerie).

**Table 2** : Valeurs des paramètres primaires et auxiliaires estimées par la méthode de covariation (Lika et al., 2011a, 2011b; Marques et al., 2018).

Paramètres du DEB	Unité	Valeurs
<b>Paramètres primaires</b>		
$z$ , zoom factor *	–	5.942
$zm$ , zoom factor for male *		9.241
$\{F_m\}$ , maximum specific searching rate	$L d^{-1} cm^{-2}$	6.5
$\kappa_X$ , digestion efficiency of food to reserve	–	0.8
$\dot{v}$ , energy conductance *	$cm d^{-1}$	0.02781
$\kappa$ , allocation fraction to soma *	–	0.7524
$\kappa_R$ , reproduction efficiency	–	0.95
$[p_M]$ , volume-specific somatic maintenance *	$J cm^{-3}d^{-1}$	20.25
$k_j$ , maturity maintenance rate coefficient	$d^{-1}$	0.002
$[E_G]$ , specific cost for structure	$J cm^{-3}$	5216
$E_H^h$ , energy maturity at hatching *	J	0.04711
$E_H^b$ , energy maturity at birth *	J	0.2668
$E_H^j$ , energy maturity at metamorphosis *	J	1.542
$E_{Hf}^p$ , energy maturity at puberty for female *	J	3.34E+05
$E_{Hm}^p$ , energy maturity at puberty for male *		3.33E+05
$\ddot{h}_a$ , Weibull aging acceleration *	$d^{-2}$	1.49E-10
$S_G$ , Gompertz stress coefficient	–	0.0001
<b>Paramètres auxiliaires</b>		
$\delta_{M.emb}$ , shape coefficient embryos *	–	0.09897
$\delta_M$ , shape coefficient *	–	0.2145
f1 scaled functional response for field data *	-	1
f2 scaled functional response (de Almeida Ozório et al., 2009) *	-	1.07
f3 scaled functional response (Ribeiro et al., 2008) *	-	1.291
f4 scaled functional response (Olmedo et al., 2000) *	-	1.2
f5 scaled functional response for SilvGal2011 *	-	1.18
$T_A$ , Température d'Arrhenius *	K	5540

\* Paramètres estimés par le modèle dit “non fixés”.

L'estimation des paramètres du modèle repose donc sur la qualité et la quantité de données disponibles. Pour ce faire, le modèle requiert deux types de données comprenant les données réelles et les pseudo-données.

Les données réelles sont de deux types :

- Les données zero variées qui correspondent à une caractéristique de l'organisme à un temps unique t.
- Les données univariées qui comprennent des données appariées, où une variable est indépendante (par exemple, le temps, la température) et l'autre dépendante (par exemple, la masse, la consommation d'oxygène).

Les pseudo-données sont un ensemble de valeurs de paramètres pour un organisme généralisé obtenu à partir d'une vaste collection de paramètres estimés pour une grande variété d'espèces. Le concept de pseudo-données est utilisé pour éviter une combinaison irréaliste de paramètres. L'ensemble des données utilisées pour paramétriser le modèle DEB sont présentées Table 3.

Compte tenu des données disponibles, certains paramètres (Table 2) ne peuvent être estimés, ils sont alors dit fixés.

**Table 3** : Données zero-variées et univariées utilisées pour l'estimation des paramètres du modèle DEB de la Dorade rose. Les références des données observées, la valeur modélisée par le modèle DEB et l'erreur relative (RE) associées sont précisées.

Zero-Variate data	Experimental data	Modeled data	Relative Error	Sources
Age at hatching (14°C) (days)	4	4.946	0.2366	(Silva and Galante, 2011)
Age at hatching (18°C) (days)	3	3.795	0.2648	(Silva and Galante, 2011)
Age at birth (14°C) (days)	13	10.2	0.215	(Silva and Galante, 2011)
Age at birth (18°C) (days)	9	7.828	0.1302	(Silva and Galante, 2011)
Age at puberty for female (days)	2920	1237	0.5765	(Krug, 1998)
Age at puberty for male (days)	2372	1755	0.2603	(Krug, 1998)
Life span (days)	7300	3.15E+04	3.316	(Gueguen, 1969)
Length at hatching (14°C) (cm)	0.37	0.3044	0.1774	(Peleteiro et al., 1997)
Length at hatching bis (14°C) (cm)	0.34	0.3044	0.1048	(Silva and Galante, 2011)
Length at hatching (18°C) (cm)	0.39	0.3044	0.2196	(Silva and Galante, 2011)
Length at birth (14°C) (cm)	0.492	0.2504	0.4911	(Peleteiro et al., 1997)
Length at birth (14°C) bis (cm)	0.49	0.2504	0.4891	(Silva and Galante, 2011)
Length at birth (18°C) (cm)	0.49	0.2504	0.4891	(Silva and Galante, 2011)
Length at puberty for female (cm)	36	24.57	0.3174	(Krug, 1998)
Length at puberty for male (cm)	30	37.33	0.2442	(Krug, 1998)
Ultimate total length (cm)	70	58.63	0.1625	(Gueguen, 1969)
Wet weight at hatching (14°C) (g)	0.00025	0.0002207	0.117	(Silva and Galante, 2011)
Wet weight at hatching (18°C) (g)	0.00025	0.0002207	0.117	(Silva and Galante, 2011)
Wet weight at birth (14°C) (g)	0.00027	0.0003832	0.4191	(Silva and Galante, 2011)
Wet weight at birth (18°C) (g)	0.00033	0.0003832	0.1611	(Silva and Galante, 2011)
Ultimate wet weight (g)	4616	4473	0.03101	(Gueguen, 1969)
Univariate data				
Number of oocytes ~ Length (cm), year 1984		Figure 3.a	0.4022	(Krug, 1990)

Number of oocytes ~ Length (cm), year 1985	Figure 3.a	0.405	(Krug, 1990)
Number of oocytes ~ Length (cm), year 1986	Figure 3.a	0.5173	(Krug, 1990)
Number of oocytes ~ Length (cm), year 1987	Figure 3.a	0.3244	(Alcazar et al., 1987)
Wet weight (g) ~ Time (days), at f= 0.6	Figure 3.b	0.1616	(de Almeida Ozório et al., 2009)
Wet weight (g) ~ Time (days), at f= 0.8	Figure 3.b	0.1758	(de Almeida Ozório et al., 2009)
Wet weight (g) ~ Time (days), at f= 1	Figure 3.b	0.1723	(de Almeida Ozório et al., 2009)
Wet weight (g) ~ Length (cm) at 19°C	Figure 3.c	0.5371	(Olmedo et al., 2000)
Wet weight (g) ~ Length (cm) vs	Figure 3.c	0.5307	(Sánchez, 1982)
Change in length ( $\text{cm} \cdot \text{d}^{-1}$ ) ~ Length at first capture (cm)	Figure 3.d	0.8095	Juan Gil comm pers.
Change in weight ( $\text{g} \cdot \text{d}^{-1}$ ) ~ Weight at first capture (g)	Figure 3.e	0.543	Juan Gil comm pers.
Length (cm) ~ Time since hatching (days)	Figure 3.f	0.4421	(Fernandez-Pato et al., 1990)
Fork length (cm) ~ Time since hatching (days)	Figure 3.g	0.1326	(Higgins et al., 2015)
Length (cm) ~ Time since hatching (days)	Figure 3.h	0.4685	(Peleteiro et al., 1997)
Length (cm) ~ Time since hatching (days)	Figure 3.i	0.3619	(Silva et al., 2009)
Length (cm) ~ Time since hatching (days)	Figure 3.j	0.1076	(Sobrino and Gil, 2001)
Change in length (cm) ~ Time (days) at 19°C	Figure 3.k	0.379	(Olmedo et al., 2000)
Wet weight (g) ~ Time since hatching (days)	Figure 3.l	0.1232	(Pinho et al., 2014)
Dry weight (g) ~ Time since hatching (days)	Figure 3.m	0.1582	(Ribeiro et al., 2008)

La température d'Arrhenius ( $T_A$ ) fournit des informations sur la variation des taux métaboliques en fonction de la température et peut être calculée à partir des valeurs observées du taux métabolique mesuré à différentes températures (Eq.2).

$$\dot{k}(T) = \dot{k}(T_1) \cdot e^{\left(\frac{T_A - T}{T_1}\right)} \quad [Eq. 2]$$

$\dot{k}(T)$  : Taux à la température T (K)

$\dot{k}(T_1)$  : Taux à la température de référence ( $T_1$ )

$T_A$  : Température d'Arrhenius

$T_1$  : Température de référence (K)

Les données qui sont liées à des taux, comme l'âge à la naissance ou à la puberté, ou la reproduction à une certaine taille, sont couplées avec des données de température correspondante. La température des données expérimentales a été indiquée quand l'information était disponible. Pour les données issues de prélèvements réalisées en milieu naturel, la température a été déterminée en réalisant des climatologies. Les données de température ont été extraites à partir de réanalyses issues de la base de données Copernicus ([https://resources.marine.copernicus.eu/product-detail/GLOBAL\\_MULTIYEAR\\_PHY\\_001\\_030/INFORMATION](https://resources.marine.copernicus.eu/product-detail/GLOBAL_MULTIYEAR_PHY_001_030/INFORMATION), consultée le 28/06/2022). La profondeur et l'emprise spatiale pour chaque donnée sont indiquées en Table 4. La valeur moyenne de température a été retenue pour corriger les calculs du modèle et tenir compte de son effet.

**Table 4** : Valeurs de températures moyennes associées à l'emprise spatiale et temporelle des données collectées en milieu naturel

Publications	N	S	O	E	Mois	Années	Profondeur (m)	Température moyenne (°C)
Gueguen (1969)	49	43	-7	0	Septembre-octobre	1993-2020	200	11.8
Krug (1998)	42	38	-1	6	Tous	1993-2020	200	13.87
Sanchez (1982)	44	43	-5	-1	Septembre	1993-2020	100	12.18
Pinho et al., 2014	41	36	-33	-23	Tous	1998-2010	200	14.36
Sobrino and Gil (2001)	36	36	-6	-5	Tous	1993-2003	100	15.32
Higgins et al., 2015 et Krug (1990)	41	36	-33	-23	Tous	1998-2010	200	14.37
Alcazar et al., 1987	44	43	-5	-1	Septembre	1993-2020	100	12.18
Juan Gil Comm.pers	36	36	-6	-5	Tous	1993-2020	100	14.36

Pour la paramétrisation du modèle, nous avons fait l'hypothèse que la valeur de la réponse fonctionnelle en milieu naturel à  $f = 1$  pour laquelle nous supposons que les animaux sont nourris en conditions ad libitum. Les données expérimentales ont été non fixées à l'exception des données d'Olmedo et al (2008) afin d'éviter une valeur de  $f$  aberrante.

A partir de ces données, les paramètres de la DEB ont été estimés en utilisant la méthode de covariation (Lika et al., 2011a, 2011b), qui vise à rechercher la combinaison de paramètres (Table 1) qui minimise la différence entre les observations et les prédictions. L'approximation des valeurs des paramètres est effectuée à l'aide d'une optimisation numérique de Nelder-Mead afin de minimiser la différence entre les valeurs observées et prédites sur la base d'un critère des moindres carrés pondérés. L'évaluation de l'estimation des paramètres est évaluée en calculant l'erreur quadratique moyenne symétrique (SMSE) variant entre 0 et 1 et l'erreur relative moyenne (MRE) qui peut varier entre 0 et  $\infty$ . Pour chaque donnée univariée et zéro-variée, l'erreur relative a été calculée comme le rapport entre la valeur de l'erreur absolue et la valeur de la variante.

L'estimation des paramètres de paramètres a été réalisée avec les modules AmPtool (<https://github.com/add-my-pet/AmPtool>) et DEBTool ([https://github.com/add-my-pet/DEBtool\\_M/](https://github.com/add-my-pet/DEBtool_M/)) sous Matlab 2021b.

La paramétrisation fait appel à quatre fichiers différents (Marques et al., 2018) :

- mydata\_Pagellus\_bogaraveo.m contient les données pour ajuster le modèle (données à zéro variées et univariées), y compris les références. Ce fichier contient également les coefficients de pondération pour toutes les données.
- predict\_Pagellus\_bogaraveo.m contient le code permettant de relier les données observées aux résultats du modèle, on y retrouve les équations auxiliaires.
- pars\_Pagellus\_bogaraveo.m contient les valeurs de paramètre au début de la procédure d'optimisation.
- run\_Pagellus\_bogaraveo.m : contient les paramètres de la procédure d'optimisation.

## Résultats et Discussion

### 1) Qualité d'ajustement du modèle DEB

L'exhaustivité (ou *completeness*) des données réelles dans le modèle abj-DEB développé pour *P.bogaraveo* était de 3 (Lika et al., 2011a). Les valeurs des paramètres sont résumées en Table 2. L'ajustement global du modèle a donné une erreur relative absolue moyenne (MRE) de 0.417 et une erreur quadratique moyenne (SMSE) de 0.222. Concernant les données zero-variées, les données d'âge, de poids et de taille à éclosion ainsi que le poids et la taille maximal

présentes des erreurs relatives faibles ( $RE < 0.27$ ). L'erreur relative pour les âges à la naissance est également peu élevée ( $RE < 0.215$ ), à l'inverse des tailles pour ce même stade ( $RE \sim 0.48$ ). La durée de vie totale est en revanche très mal estimée ( $RE = 3.3116$ ). L'écart observé entre les données prédictes et modélisées pour l'âge et la taille à la puberté peut s'expliquer par le fait que ces données reposent sur des ogives de maturité. Cette dernière établit le pourcentage d'individus matures en fonction de la taille ou de l'âge et définit la taille et l'âge de première maturité pour lesquels 50 % des individus sont matures, ce qui implique nécessairement la présence de variabilité dans ces données.

Concernant les données univariées, les données de poids en fonction du temps (Figure 3b, 3l, 3m) sont bien estimées ( $0.1232 < RE < 0.1758$ ). La Figure 3b présente la taille en fonction du poids, le basculement des valeurs observé pour des individus de 0.5 cm correspond certainement à un stade de transition entre l'embryon et la larve qui commence à se nourrir. Les données après cette transition de phase sont par contre mal estimées d'où une erreur relative de 0.4421. Les données issues de capture, marquage, recapture (Figure 3.d, e), de changement dans la taille au cours du temps (Figure 3.k) présentent une grande variabilité dans les données conduisant à des valeurs d'erreur standard relativement élevées ( $0.379 < RE < 0.8$ ). Le nombre d'oocytes en fonction de la taille (Figure 3a) montrent une différence entre les données de Krug (1990) et Alcazar et al (1987) qui est lié à la différence de température utilisée pour corriger les taux métaboliques (les données étant issues de deux zones différentes) (Table 3). Les données de taille en fonction du temps sont relativement bien ajustées pour des individus avancés dans le développement avec une RE située entre 0.1 et 0.13 (Figure 3.g, j). En revanche les données d'embryons/juvéniles sont moins bien ajustées au modèle (Figure 3.f, h, i), la valeur de RE oscillant entre 0.36 et 0.46.

Pour l'ensemble des données issue de milieu naturel, la différence entre données observées et modélisées pourraient être liée à l'utilisation d'une température constante et des conditions alimentaires *ad libitum* dans le modèle bien loin des conditions de terrain qui présentent une nourriture et une température variables. Par ailleurs, il existe un risque d'erreur inhérent à la variabilité des sources de données. Par exemple, les données prélevées sur le terrain varieront probablement d'un endroit à l'autre et peuvent être affectées par l'historique des valeurs de température et de disponibilité en nourriture.

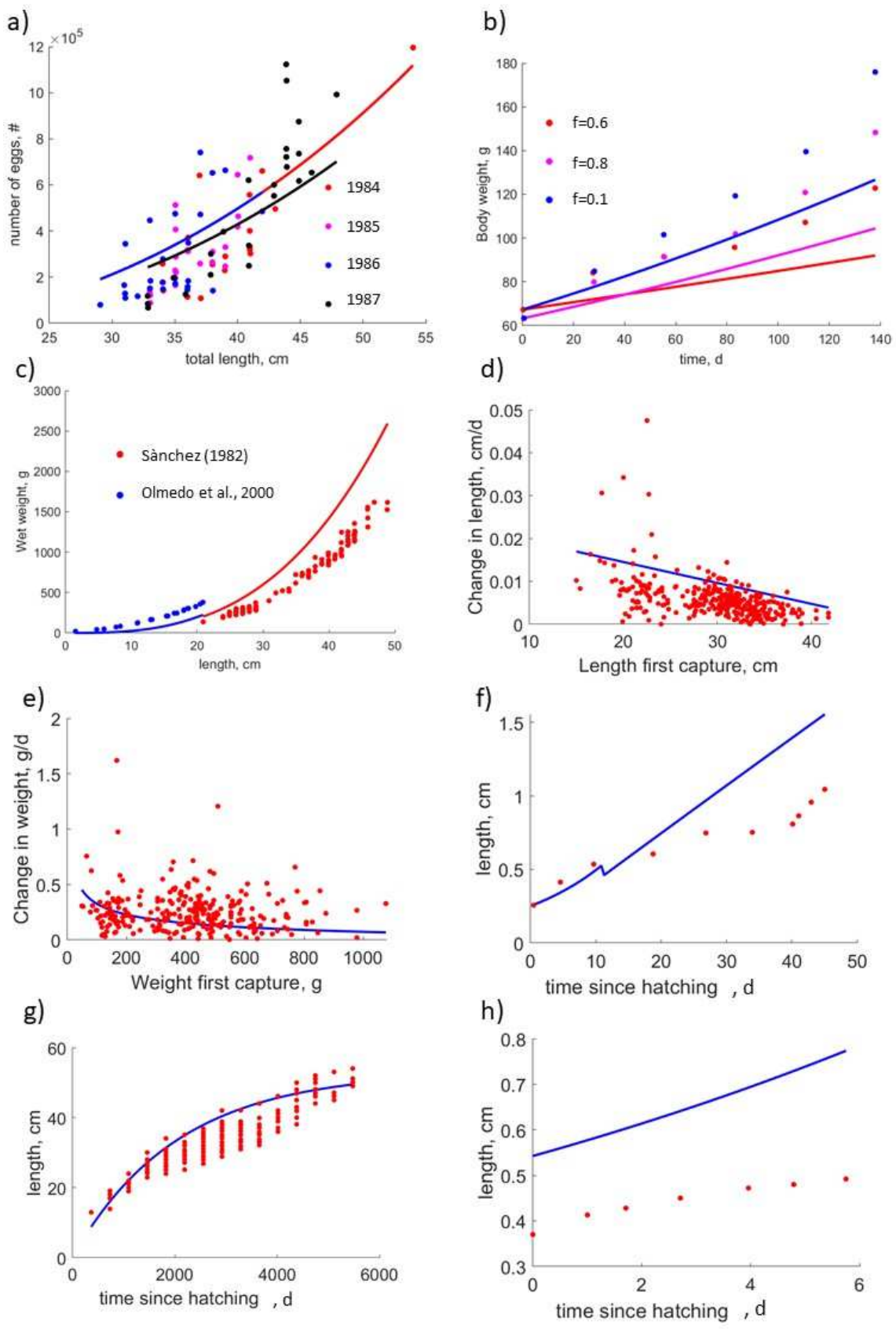
## 2) Paramètres estimés

La méthode de covariation utilise de nombreux types d'ensembles de données réelles dans la procédure d'estimation des paramètres, et généralement, plus le nombre de données utilisées dans l'estimation est important, plus les paramètres sont fiables. Les valeurs du zoom factor  $z$  et du coefficient de forme  $\delta_M$  peuvent être considérées comme relativement robustes puisqu'ils ont pu être estimés à partir des données zero-variées de tailles et des données univariées de poids~âge ou encore de taille~poids (Lika et al., 2011b). La faible robustesse des données de taille à la puberté peut limiter l'estimation de kappa  $\kappa$ , nous disposons néanmoins

d'information sur le taux de reproduction en nombre d'œufs par unité de temps grâce aux données de Krug (1990) et Alcazar et al, 1987 (Figure 3.a). Le paramètre  $k_J$  ne peut être estimé car des données sur la reproduction à différents niveaux de nourriture sont requis. De même pour le coefficient de stress de Gomertz  $S_G$ , la survie en fonction de l'âge est requis pour pouvoir l'estimer.

Les valeurs de  $f$  relativement élevées au-dessus de 1 pour les données expérimentales peuvent se justifier par des conditions d'accès et de qualité de la nourriture supérieures à celles en milieu naturel.

Par ailleurs, la température d'Arrhenius a été estimée par le modèle et n'a pas pu être déterminée à priori. Nous avons donc corrigé les taux métaboliques en utilisant ce seul paramètre. Des expériences en laboratoire basées sur des mesures de consommation d'oxygène à différentes températures par exemple permettraient d'estimer la température d'Arrhenius mais aussi de fournir une plage de tolérance de température spécifique à l'espèce (Kooijman, 2009).



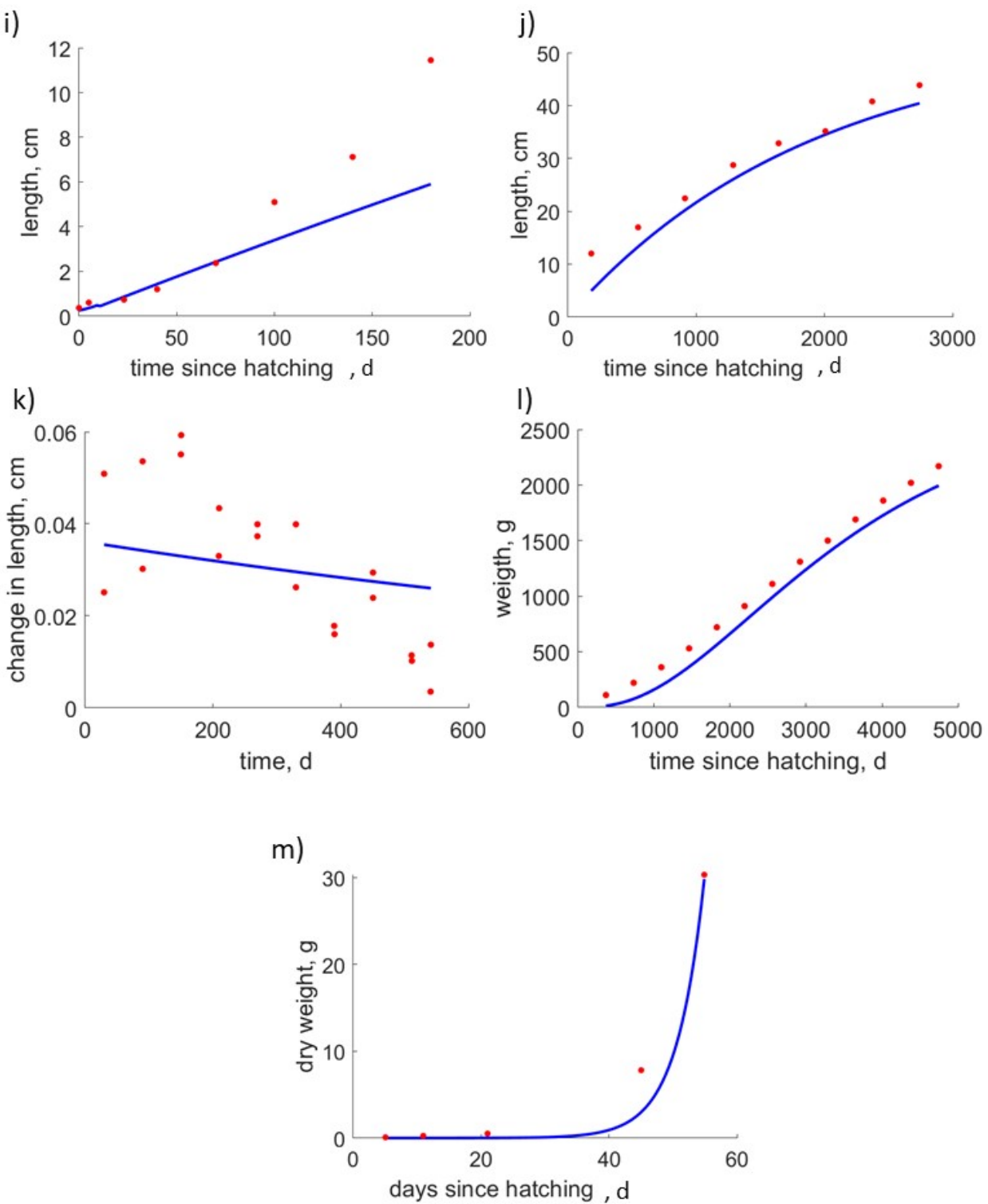


**Figure 3 :** Ajustement du modèle DEB (courbes bleues) et valeurs expérimentales/de terrain (points rouges) pour les données univariées : a) Nombre d'œufs en fonction de la taille (Krug, 1990), b) Poids frais en fonction du temps à différents niveaux de disponibilité en nourriture, en rouge  $f=0.6$ , en rose  $f=0.8$  et en bleu  $f=1$  (de Almeida Ozório et al., 2009), c) Poids frais en fonction de la taille, en bleue les données d' Olmedo et al., 2000 et en rouge de Sanchez (1982), d) Changement dans la taille en fonction de la taille à première capture (Juan Gil comm pers), e) Changement dans le poids frais en fonction du poids frais à première capture (Juan Gil comm pers), f) Taille en fonction du temps (Fernandez-Pato et al., 1990), g) longueur à la fourche en fonction du temps (Higgins et al., 2015), h) Taille en fonction du temps (Peleteiro et al., 1997) , i) Taille en fonction du temps (Silva et al., 2009), j) Taille en fonction du temps (Sobrino and Gil, 2001), k) Changement dans la taille en fonction du temps (Olmedo et al., 2000), l) Poids frais en fonction du temps (Pinho et al., 2014), m) Poids sec en fonction du temps (Ribeiro et al., 2008).

## Références

- Alcazar, J.L., Carrasco, J.F., Llera, J.A., Mendez, M., Ortea, J.A., Vizcaaino, A., 1987. Aportacion al estudio del besugo en el Principado de Asturias. Recur. Pesq. Astur. 4, 88.
- Augustine, S., Gagnaire, B., Adam-Guillermin, C., Kooijman, S.A.L.M., 2012. Effects of uranium on the metabolism of zebrafish, *Danio rerio*. Aquat. Toxicol. 118–119, 9–26.  
<https://doi.org/10.1016/j.aquatox.2012.02.029>
- Bodiguel, X., Maury, O., Mellon-Duval, C., Roupsard, F., Le Guellec, A.-M., Loizeau, V., 2009. A dynamic and mechanistic model of PCB bioaccumulation in the European hake (*Merluccius merluccius*). J. Sea Res. 62, 124–134. <https://doi.org/10.1016/j.seares.2009.02.006>
- de Almeida Ozório, R.O., Andrade, C., Freitas Andrade Timóteo, V.M., Castanheira da Conceição, L.E., Pinheiro Valente, L.M., 2009. Effects of Feeding Levels on Growth Response, Body Composition, and Energy Expenditure in Blackspot Seabream, *Pagellus bogaraveo*, Juveniles. J. World Aquac. Soc. 40, 95–103.  
<https://doi.org/10.1111/j.1749-7345.2008.00231.x>
- Eichinger, M., Loizeau, V., Roupsard, F., Le Guellec, A.M., Bacher, C., 2010. Modelling growth and bioaccumulation of Polychlorinated biphenyls in common sole (*Solea solea*). J. Sea Res. 64, 373–385.  
<https://doi.org/10.1016/j.seares.2010.05.005>
- Fabri-Ruiz, S., 2018. Modèles de distribution et changements environnementaux: application aux faunes d'échinides de l'océan Austral et écorégionalisation. Université Bourgogne Franche-Comté; Université libre de Bruxelles (1970-....).
- Fernandez-Pato, C.A., Martinez-Tapia, C., Chereguini, O., Garcia-Banda, I., 1990. Spawn, hatching, and larvae rearing of black-spot sea bream: (*Pagellus bogaraveo* b.) first experiences in the oceanographic center of Santander (Spain) in order to its culture. ICES CM.
- Gueguen, J., 1969. Croissance de la dorade, *Pagellus centrodontus* Delaroche. Rev. Trav. Inst. Pêch. Marit. 33, 251–264.
- Higgins, R.M., Diogo, H., Isidro, E.J., 2015. Modelling growth in fish with complex life histories. Rev. Fish Biol. Fish. 25, 449–462. <https://doi.org/10.1007/s11160-015-9388-8>
- Jusup, M., Klanjscek, T., Matsuda, H., Kooijman, S.A.L.M., 2011. A Full Lifecycle Bioenergetic Model for Bluefin Tuna. PLoS ONE 6, e21903. <https://doi.org/10.1371/journal.pone.0021903>
- Jusup, M., Sousa, T., Domingos, T., Labinac, V., Marn, N., Wang, Z., Klanjšček, T., 2017. Physics of metabolic organization. Phys. Life Rev. 20, 1–39. <https://doi.org/10.1016/j.plrev.2016.09.001>
- Kooijman, B., 2009. Dynamic Energy Budget Theory for Metabolic Organisation, 3rd ed. Cambridge University Press, Cambridge. <https://doi.org/10.1017/CBO9780511805400>
- Kooijman, S.A.L.M., Pecquerie, L., Augustine, S., Jusup, M., 2011. Scenarios for acceleration in fish development and the role of metamorphosis. J. Sea Res. 66, 419–423.  
<https://doi.org/10.1016/j.seares.2011.04.016>
- Krug, H., 1998. Variation in the reproductive cycle of the blackspot seabream, *Pagellus bogaraveo* (Brünnich, 1768) in the Azores. Arquipél. Life Mar. Sci. 16, 37–47.
- Krug, H.M., 1990. The Azorean blackspot seabream, *Pagellus bogaraveo* (Bruennich, 1768) (Teleostei, Sparidae). Reproductive cycle, hermaphroditism, maturity and fecundity. Cybium 14, 151–159.

Lika, K., Kearney, M.R., Freitas, V., van der Veer, H.W., van der Meer, J., Wijsman, J.W.M., Pecquerie, L., Kooijman, S.A.L.M., 2011a. The “covariation method” for estimating the parameters of the standard Dynamic Energy Budget model I: Philosophy and approach. *J. Sea Res.* 66, 270–277.  
<https://doi.org/10.1016/j.seares.2011.07.010>

Lika, K., Kearney, M.R., Kooijman, S.A.L.M., 2011b. The “covariation method” for estimating the parameters of the standard Dynamic Energy Budget model II: Properties and preliminary patterns. *J. Sea Res.* 66, 278–288. <https://doi.org/10.1016/j.seares.2011.09.004>

Marques, G.M., Augustine, S., Lika, K., Pecquerie, L., Domingos, T., Kooijman, S.A.L.M., 2018. The Amp project: Comparing species on the basis of dynamic energy budget parameters. *PLOS Comput. Biol.* 14, e1006100. <https://doi.org/10.1371/journal.pcbi.1006100>

Olmedo, M., Peleteiro, J.B., Linares, F., Álvarez-Blázquez, B., Gómez, C., Ortega, A., 2000. Experience with ongrowing Muvenile blackspot sea bream born in captivity, in tanks at different temperatures. *Cah. Options Méditerranéennes* 153–156.

Pecquerie, L., Johnson, L.R., Kooijman, S.A.L.M., Nisbet, R.M., 2011. Analyzing variations in life-history traits of Pacific salmon in the context of Dynamic Energy Budget (DEB) theory. *J. Sea Res.* 66, 424–433.  
<https://doi.org/10.1016/j.seares.2011.07.005>

Pecquerie, L., Petitgas, P., Kooijman, S.A.L.M., 2009. Modeling fish growth and reproduction in the context of the Dynamic Energy Budget theory to predict environmental impact on anchovy spawning duration. *J. Sea Res.* 62, 93–105. <https://doi.org/10.1016/j.seares.2009.06.002>

Peleteiro, J.B., Olmedo, M., Gomez, C., Alvarez-Blázquez, B., 1997. Study of reproduction in captivity of blackspot sea bream (*Pagellus bogaraveo* b.). Embryonic development and consumption of vitelline sac.

Pinho, M., Diogo, H., Carvalho, J., Pereira, J.G., 2014. Harvesting juveniles of blackspot sea bream (*Pagellus bogaraveo*) in the Azores (Northeast Atlantic): biological implications, management, and life cycle considerations. *ICES J. Mar. Sci.* 71, 2448–2456. <https://doi.org/10.1093/icesjms/fsu089>

Ribeiro, L., Couto, A., Olmedo, M., Álvarez-Blázquez, B., Linares, F., Valente, L.M.P., 2008. Digestive enzyme activity at different developmental stages of blackspot seabream, *Pagellus bogaraveo* (Brunnich 1768). *Aquac. Res.* 39, 339–346. <https://doi.org/10.1111/j.1365-2109.2007.01684.x>

Sánchez, F., 1982. Preliminary fishing and biological data about red sea-bream (*Pagellus bogaraveo* b.) in the Cantabrian Sea (N. Spain). Presented at the ICES 1982 (Collected Papers),, Publisher ICES COPENHAGEN (DENMARK), p. 11 pp.

Sanchez, F., 1982. Preliminary fishing and biological data about red sea-bream (*Pagellus ogaraveo* B.) in the Cantabrian Sea (N. Spain). *ICES CM.*

Silva, P., Galante, M.H., 2011. Influence of temperature on muscle fibre hyperplasia and hypertrophy in larvae of blackspot seabream, *Pagellus bogaraveo*. *Aquac. Res.* 10.

Silva, P., Valente, L.M.P., Olmedo, M., Galante, M.H., Monteiro, R.A.F., Rocha, E., 2009. Hyperplastic and hypertrophic growth of lateral muscle in blackspot seabream *Pagellus bogaraveo* from hatching to juvenile. *J. Fish Biol.* 74, 37–53. <https://doi.org/10.1111/j.1095-8649.2008.02122.x>

Sobrino, I., Gil, J., 2001. Studies on age determination and growth pattern of the red (Blackspot) seabream *Pagellus bogaraveo* (Brunnich, 1768) from the Strait of Gibraltar (ICES 9a/SW Spain): Application to the species migratory pattern.

van der Meer, J., 2006. An introduction to Dynamic Energy Budget (DEB) models with special emphasis on parameter estimation. *J. Sea Res.* 56, 85–102. <https://doi.org/10.1016/j.seares.2006.03.001>

van der Veer, H.W., Cardoso, J.F.M.F., Peck, M.A., Kooijman, S.A.L.M., 2009. Physiological performance of plaice *Pleuronectes platessa* (*L*).: A comparison of static and dynamic energy budgets. *J. Sea Res.* 62, 83–92.  
<https://doi.org/10.1016/j.seares.2009.02.001>

van der Veer, H.W., Kooijman, S.A.L.M., van der Meer, J., 2003. Body size scaling relationships in flatfish as predicted by Dynamic Energy Budgets (DEB theory): implications for recruitment. *J. Sea Res.* 50, 257–272.  
<https://doi.org/10.1016/j.seares.2003.05.001>

Annexe 4  
Communications présentées lors de colloques

XVII international Symposium on Oceanography of the Bay of Biscay (ISOBAY 17) [17ème symposium d'océanographie du golfe de Gascogne], 1-4 Juin 2021

ICES 2021 Annual Science Conference [Conférence Scientifique Annuelle du CIEM 2021], 6-10 Septembre 2021

Huitièmes Rencontres de l'Ichtyologie en France, Paris, 14-18 mars 2022

# XVII international Symposium on Oceanography of the Bay of Biscay (ISOBAY 17)

**Bay of Biscay** **ISOBAY 17: XVII International Symposium on Oceanography of the Bay of Biscay** **Ifremer** **PANDORA** **FRANCE PECHE**

Identifying potential habitats of a locally overexploited species: case study of the blackspot seabream in the Bay of Biscay

Lola De Cubber, Verena Trenkel, Guzman Diez, Juan Gil-Herrera, Ana Maria Novoa Pabon, David Eme & Pascal Lorance

lola.decubber@gmail.com

## Introduction

Demersal species  
Vast spatial distribution with 3 main stocks (Atlantic, Azores, East Mediterranean Sea)  
Potential habitats probably quite wide (young close to the coast – adults further, mobile species migrating over long distances)

World Register of Marine Species  
<http://www.marinespecies.org/aphia.php?p=taxdetails&t=127056&sub>

Landing (t)  
Year

2

## Introduction

Demersal species  
Vast spatial distribution with 3 main stocks (Atlantic, Azores, East Mediterranean Sea)  
Potential habitats probably quite wide (young close to the coast – adults further, mobile species migrating over long distances)

World Register of Marine Species  
<http://www.marinespecies.org/aphia.php?p=taxdetails&t=127056&sub>

Landing (t)  
Year

Stock collapse in the Bay of Biscay  
Better status in the Azores and Mediterranean Sea

3

## Introduction

Demersal species  
Vast spatial distribution with 3 main stocks (Atlantic, Azores, East Mediterranean Sea)  
Potential habitats probably quite wide (young close to the coast – adults further, mobile species migrating over long distances)

World Register of Marine Species  
<http://www.marinespecies.org/aphia.php?p=taxdetails&t=127056&sub>

Landing (t)  
Year

Stock collapse in the Bay of Biscay  
Better status in the Azores and Mediterranean Sea

Current spatial distribution and potential habitats ?

4

## Methods: Ensemble Species Distribution Model (ESDM)

- SDM: Estimate the presence probability of a species according to environmental variables
- ESDM: Combination of various SDMs

5

## Methods: Ensemble Species Distribution Model (ESDM)

- Occurrence data compilation
- Environmental data extraction
- Occurrence data filtering and environmental variables selection
- SDMs: Generalised Linear Model (GLM), Generalised Boosting Model (GBM), Generalised Additive Model (GAM), Artificial Neural Network (ANN), Flexible Discriminant Analysis (FDA), Random Forest (RF), Classification Tree analysis (CTA), Surface Range Envelope (SRE)
- Ensemble model: model selection with TSS > 0.5 and/or AUC ROC > 0.8
- Projection of presence probabilities on the whole geographical area
- Validation on the whole data set, presence thresholds and binary habitats maps

6

## Methods: Ensemble Species Distribution Model (ESDM)

- SDM: Estimate the presence probability of a species according to environmental variables
- ESDM: Combination of various SDMs

```

    graph TD
      1[1 Occurrence data compilation] --> 2[2 Environmental data extraction]
      2 --> 3[3 Occurrence data filtering and environmental variables selection]
      3 --> 4[4 SDMs: GLM, GAM, ANN, FDA, RF, CTA, SRE]
      4 --> 5[5 Ensemble model: model selection with TSS > 0.5 and/or AUC ROC > 0.8]
      5 --> 6[6 Projection of presence probabilities on the whole geographical area]
      6 --> 7[7 Validation on the whole data set, presence thresholds and binary habitats maps]
  
```

7

## Occurrence data

Presence / Absence data

Source: Azores\_jpap, Azores\_wav, Benthic, ENVOC, MEDETS, MPA, Observat, PFBTS, SGR, SR\_north, StratGocator

40°W 30°W 20°W 10°W 0° 10°E 20°E

8

## Occurrence data

Presence / Absence data

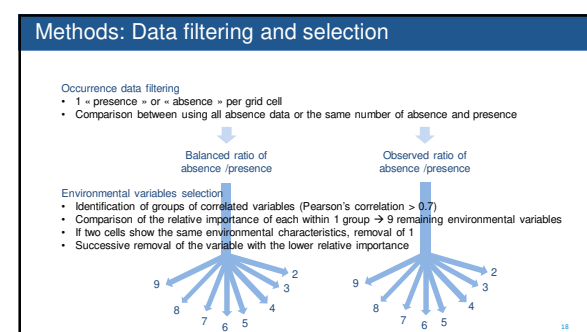
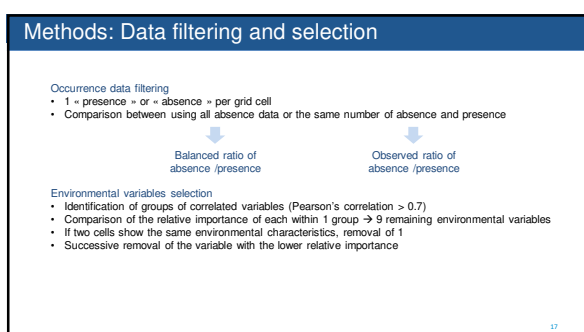
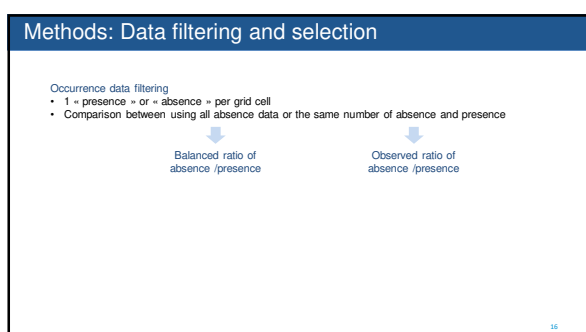
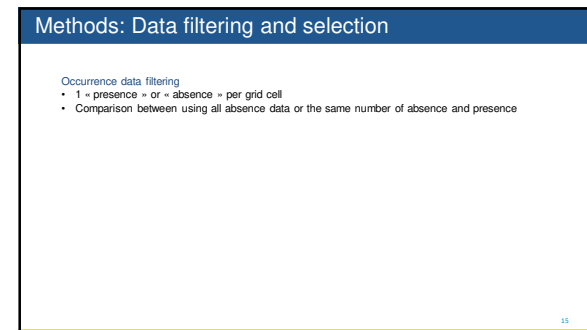
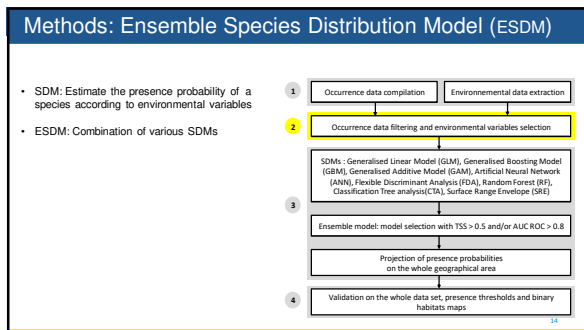
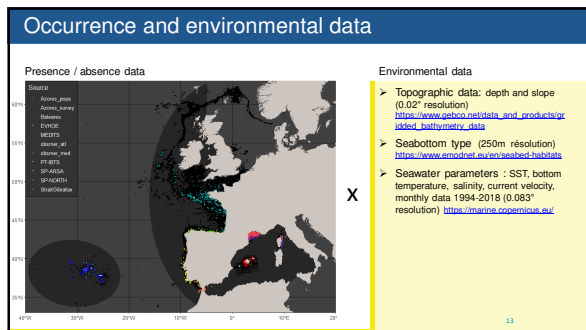
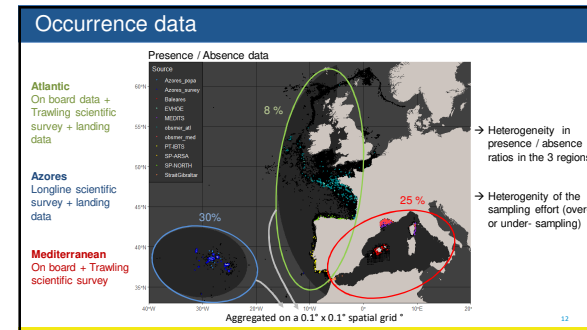
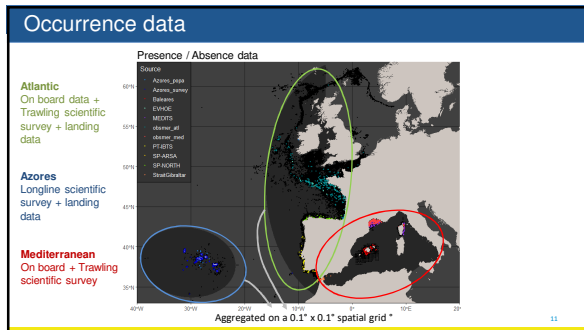
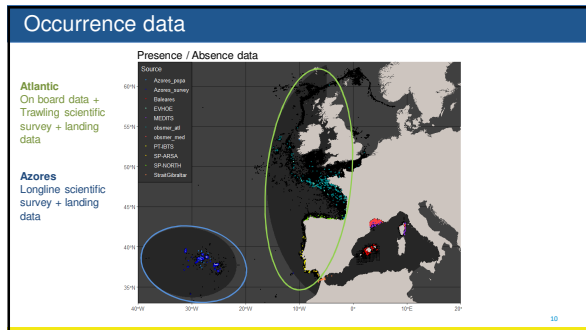
Atlantic  
On board data + Trawling scientific survey + landing data

Source: Azores\_jpap, Azores\_wav, Benthic, ENVOC, MEDETS, MPA, Observat, PFBTS, SGR, SR\_north, StratGocator

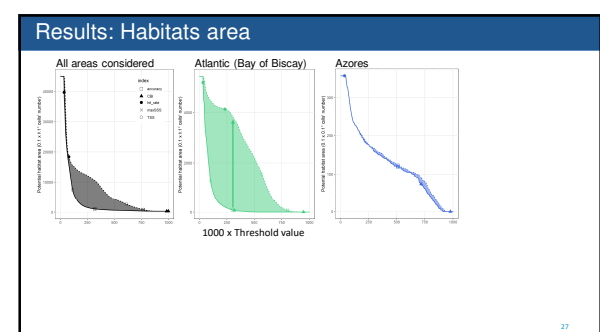
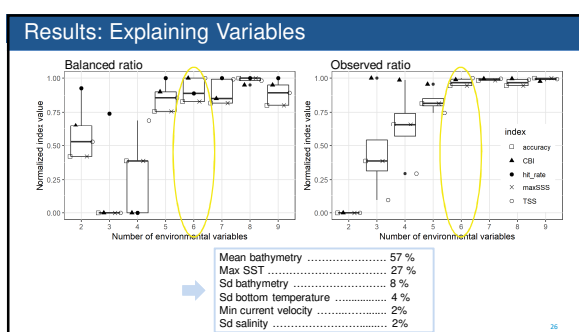
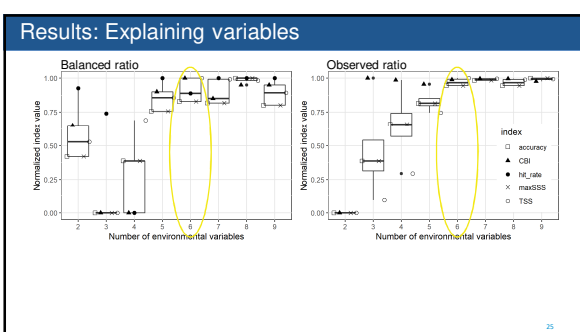
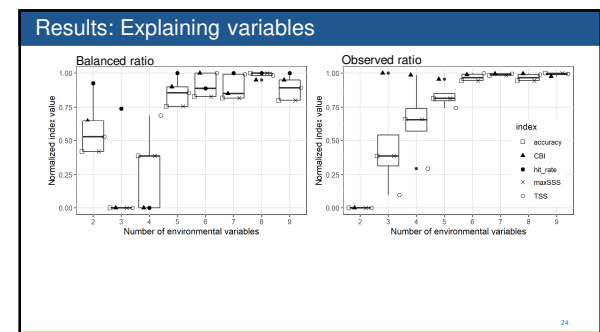
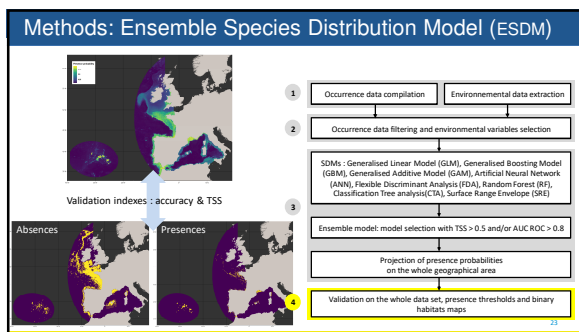
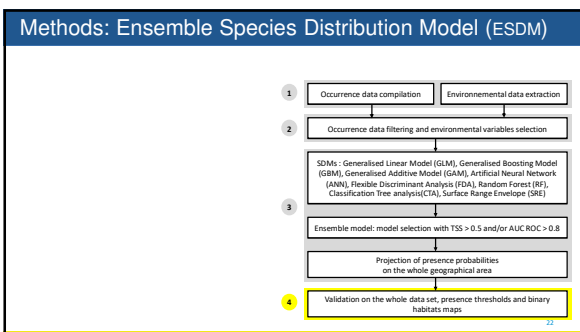
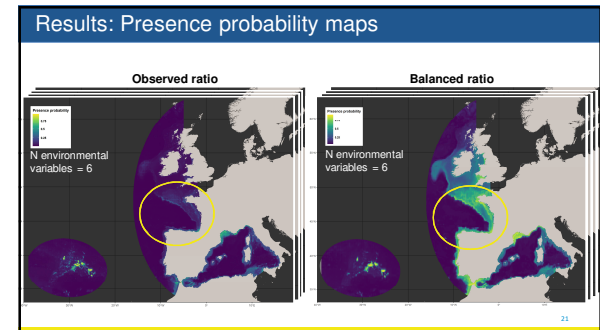
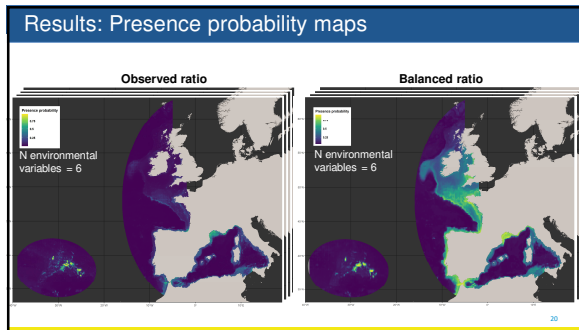
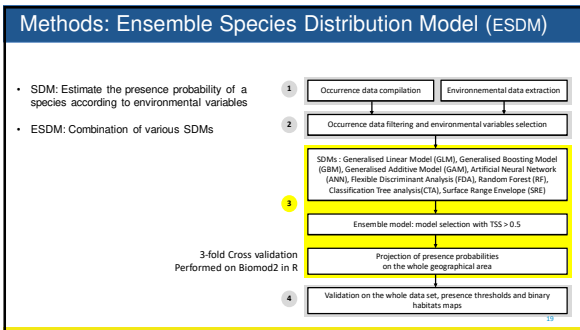
40°W 30°W 20°W 10°W 0° 10°E 20°E

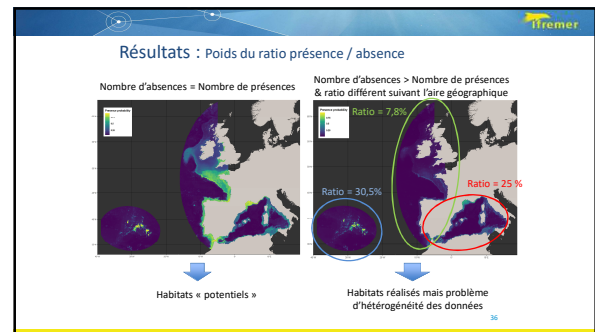
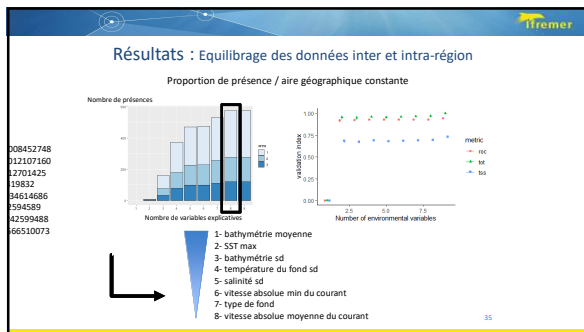
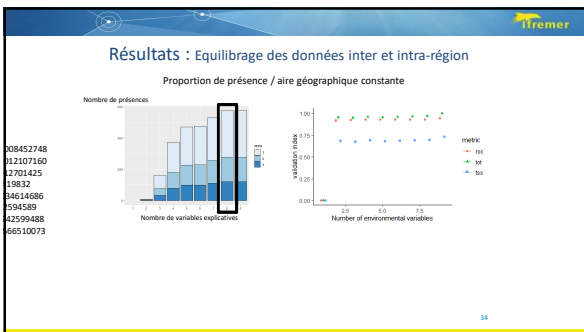
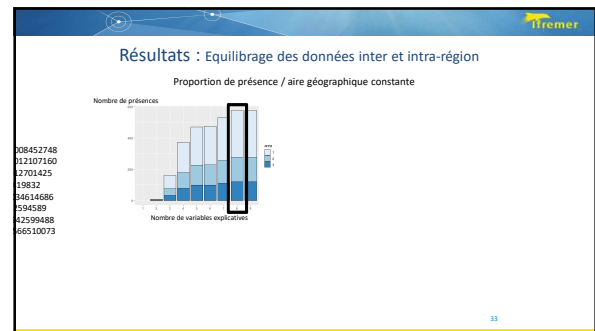
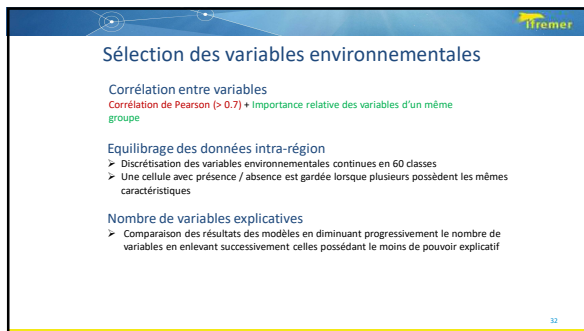
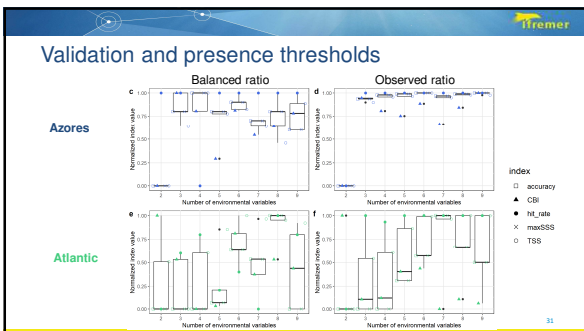
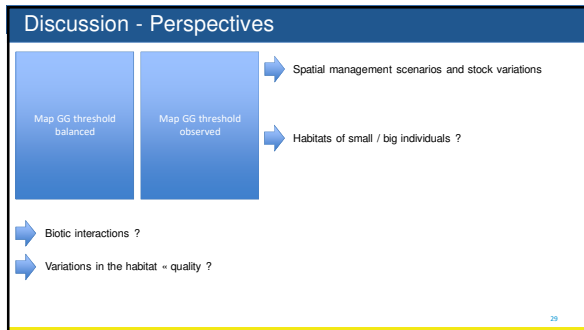
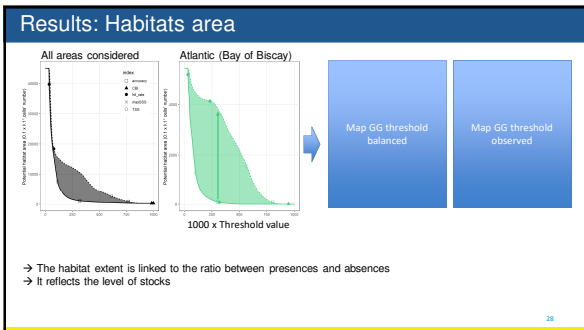
9

# XVII international Symposium on Oceanography of the Bay of Biscay (ISOBAY 17)



# XVII international Symposium on Oceanography of the Bay of Biscay (ISOBAY 17)





### Perspectives

Nombre d'absences = Nombre de présences

→ Calcul de la valeur seuil pour une carte de présence absence binnaire via le maxSS  
(Maximisation de la sensibilité et la spécificité, Liu et al., 2005)  
→ Adaptation de la valeur seuil pour une carte de présence absence binnaire en fonction de l'aire géographique.

37

### Matériels et Méthodes

	Aire totale		Atlantique		Acores		Méditerranée	
	Points	Cellules	Points	Cellules	Points	Cellules	Points	Cellules
N présences	6928	782	639	389	4872	165	1417	228
Proportion	1,7%	1,7%	1,7%	1,7%	1,7%	1,7%	1,7%	1,7%
N absences	99529	5683	74556	4626	13906	376	11067	681
Proportion	12,7%	20%	20%	20%	4%	5,6%	4%	5,6%
N total	106457	6465	75196	5015	18778	541	12484	909
Proportion	14,4%	21,6%	21,6%	21,6%	5,8%	5,8%	7,4%	7,4%

Ratio présence/N échantillon 6,5% 12% 0,8% 7,8% 25,9% 30,5% 11,4% 25%

→ Proportion de « cellules de présence » équivalente suivant les aires géographiques

38

### Matériels et Méthodes

	Aire totale		Atlantique		Acores		Méditerranée	
	Points	Cellules	Points	Cellules	Points	Cellules	Points	Cellules
N présences	6928	782	639	389	4872	165	1417	228
Proportion	1,7%	1,7%	1,7%	1,7%	1,7%	1,7%	1,7%	1,7%
N absences	99529	5683	74556	4626	13906	376	11067	681
Proportion	12,7%	20%	20%	20%	4%	5,6%	4%	5,6%
N total	106457	6465	75196	5015	18778	541	12484	909
Proportion	14,4%	21,6%	21,6%	21,6%	5,8%	5,8%	7,4%	7,4%

Ratio présence/N échantillon 6,5% 12% 0,8% 7,8% 25,9% 30,5% 11,4% 25%

→ Proportion de « cellules de présence » équivalente suivant les aires géographiques  
→ Nombre d'absences et ratio présence / N échantillon variables

39

### Matériels et Méthodes

	Aire totale		Atlantique		Acores		Méditerranée	
	Points	Cellules	Points	Cellules	Points	Cellules	Points	Cellules
N présences	6928	782	639	389	4872	165	1417	228
Proportion	1,7%	1,7%	1,7%	1,7%	1,7%	1,7%	1,7%	1,7%
N absences	99529	5683	74556	4626	13906	376	11067	681
Proportion	12,7%	20%	20%	20%	4%	5,6%	4%	5,6%
N total	106457	6465	75196	5015	18778	541	12484	909
Proportion	14,4%	21,6%	21,6%	21,6%	5,8%	5,8%	7,4%	7,4%

Ratio présence/N échantillon 6,5% 12% 0,8% 7,8% 25,9% 30,5% 11,4% 25%

→ Proportion de « cellules de présence » équivalente suivant les aires géographiques  
→ Nombre d'absences et ratio présence / N échantillon variables  
→ Déséquilibre des données au sein des aires géographiques avec des zones sur- ou sous-échantillonnées

40

### Matériels et Méthodes

	Aire totale		Atlantique		Acores		Méditerranée	
	Points	Cellules	Points	Cellules	Points	Cellules	Points	Cellules
N présences	6928	782	639	389	4872	165	1417	228
Proportion	1,7%	1,7%	1,7%	1,7%	1,7%	1,7%	1,7%	1,7%
N absences	99529	5683	74556	4626	13906	376	11067	681
Proportion	12,7%	20%	20%	20%	4%	5,6%	4%	5,6%
N total	106457	6465	75196	5015	18778	541	12484	909
Proportion	14,4%	21,6%	21,6%	21,6%	5,8%	5,8%	7,4%	7,4%

Ratio présence/N échantillon 6,5% 12% 0,8% 7,8% 25,9% 30,5% 11,4% 25%

Comment gérer les déséquilibres des données entre les différentes aires géographiques et au sein de chacune des aires géographiques ?

41

### Matériels et Méthodes

Données de présence / absence

Données de topographie : bathymétrie et pente résolution 0,02°  
[https://www.gebco.net/data\\_and\\_products/gridded\\_bathymetry.aspx](https://www.gebco.net/data_and_products/gridded_bathymetry.aspx)

Données de nature du substrat, résolution 250m  
<https://www.emodnet.eu/en/data/benthos>

Données physico-chimiques : SST, température du fond, salinité, vitesse des courants, données mensuelles 1994-2018, résolution 0,083°  
<https://marine.copernicus.eu/>

42

### Matériels et Méthodes

Données de présence / absence

Données de topographie : bathymétrie et pente résolution 0,02°  
[https://www.gebco.net/data\\_and\\_products/gridded\\_bathymetry.aspx](https://www.gebco.net/data_and_products/gridded_bathymetry.aspx)

Données de nature du substrat, résolution 250m  
<https://www.emodnet.eu/en/data/benthos>

Données physico-chimiques : SST, température du fond, salinité, vitesse des courants, données mensuelles 1994-2018, résolution 0,083°  
<https://marine.copernicus.eu/>

Agrégé sur une grille de 0,1 x 0,1 °

43

### Exploration des données brutes

Pente

Salinité

→ Des réponses potentiellement contrastées à une même variable environnementale suivant la localisation

44

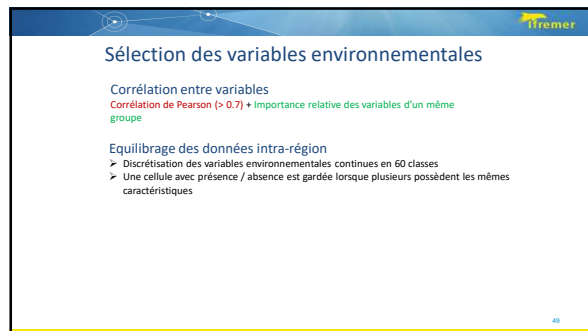
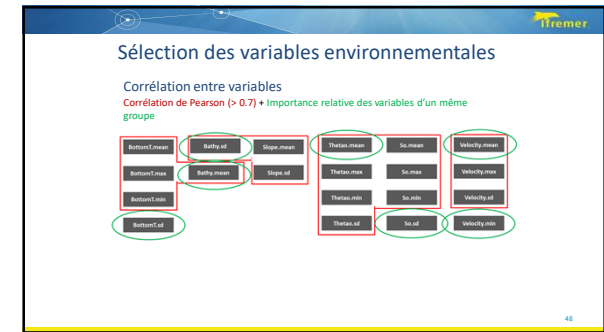
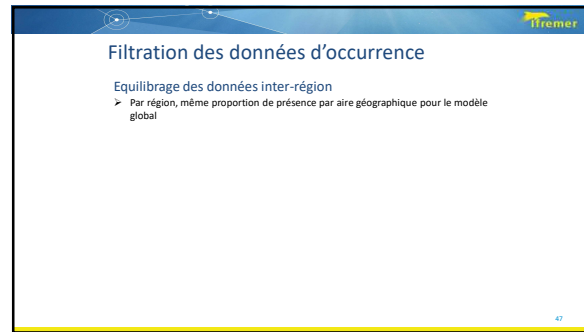
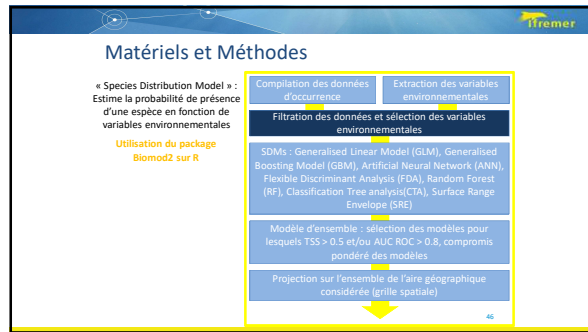
### Problématiques méthodologiques

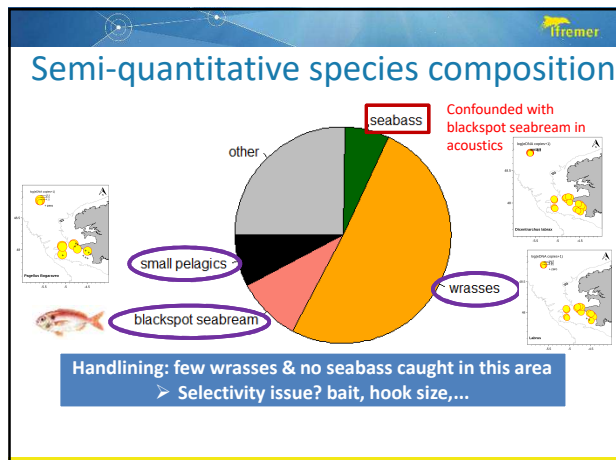
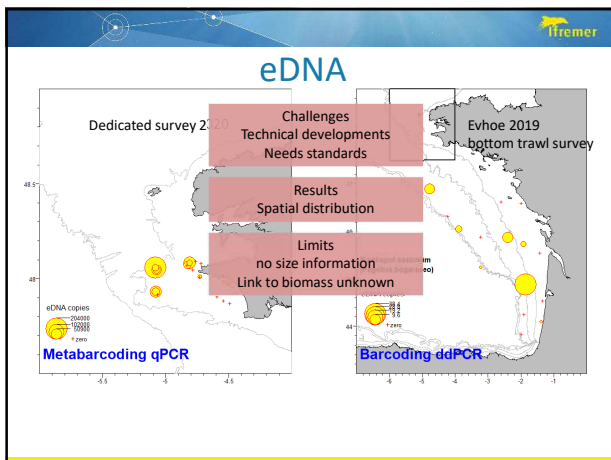
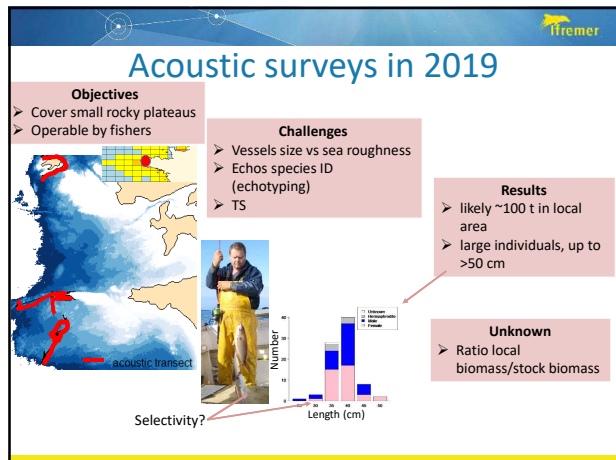
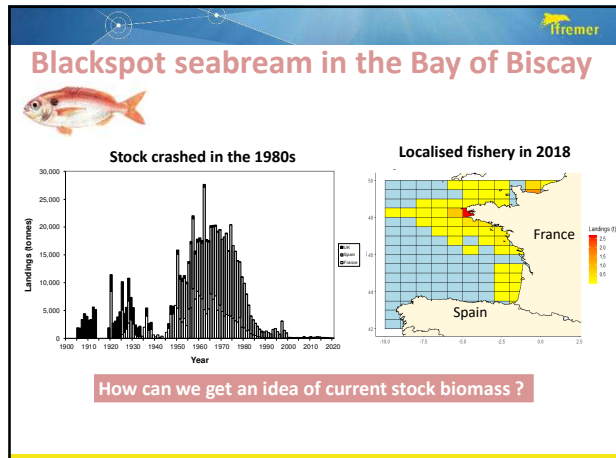
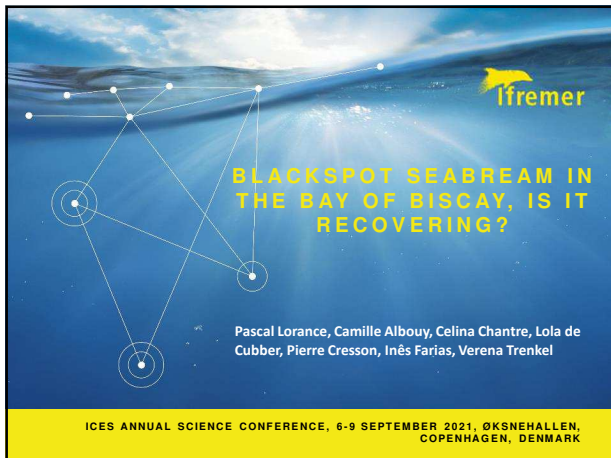
Comment intégrer les réponses potentiellement variables de la distribution *Pagellus bogaraveo* à l'environnement suivant l'aire géographique concernée ?

Comment gérer les déséquilibres générés par les données ?

45

# XVII international Symposium on Oceanography of the Bay of Biscay (ISOBAY 17)





## Acoustics vs eDNA

	Acoustics	eDNA
Method	Classical Sensitive to - weather - TS - Ecotyping standard	Needs developments for - Post processing - Link to biomass - Diffusion & degradation
Species ID	Uncertain	Reliable
Size	Representativeness?	None
Main result	Biomass	Species distribution Species composition nb of DNA copies

## Biology

Age estimation from scales

1969: 5 years old fish  
Guéguen, J. 1969. Croissance de la dorade, *Pagellus centrodontus* Delaroche. Revue des Travaux de l'Institut des Pêches Maritimes 33:251-264.

2019: 6 years

## Size-at-age 60 years later

Result

- larger size-at-age in 2019 (depleted) than 60 years ago (abundant stock)
- density-dependence?

Guéguen, J. 1969. Croissance de la dorade, *Pagellus centrodontus* Delaroche. Revue des Travaux de l'Institut des Pêches Maritimes 33:251-264.

## Habitat modelling

Species distribution models (SDM)

Species occupies only a fraction of its habitats in the Bay of Biscay

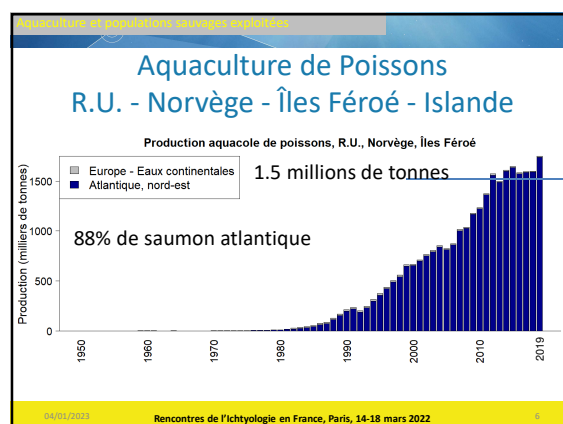
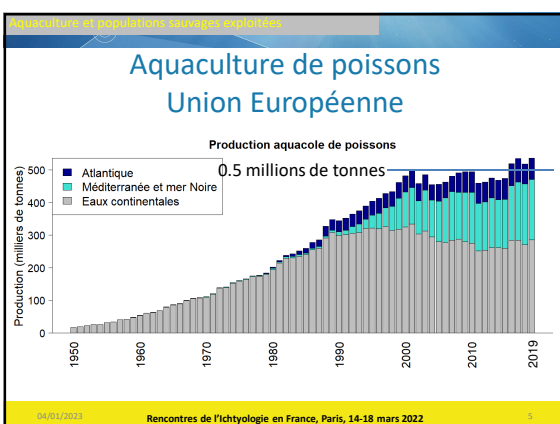
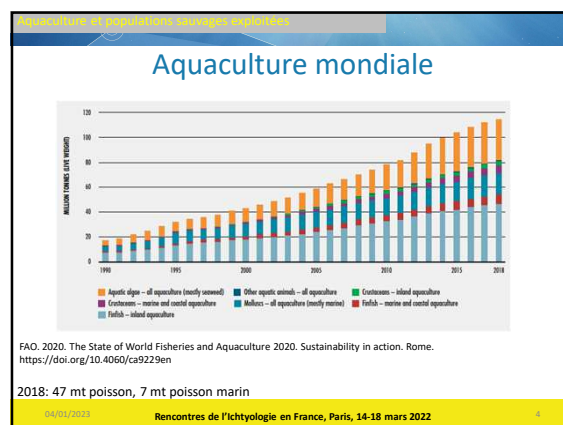
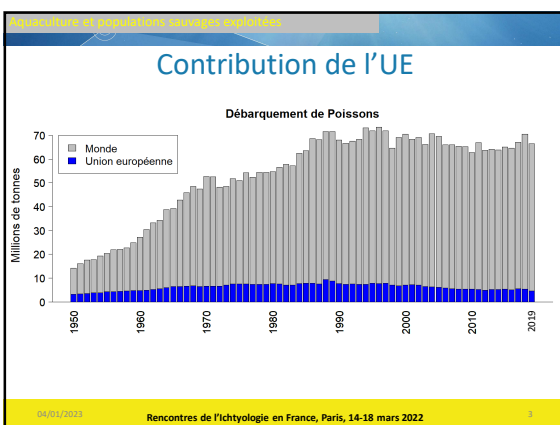
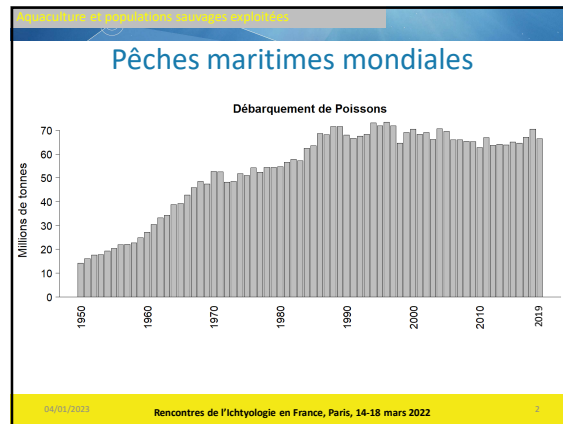
Bay of Biscay stock more depleted than other stocks

## Conclusion

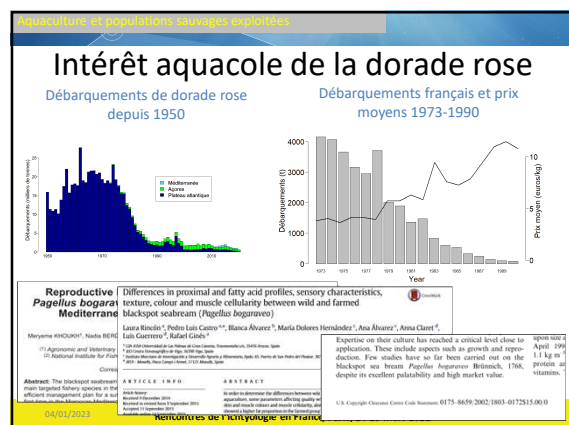
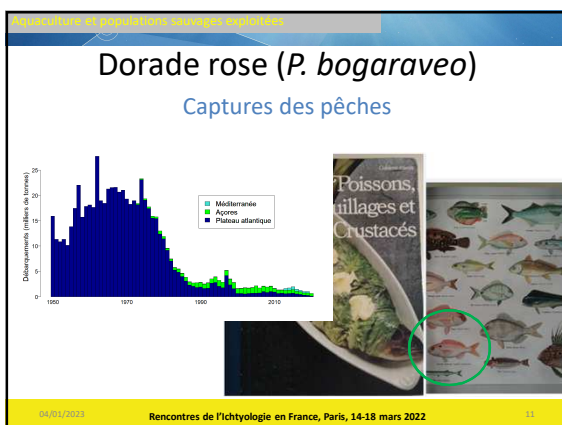
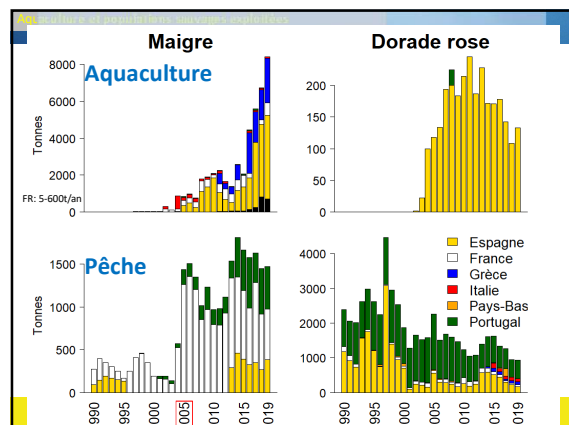
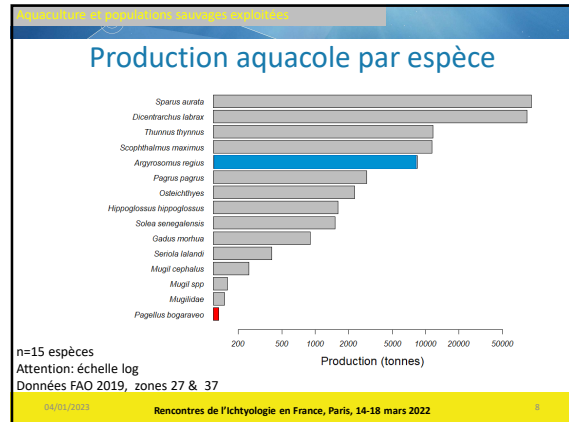
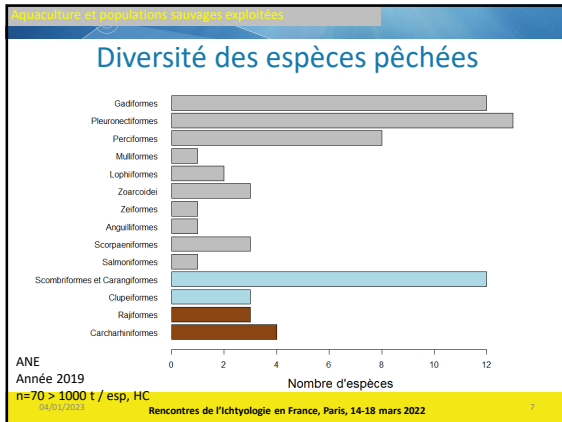
- Acoustics
  - uncertain estimate of the local biomass
- eDNA
  - estimate of spatial distribution
  - Reliable species composition
- The two methods could complement each-other
- Bay of Biscay blackspot seabream
  - stock trend still unknown
  - large/old (50 cm/13 years) fish exists
  - low biomass level possibly impacts on life history

## Acknowledgement

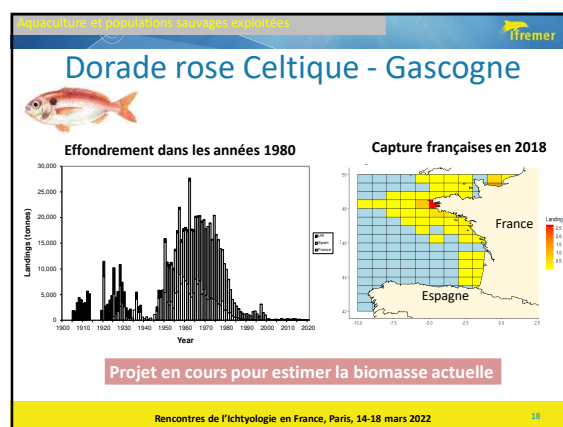
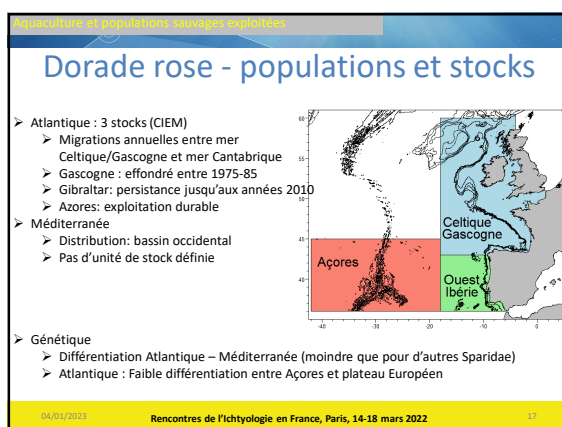
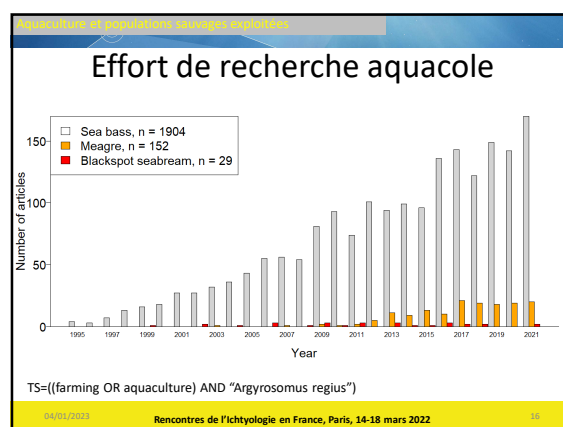
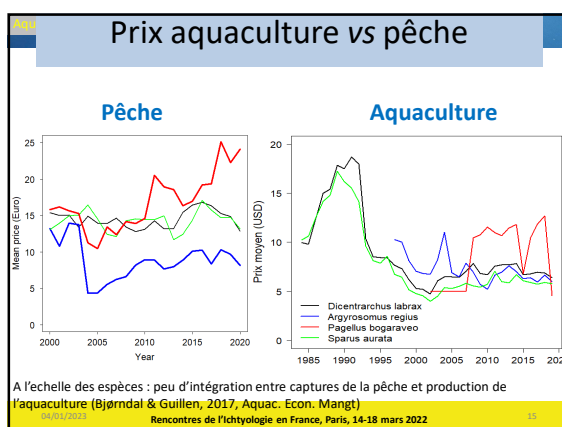
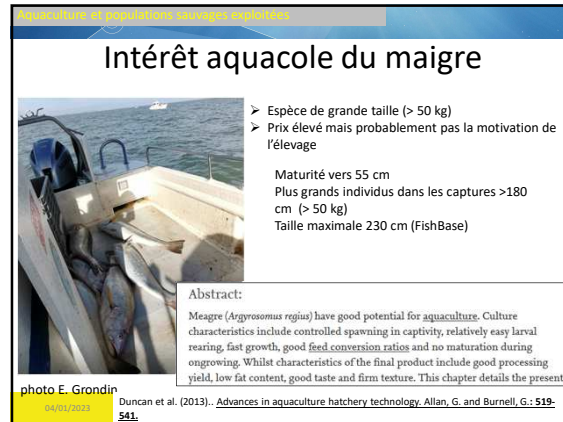
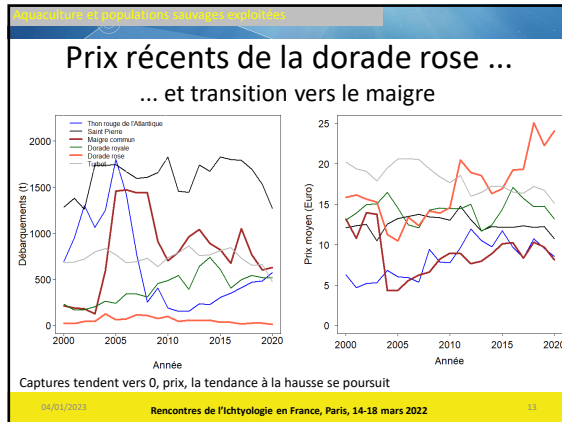
## Rencontres de l'Ichtyologie en France, Paris, 14-18 mars 2022



Rencontres de l'Ichtyologie en France, Paris, 14-18 mars 2022



## Rencontres de l'Ictyologie en France, Paris, 14-18 mars 2022



## Rencontres de l'Ichtyologie en France, Paris, 14-18 mars 2022

**Aquaculture et populations sauvages exploitées**

**Projet DynRose**

Travaux récents en cours  
➤ suivre les tendances de la populations

Rencontres de l'Ichtyologie en France, Paris, 14-18 mars 2022 19

**Aquaculture et populations sauvages exploitées**

**DynRose : approche acoustique**

**Objectifs**  
Couvrir des zones rocheuses  
Mise en œuvre par pêcheurs

**défis**  
➤ Petits navires vs mer agitée  
➤ Identification des espèces (écotyping)  
➤ Index de réflexion

**Résultats**  
➤ probablement ~100 t in local area  
➤ Grands individus >50 cm

**Inconnues**  
➤ Ratio biomasse locale/stock

Selectivity?  
Number vs Length (cm)

Rencontres de l'Ichtyologie en France, Paris, 14-18 mars 2022 20

**Aquaculture et populations sauvages exploitées**

**Semi-quantitative species composition**

Confusion acoustique bar dorade rose?

Captures: quelques labres et aucun bar  
➤ Sélectivité ? appâts, hameçons,...  
➤ Echotypage : pélagiques et Labridae exclut, bar confondu

Rencontres de l'Ichtyologie en France, Paris, 14-18 mars 2022 21

**Aquaculture et populations sauvages exploitées**

**Biologie**

**Estimation d'âge à partir des écailles**

1969: 5 anneaux de croissance  
Guéguen, J. 1969. Croissance de la dorade, *Pagellus centrodorsatus*. *Détrache: Revue des Travaux de l'Institut des Pêches Maritimes* 33:251-264.

2019: 6 anneaux  
photo Ifremer Boulogne-sur-mer

Rencontres de l'Ichtyologie en France, Paris, 14-18 mars 2022 22

**Aquaculture et populations sauvages exploitées**

**Taille aux âges – 60 ans plus tard**

Guéguen, J. 1969. Croissance de la dorade, *Pagellus centrodorsatus*. *Détrache: Revue des Travaux de l'Institut des Pêches Maritimes* 33:251-264.

Résultats  
➤ Taille-aux âges plus grandes en 2019 (stock raréfié) que 60 ans plus tôt (stock abondant)  
■ densité-dépendance?

Rencontres de l'Ichtyologie en France, Paris, 14-18 mars 2022 23

**Aquaculture et populations sauvages exploitées**

**DynRose : ADN environnemental**

**Campagne dédiée eDNA 2020**

eDNA copies  
0-1000  
1000-2000  
2000-5000  
5000-10000  
10000-20000

**Metabarcoding qPCR**

**EVHOE**

**Results Spatial distribution**

**Blackspot seabream (*Pagellus bogaraveo*)**

**Barcoding ddPCR**

**Limites**  
➤ Pas d'information sur les tailles  
➤ Lien entre nombre de copies et biomasse ?

Rencontres de l'Ichtyologie en France, Paris, 14-18 mars 2022 24

Aquaculture et populations sauvages exploitées

## Conclusion

- Acoustique
  - Estimation incertaine de la biomasse locale
- ADNe
  - Distribution spatiale
  - Identification spécifique fiable
  - Domaine en progrès rapide
- Stock de Celtique / Gascogne
  - Tendance récente inconnue
  - Présence de grands/vieux individus (50 cm/13 ans)
  - Faible niveau de la biomasse a probablement un impact sur les traits d'histoire de vie (taille-aux-âges)

**Objectif de l'ADNe : observer la dynamique de reconstitution d'une population effondrée**

Rencontres de l'Ichtyologie en France, Paris, 14-18 mars 2022 25

Aquaculture et populations sauvages exploitées

## Travaux à poursuivre

- ADNe
  - Projet shift EDNA : ANR franco-Suisse avec l'École polytechnique de Zurich (ETHZ)
  - Point d'échantillonnage Pointe du Raz 2022-2024
  - objectif : abondance et distribution
- Modélisation DEB (Dynamic Energy Budget)
  - objectif : comprendre la stratégie vitale énergétique

04/01/2023 Rencontres de l'Ichtyologie en France, Paris, 14-18 mars 2022 26

Aquaculture et populations sauvages exploitées

## Maigre – populations et stocks

- golfe de Gascogne
  - frayerie Gironde
- Autres lieux de capture
  - Méditerranée (Egypte)
  - Portugal
  - Mauritanie

Il n'y a ni d'évaluation de stocks ni de régulation de la pêche, sauf un taille minimale de 30 cm

04/01/2023 Rencontres de l'Ichtyologie en France, Paris, 14-18 mars 2022 27

Aquaculture et populations sauvages exploitées

## Projet ACOST

- Objectif pour le maigre\*
  - estimation d'abondance par marquage recapture génétique (CKMR)
- Avancement: échantillon collecté
  - histogramme de longueur (N=2489)
  - trois autres espèces sont étudiées avec d'autres objectifs

04/01/2023 Rencontres de l'Ichtyologie en France, Paris, 14-18 mars 2022 28

Aquaculture et populations sauvages exploitées

## Conclusion

- Pisciculture marine en augmentation
- Elevage porte sur des espèces chères avec prix des poissons d'élevage inférieurs à ceux des poissons sauvages
- motivation de l'aquaculture
  - Dorade rose : haute valeur
  - Maigre : caractéristiques biologiques et valeur
- succès de l'aquaculture
  - Dorade rose : semble compromis
  - Maigre : en développement rapide
- Abondances des populations sauvages non quantifiée
  - l'haleutique du futur est arrivé!
    - dorade rose : suivi par ADNe
    - maigre : approche CKMR

04/01/2023 Rencontres de l'Ichtyologie en France, Paris, 14-18 mars 2022 29

Aquaculture et populations sauvages exploitées

## Remerciements

Contributrices, contributeurs:  
Lola de Cubber, IRD, URM Marbec  
Juan Gil, IEO Cadiz  
Mario Pinho, University of the Azores  
Pôle sclérochronologie, Ifremer

projet H2020 PANDORA  
projet FFP DynRose  
projet FFP ACOST

projet ANR GenoPopTaille

04/01/2023 Rencontres de l'Ichtyologie en France, Paris, 14-18 mars 2022 30